

Regional impacts of offshore wind farms on the North Sea hydrodynamics

Dissertation

zur Erlangung des Doktorgrades der Naturwissenschaften
an der Fakultät für Mathematik, Informatik und Naturwissenschaften
Fachbereich Geowissenschaften
der Universität Hamburg

vorgelegt von

Nils Christiansen

Hamburg, 2022

Fachbereich Erdsystemwissenschaften

Datum der Disputation:

21.04.2023

Gutachter:innen der Dissertation:

Prof. Dr. Corinna Schrum

Dr. Thomas Pohlmann

Zusammensetzung der Prüfungskommission:

Prof. Dr. Corinna Schrum

Dr. Thomas Pohlmann

Dr. Ute Daewel

Prof. Dr. Dirk Notz

Prof. Dr. Jürgen Scheffran

Vorsitzender des Fach-Promotionsausschusses

Erdsystemwissenschaften:

Prof. Dr. Hermann Held

Dekan der Fakultät MIN:

Prof. Dr. Ing. Nobert Ritter

Abstract

As part of the transition to more sustainable energy generation and the reduction of anthropogenic greenhouse gas emissions, offshore wind energy has developed rapidly over the past decade. As a result, the economic use of the coastal ocean is continuously increasing, and with it the interactions between anthropogenic impacts and the marine environment. In light of offshore wind development, this dissertation investigates the physical effects of offshore wind farms on the hydrodynamics of the North Sea, a global hotspot for offshore renewable energy.

Offshore wind farms affect the physics in the atmosphere and ocean by extracting energy and disturbing incoming horizontal winds and currents. The associated effects occur on a variety of horizontal scales, from local mixing at turbine foundations to large-scale wind speed reductions. This thesis demonstrates how these wind farm effects influence hydrodynamics on regional and seasonal scales, providing essential knowledge about the implications for ocean physics. Using three-dimensional numerical modeling, the thesis presents new and existing parameterization approaches to account for wind speed reduction and additional structure-induced mixing from offshore wind farms in regional hydrostatic models.

Sectioned into three individual studies, this dissertation illustrates the physical implications of surface wind speed reduction and underwater structure drag on wind-driven processes and local mixing, respectively. In this context, the so-called wind wakes are shown to associate with changes in wind-induced currents and mixing, whereas the oceanic wakes particularly influence the local turbulence and horizontal circulation. Thereby, the changes in ocean physics do not remain local, but propagate through advection and baroclinic currents into the far field of offshore wind farms. The emerging large-scale anomalies translate to current speeds, surface elevation or vertical velocities. Eventually, both wind farm effects alter the vertical density stratification and cause regional perturbations of the seasonal pycnocline of about $\pm 5\text{--}10\%$ on average.

This dissertation emphasizes that physical implications from wind speed reduction and underwater structure drag can emerge on similar magnitudes, although being driven by different mechanism and originating on different spatial scales. The monthly-mean wake effects in the atmosphere and ocean are shown to cause large-scale restructuring and spatiotemporal redistributions of ocean physics within natural variability. In this context, the wake effects, particularly wind wake effects, show strong variability and

sensitivity to local conditions such as tidal stirring, which can disturb initial signals from wind speed reduction and attenuate wake effects by 50 % or more.

While the outcomes advance the knowledge about regional implications from offshore wind energy production, changes in the physical environment indicate potential consequences for physically determined ecosystem dynamics. Questions remain open about the interaction of the wind farm effects and possible mitigation strategies or beneficial use of physical implications from offshore wind farms.

Zusammenfassung

Im Zuge des Wandels zu einer nachhaltigeren Energieerzeugung und der Verringerung der anthropogenen Treibhausgasemissionen hat sich die Offshore-Windenergie in den letzten zehn Jahren rasant entwickelt. Folglich nimmt die wirtschaftliche Nutzung des Küstenmeeres kontinuierlich zu und damit auch die Wechselwirkungen zwischen anthropogenen Einflüssen und der Meeresumwelt. Vor dem Hintergrund der Entwicklung der Offshore-Windenergie untersucht diese Arbeit die physikalischen Auswirkungen von Offshore-Windparks auf die Hydrodynamik der Nordsee, einem globalen Hotspot für erneuerbare Offshore-Energie.

Offshore-Windparks beeinflussen die Physik in der Atmosphäre und im Ozean, indem sie Energie entziehen und die eintreffenden horizontalen Strömungen stören. Die damit verbundenen Auswirkungen treten auf verschiedenen horizontalen Skalen auf, von der lokalen Durchmischung an den Fundamenten der Turbinen bis hin zur großräumigen Verringerung der Windgeschwindigkeit. In dieser Arbeit wird verdeutlicht, wie diese Windparkeffekte die Hydrodynamik auf regionalen und saisonalen Skalen beeinflussen, und damit wichtige Erkenntnisse über die Folgen für die Ozeanphysik geliefert. Unter Verwendung dreidimensionaler numerischer Modellierung werden in dieser Arbeit neue und bestehende Parametrisierungsansätze vorgestellt, welche die Verringerung der Windgeschwindigkeit und zusätzliche strukturbedingte Vermischung durch Offshore-Windparks in regionalen hydrodynamischen Modellen zu berücksichtigen.

Aufgeteilt in drei Einzelstudien veranschaulicht diese Dissertation die physikalischen Auswirkungen der Verringerung der Windgeschwindigkeit an der Oberfläche und des Strukturwiderstands unter Wasser auf windgetriebene Prozesse bzw. die lokale Durchmischung. In diesem Zusammenhang wird gezeigt, dass die so genannten Wirbelschleppen mit Veränderungen der windinduzierten Strömungen und Vermischung einhergehen, während die ozeanischen Nachlaufeffekte insbesondere die lokale Turbulenz und die horizontale Zirkulation beeinflussen. Dabei bleiben die ozeanphysikalischen Veränderungen nicht lokal, sondern breiten sich durch Advektion und barokline Strömungen bis in das Fernfeld von Offshore-Windparks aus. Die entstehenden großräumigen Anomalien schlagen sich in Strömungsgeschwindigkeiten, Oberflächenhöhe oder vertikalen Geschwindigkeiten nieder. Letztendlich verändern beide Windparkeffekte die vertikale Dichteschichtung und verursachen regionale Störungen der saisonalen Pyknokline von durchschnittlich $\pm 5-10\%$.

In dieser Dissertation wird deutlich, dass die physikalischen Auswirkungen der Verringerung der Windgeschwindigkeit und des Widerstands von Unterwasserstrukturen in ähnlicher Größenordnung auftreten können, obwohl sie durch unterschiedliche Mechanismen angetrieben werden und auf unterschiedlichen räumlichen Skalen entstehen. Es wird gezeigt, dass die Nachlaufeffekte in der Atmosphäre und im Ozean im Monatsmittel großräumige Umstrukturierungen und räumlich-zeitliche Umverteilungen der Ozeanphysik innerhalb der natürlichen Variabilität verursachen. In diesem Zusammenhang zeigen die Nachlaufeffekte, insbesondere die Wirbelschleppeneffekte, eine starke Variabilität und Empfindlichkeit gegenüber lokalen Bedingungen, wie z. B. der Gezeitendurchmischung, welche die ursprünglichen Signale der Windgeschwindigkeitsreduzierung stören kann und die Nachlaufeffekte um 50 % oder mehr abschwächt.

Während die Ergebnisse das Wissen über die regionalen Auswirkungen der Offshore-Windenergieerzeugung vorantreiben, deuten Veränderungen in der physikalischen Umwelt auf potenzielle Folgen für die physikalisch geprägte Ökosystemdynamik hin. Es bleiben offene Fragen über die Wechselwirkung der Windparkeffekte und mögliche Abmilderungsstrategien oder die vorteilbringende Nutzung der physikalischen Auswirkungen von Offshore-Windparks.

List of Publications

Publications related to this dissertation:

Study I

Christiansen, N., Daewel, U., Djath, B. and Schrum, C. (2022). Emergence of large-scale hydrodynamic structures due to atmospheric offshore wind farm wakes. *Frontiers in Marine Science* 9:818501. doi: 10.3389/fmars.2022.818501

Study II

Christiansen, N., Daewel, U. and Schrum, C. (2022). Tidal mitigation of offshore wind wake effects in coastal seas. *Frontiers in Marine Science* 9:1006647.
doi: 10.3389/fmars.2022.1006647

Study III

Christiansen, N., Carpenter, J.R., Daewel, U., Suzuki, N. and Schrum, C. (2022). Regional modeling of structure-induced mixing at offshore wind farm sites. (to be submitted)

Contents

Abstract.....	i
Zusammenfassung.....	iii
List of Publications.....	v
Contents.....	vii
1 Introduction.....	1
2 Study I – The Impact of Wind Wakes.....	11
3 Study II – Tidal Mitigation of Wake Effects.....	35
4 Study III – Regional Modeling of Structure Drag.....	53
5 Discussion and Outlook.....	93
References.....	103
Acknowledgements.....	107
Eidesstattliche Versicherung Declaration on Oath.....	109

1 Introduction

Wind energy is one of the most important sources of renewable energy, used both on land and at sea for sustainable power generation. In Europe, wind energy production reached a total capacity of 236 GW in 2021, covering about 15% of the European electricity demand (WindEurope, 2022). While the offshore production accounted for only 12% of the total capacity, 116 offshore wind farms with a total of 5402 wind turbines had already been commissioned in European waters by the end of 2020 (WindEurope, 2021), of which 79% are located in the North Sea (Figure 1). In view of climate change mitigation strategies and the need for reduction in greenhouse gas emissions, the share of renewable energies will increase strongly in the coming years, having an impact on offshore wind energy development. Starting from about 28 GW offshore wind capacity (including UK) in 2021 (WindEurope, 2022), EU's Offshore Renewable Energy Strategy (European Commission, 2020) is targeting a capacity of at least 60 GW by 2030 and 300 GW by 2050 (excluding UK), implying a massive expansion of offshore wind infrastructure in the European shelf seas. While these plans represent important steps toward more sustainable energy production, the expansion of offshore wind energy entails extensive development of coastal seas, increasing anthropogenic pressures on the marine environment and creating potential conflicts between humans and nature. It is therefore essential to investigate the effects of offshore wind energy production on the ocean and to determine the possible consequences for the marine environment.

A new member in the marine environment

As offshore wind turbines form new artificial stressors in the marine system, the environment must adapt to the man-made structures. This concerns ecological as well as physical processes below and above sea level. In recent years, there has been increasing research on the environmental impacts of offshore wind turbines, particularly from an ecological perspective. In this context, the artificial stressors can affect the different marine receptors both positively and negatively. For instance, offshore wind turbines can threaten birds and marine mammals through collision, noise emissions and electromagnetic fields during construction and operation phases of the devices (Inger et al., 2009; Boehlert and Gill, 2010; Bergström et al., 2014). On the other hand, wind turbines are suggested to create artificial reefs, attracting benthic and pelagic species by providing new settlement habitats and recruitment areas (Boehlert and Gill, 2010; Mineur et al., 2012; Bergström et al., 2014). By this, the artificial structures can increase the

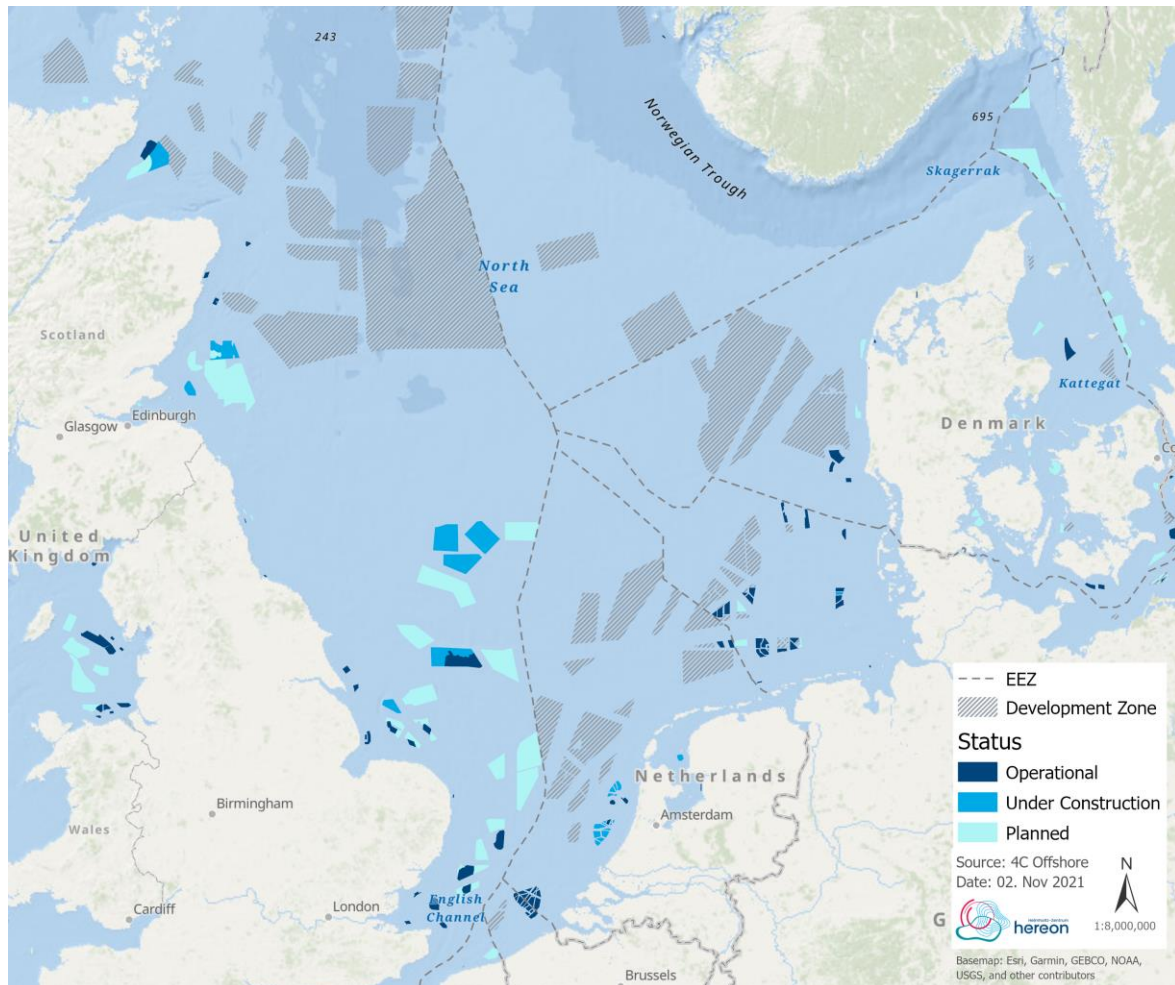


Figure 1 | Map of European offshore wind energy in the North Sea (status as of November 2, 2021). The data have been obtained from <https://www.4coffshore.com/offshorewind/>.

biodiversity and abundance of different species at offshore wind farms (Inger et al., 2009; Boehlert and Gill, 2010), leading to spatial redistribution in the marine environment at various trophic levels.

In addition to the local biological processes, environmental effects of offshore wind farms are expected to result from physical changes and associated biogeochemical processes (Clark et al., 2014). Effects on the physical environment are essentially due to changes in kinetic energy in the atmosphere and the ocean caused by the physical presence of the offshore wind turbines and their operation. More precisely, the wind turbine rotors extract momentum from the wind field, while the wind turbine foundations obstruct the horizontal currents. These two effects influence wind-driven and depth-averaged currents, respectively, and have the potential to alter local ocean dynamics near offshore wind farms.

Above sea level, the drag of wind turbine rotors results in downstream reduction in wind speed associated with changing pressure and increasing turbulence (Djath et al., 2018). These atmospheric wakes develop at hub height of wind turbines, but extend vertically and strike the water surface at a distance of about 10 rotor diameters from the respective wind turbines (Christiansen and Hasager, 2005; Frandsen et al., 2006). These effects do not only occur at individual turbines, but are bundled behind offshore wind farms to form large wind farm wake structures (Frandsen et al., 2006), which affect the wind field near the sea surface. Using in situ measurements and satellite data (Figure II), recent studies have obtained information about the magnitude of atmospheric wakes, showing that the wind speed reductions near the sea surface depend strongly on the local conditions. Wake dispersion and thus wake length is a function of turbulence and atmospheric stability in the boundary layer (Emeis, 2010; Djath et al., 2018; Platis et al., 2020), whereas the wake intensity is primarily determined by the wind farm properties (Djath et al., 2018). In this context, thermally stable atmospheric conditions allow wind wakes to extend several tens of kilometers, resulting in wind wakes being observed more than 50 km downstream of wind farms (Djath et al., 2018; Djath and Schulz-Stellenfleth, 2019; Cañadillas et al., 2020).

At the sea surface, the induced wind speed reductions imply lower wind stress at the boundary, affecting wind-driven processes and vertical exchange between atmosphere and ocean (Akhtar et al., 2022). First idealized studies have shown that the reductions in wind stress decrease the horizontal surface currents and change associated Ekman dynamics along the wind wakes (Ludewig, 2015). In this process, upwelling and downwelling emerges from divergence and convergence of surface water perpendicular to the downstream wake axis (Broström, 2008; Paskyabi and Fer, 2012; Ludewig, 2015). For an idealized stratified water column, Ludewig (2015) identified vertical velocities on the order of meters per day triggered by the surface changes under steady wind conditions. The vertical transport was shown to change temperature and salinity stratification and influence the local pycnocline. Recent observations by Floeter et al. (2022) provided empirical evidence of upwelling/downwelling dipoles in the German Bight by measuring water property transects through offshore wind farms, showing diagonal excursions of the thermocline perpendicular to the prevailing wind direction of about 10–14 m over a distance of 10–12 km.

Below sea level, the effects of surface wind speed reduction are complemented by the hydrodynamic wake effects at wind turbine foundations. The drag by the underwater cylinders changes flow characteristics locally by blocking horizontal currents and generating turbulence downstream of the piles (Williamson, 1996; Sumer and Fredsøe,

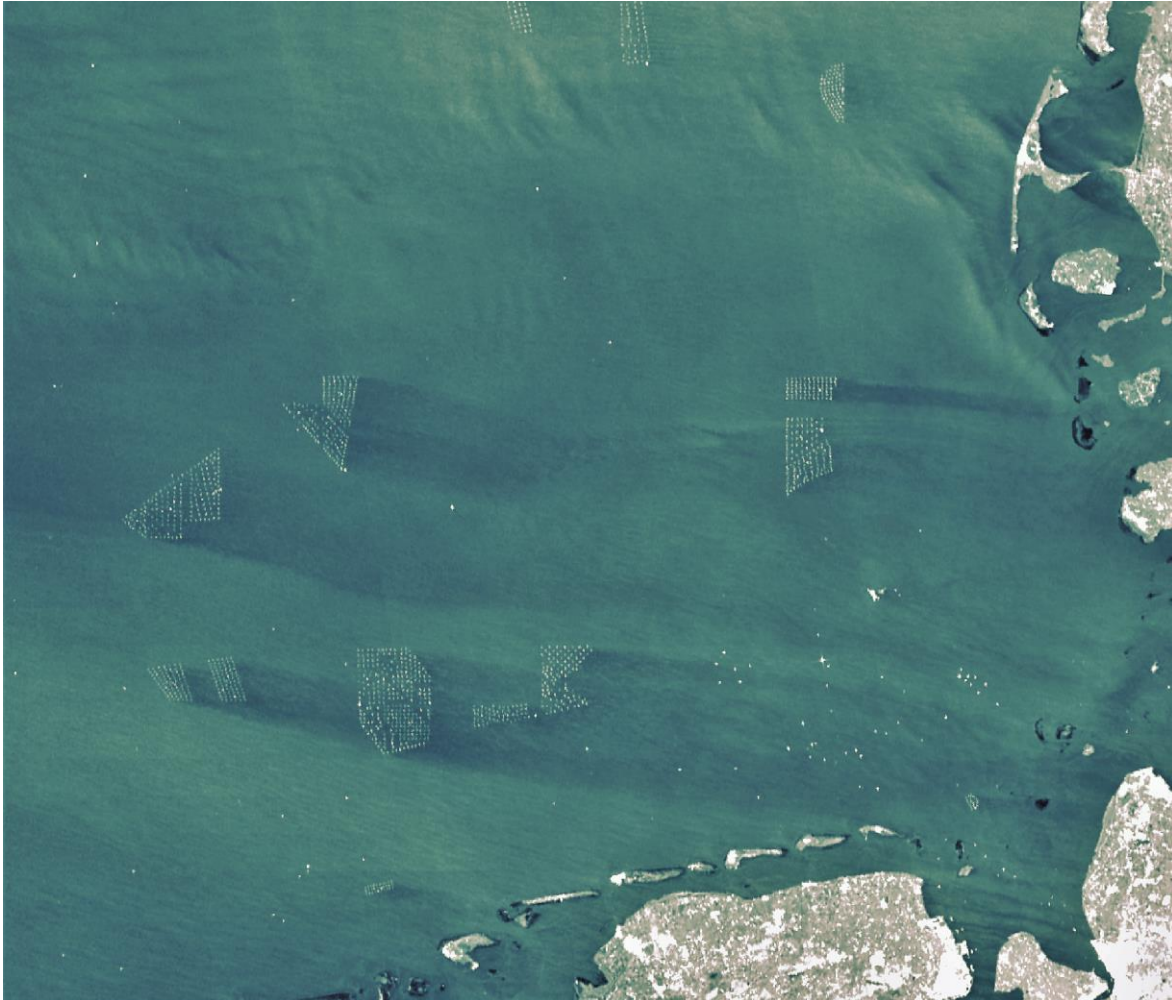


Figure II | Example of surface wind speed reductions (atmospheric wakes) in the German Bight on April 1, 2020. The figure shows satellite SAR data obtained from the Copernicus Sentinel-1 program (<https://sentinels.copernicus.eu/web/sentinel/missions/sentinel-1>), courtesy of Bughsin' Djath.

2006; Grashorn and Stanev, 2016). In this context, structure drag depends on local hydrodynamic conditions, such as free-stream flow turbulence, and structure properties, such as surface roughness, which determine the magnitude of induced wake turbulence and the characteristics of the hydrodynamic wake effects (Shih et al., 1993; Williamson, 1996; Dorrell et al., 2022). Under shelf-sea conditions, the pile effects are assumed highly turbulent and three-dimensional (Dorrell et al., 2022). Using satellite imaging and in situ measurements, recent studies detected wakes of at least 1 km in length (Vanhellemont and Ruddick, 2014; Forster, 2018; Schultze et al., 2020), for example in the shallow turbulent waters near the Thames Estuary (Figure III), where hydrodynamic wakes can trap suspended particulate matter (Baeye and Fettweis, 2015).

The additional turbulence from wind turbine foundations mixes the water column and changes physical and biogeochemical processes. Schultze et al. (2020) estimated that

additional mixing of a single monopile accounts for about 7–10% of the mixing occurring in the bottom mixed layer. In shallow waters, the structure-induced mixing affects the sedimentation and sediment resuspension downstream of the foundations, increasing the turbidity and resulting in turbid plumes behind wind turbines (Vanhellemont and Ruddick, 2014; Baeye and Fettweis, 2015). In deeper stratified waters, on the other hand, wake turbulence is associated with destratification of the water column and changes in temperature and salinity distributions (Floeter et al., 2017; Schultze et al., 2020). In situ measurements by Floeter et al. (2017) indicated that mixing may extend throughout the wind farm area due to changing tidal currents, leading to a doming of the mixed layer depth due to declining stratification and enhancing the nutrient supply in the depleted surface mixed layer.

Need for further investigations

Despite knowledge about their local physical and ecological consequences, potential regional implications of atmospheric and hydrodynamic wake effects on the ocean remain poorly represented in the literature to date. The physical stressors have yet been addressed primarily at local scales, but in view of recent and future offshore wind development wind farm effects may become much more regional.

In context of additional structure-induced mixing, Carpenter et al. (2016) made first assumptions about the impact of extensive offshore wind development in the German Bight. Based on theoretical drag models for turbulent kinetic energy production, the study suggested significant impact by the additional turbulence on the development of stratification and extraction of tidal energy by wind turbines of about 4–20 % of the bottom boundary layer extraction (Carpenter et al., 2016). Using regional-scale numerical modeling, Rennau et al. (2012) and Cazenave et al. (2016) showed that wind farm mixing may influence not only local processes but mixed waters can propagate and change density stratification in the far field of wind farms. At this, Rennau et al. (2012) demonstrated changes in bottom water salinity several tens of kilometers along the westerly Baltic inflow for realistic wind farm scenarios in the western Baltic Sea. However, the changes of about 0.02 g/kg did not appear to influence the regional stratification significantly.

On the other hand, Ludewig (2015) has given first insights into the magnitude of the atmospheric wake effects and associated changes in the hydrodynamics, showing that wind farms can affect the marine environment far beyond their locations. Using future offshore wind scenarios for the German Bight, the study revealed large-scale anomalies

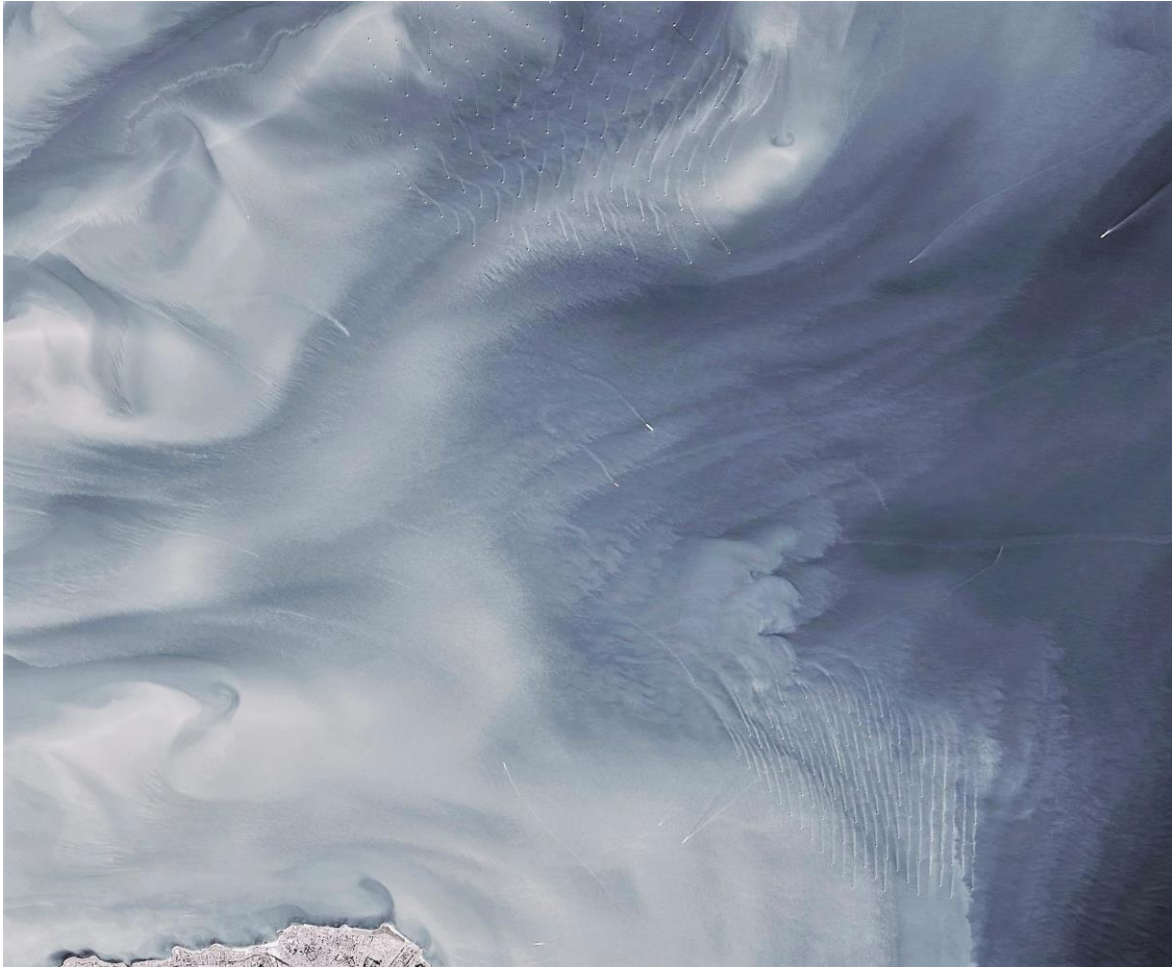


Figure III | Example of sediment plumes (hydrodynamic wakes) near the Thames Estuary on June 30, 2015. The figure shows data from the Landsat 8 satellite, processed and provided by the NASA Earth Observatory (<https://landsat.visibleearth.nasa.gov/view.php?id=89063>). The original figure was modified by image processing.

in atmospheric and hydrodynamic parameters, e.g. horizontal surface currents or sea surface elevation, which eventually affected temperature and salinity distributions over areas covered by offshore wind farms and well beyond. At this, daily mean changes in sea surface temperature occurred on the order of $\pm 0.1^{\circ}\text{C}$. However, the simulations were limited to a three-day period and thus did not provide information about the long-term impact on, for example, seasonal stratification development or persistent hydrodynamic changes.

The previous investigations provided preliminary insights into the processes associated to large-scale wind speed reduction and structure-induced mixing, and addressed their potential environmental consequences for the coastal ocean. However, further analysis on the regional spatial scale and the seasonal temporal scale of the processes is missing. Questions remain about the different magnitudes of atmospheric and hydrodynamic

wake effects under realistic conditions and their interaction in the marine environment. Indications of large-scale changes in temperature and salinity raise questions about the implications for the seasonal stratification development and the associated ecosystem dynamics. Especially in stratified regions, perturbations of stratification conditions could feed back on ecological processes and create a 'new normal' for shelf sea dynamics (Dorrell et al., 2022). In view of future development, offshore wind energy will play an important role in the future coastal ocean, implying the need for further regional impact assessment of wake effects and a better understanding of the atmospheric and hydrodynamic processes.

Motivated by the potential consequences of physical offshore wind farm effects, this study aims to advance the understanding of how coastal systems adapt to these anthropogenic stressors, and to raise awareness of potential side effects of climate change mitigation strategies. Specifically, the focus is on the long-term impact of the previously underestimated atmospheric wind wake effects, with a special emphasis on seasonal stratification development in summer, and on the processes determining the magnitudes of the effects. In addition, this thesis addresses the cross-scale modeling of turbulent wakes at wind turbine foundations, aiming to determine the scale of the hydrodynamic wake effects and their impact on regional ocean dynamics. The following research questions compromise the objectives of this thesis:

-
- Q1 How can offshore wind farm effects be integrated into regional-scale models?**
 - Q2 What are the physical effects of atmospheric and hydrodynamic wakes?**
 - Q3 Can offshore wind farm effects change regional ocean dynamics?**
-

Approach and outline

Focus of this thesis is the southern North Sea, a region strongly affected by the development in offshore wind energy due to its shallow water depths and stable wind resources. The southern North Sea, as part of the North Sea shelf region, is governed by tidal energy from the open ocean, continental influences and wind forcing, all determining the dynamics of the shallow North Sea waters (Sündermann and Pohlmann, 2011). Wind stress and bottom friction create turbulence in the surface and bottom layers (Simpson and Sharples, 2012), resulting in regimes of permanently mixed waters, frontal areas, and seasonally stratified deeper regions (Otto et al., 1990; van Leeuwen et al., 2015). The physical regimes make the southern North Sea a complex system of varying

conditions, but allow investigating the influence of offshore wind farm effects under different hydrodynamic circumstances.

For impact analysis, this thesis considers realistic offshore wind scenarios based on recent offshore wind development data (Figure I). Specifically, investigations focus on the current states of fully commissioned offshore wind farms in the German Bight and the southern North Sea. This includes wind farms located mainly in well-mixed waters, but also in stratified regimes, enabling to address the impact on seasonal stratification and the role of tidal mixing. All studies are grounded on three-dimensional hydrodynamic modeling, which allows studying specific case studies with and without wind farms and do pre-post analysis, without the need for in situ measurements at wind farm sites. Here, the Semi-implicit Cross-scale Hydroscience Integrated System Model (Zhang et al., 2016) is used, a hydrostatic model using Reynolds-averaged Navier-Stokes equations and the Boussinesq approximation. The SCHISM model is based on unstructured horizontal grids that enable to resolve cross-scale wake effects from offshore wind farms in the regional model domain of the southern North Sea.

Within the frame of this thesis, the impact analysis of offshore wind farm effects is divided into three subchapters, each of which corresponds to an independent study. In the first part (**Study I**), a new observation-based empirical wind wake model is introduced that allows parameterizing surface wind speed reductions at wind farm sites through the atmospheric boundary forcing in the hydrodynamic model. Using this wind wake parameterization, **Study I** highlights the regional impacts of the atmospheric wake effect in the southern North Sea during the summer season. For the first time, the study shows long-term impact of wake-related wind speed reductions on hydrodynamic processes and associated consequences for the seasonal development of stratification in the coastal waters of the southern North Sea.

Based on indications by the first study on potential influence of local hydrodynamics on occurring wake effects, **Study II** investigates the importance of the environmental conditions on the magnitude of the processes related to wind wakes. **Study II** demonstrates how tidal currents and associated mixing in the southern North Sea determine the response of hydrodynamics to the atmospheric wakes, helping to assess the expected magnitudes of the atmospheric wake impact in different marine environments. In this context, the study shows that hydrodynamic conditions play an important role in mitigating the effects of surface wind speed reduction.

Ultimately, **Study III** completes the overall story of physical stressors from offshore wind farms by incorporating effects of structure-induced mixing into the hydrodynamic

model. In order to assess the regional impact of the hydrodynamic wake effects, **Study III** evaluates the difficulties of different existing approaches of including the small-scale processes at wind turbine foundations into the large-scale hydrostatic model framework. Using the German Bight as a case study, the study presents the magnitude of structure-induced mixing and long-term consequences for horizontal circulation and stratification, emphasizing the need for regional consideration of the small-scale wake effects.

All three studies contribute to the overarching research questions and goal of determining the impact of offshore wind farms on North Sea hydrodynamics. The outcomes of the studies are summarized at the end of this thesis, discussing the significance of the results and giving an outlook with regard to increasing offshore wind development in marine environments and future research needs.

2 Study I – The Impact of Wind Wakes

This chapter contains the first paper, published in *Frontiers in Marine Science – Coastal Ocean Processes*:

Christiansen, N., Daewel, U., Djath, B. and Schrum, C. (2022). **Emergence of Large-Scale Hydrodynamic Structures Due to Atmospheric Offshore Wind Farm Wakes**. *Front. Mar. Sci.* 9:818501. doi: 10.3389/fmars.2022.818501

Author Contributions:

NC implemented the wake parameterization, set up the numerical model, performed the data analysis and wrote the manuscript. UD and CS contributed to the data analysis, discussion and design of the study. BD performed statistical analysis and contributed to the parameterization section. CS initiated the study. All authors revised and approved the manuscript.



Comment:

Minor errors have been identified in the published article: In Figure 6b, the x-axis is mislabeled, showing the actual velocity profiles, not the differences. Figure 6, 7b & 8b should show the averaged differences for hourly output data, but daily means were mistakenly averaged. This may reduce the local magnitudes by a maximum of 40%, but the story of the figures remains.



Emergence of Large-Scale Hydrodynamic Structures Due to Atmospheric Offshore Wind Farm Wakes

Nils Christiansen^{1*}, Ute Daewel¹, Bughsin Djath¹ and Corinna Schrum^{1,2}

¹ Institute of Coastal Systems, Helmholtz-Zentrum Hereon, Geesthacht, Germany, ² Center for Earth System Research and Sustainability, Institute of Oceanography, Universität Hamburg, Hamburg, Germany

OPEN ACCESS

Edited by:

Harshinie Karunaratna,
Swansea University, United Kingdom

Reviewed by:

Michela De Dominicis,
University of Southampton,
United Kingdom

José Pinho,
University of Minho, Portugal

*Correspondence:

Nils Christiansen
nils.christiansen@hereon.de

Specialty section:

This article was submitted to
Coastal Ocean Processes,
a section of the journal
Frontiers in Marine Science

Received: 19 November 2021

Accepted: 13 January 2022

Published: 03 February 2022

Citation:

Christiansen N, Daewel U, Djath B
and Schrum C (2022) Emergence
of Large-Scale Hydrodynamic
Structures Due to Atmospheric
Offshore Wind Farm Wakes.
Front. Mar. Sci. 9:818501.
doi: 10.3389/fmars.2022.818501

The potential impact of offshore wind farms through decreasing sea surface wind speed on the shear forcing and its consequences for the ocean dynamics are investigated. Based on the unstructured-grid model SCHISM, we present a new cross-scale hydrodynamic model setup for the southern North Sea, which enables high-resolution analysis of offshore wind farms in the marine environment. We introduce an observational-based empirical approach to parameterize the atmospheric wakes in a hydrodynamic model and simulate the seasonal cycle of the summer stratification in consideration of the recent state of wind farm development in the southern North Sea. The simulations show the emergence of large-scale attenuation in the wind forcing and associated alterations in the local hydro- and thermodynamics. The wake effects lead to unanticipated spatial variability in the mean horizontal currents and to the formation of large-scale dipoles in the sea surface elevation. Induced changes in the vertical and lateral flow are sufficiently strong to influence the residual currents and entail alterations of the temperature and salinity distribution in areas of wind farm operation. Ultimately, the dipole-related processes affect the stratification development in the southern North Sea and indicate potential impact on marine ecosystem processes. In the German Bight, in particular, we observe large-scale structural change in stratification strength, which eventually enhances the stratification during the decline of the summer stratification toward autumn.

Keywords: offshore, wind farms, atmospheric wakes, 3D hydrodynamic modeling, North Sea, stratification

INTRODUCTION

With sustainable energy generation through offshore wind farms, kinetic energy is withdrawn from the atmosphere and consequently horizontal momentum reduces on the leeward side of the respective wind turbines. The consequences of this energy extraction are atmospheric wakes, which are characterized by the downstream reduction of the mean wind speed and the development of increased turbulence along the wind speed deficit (Lissaman, 1979; Fitch et al., 2012, 2013; Volker et al., 2015; Akhtar et al., 2021). In large wind turbine clusters, the individual wakes merge downstream into a single wind farm related wake structure, whereby wind direction and wind turbine layout play an important role (Frandsen, 1992; Li and Lehner, 2013).

By using in-situ airborne measurements and satellite Synthetic Aperture Radar (SAR) data, recent studies observed atmospheric wakes behind offshore wind farms in the North Sea and derived information about spatial extension and intensity of wind farm wakes (Christiansen and Hasager, 2005, 2006; Li and Lehner, 2013; Emeis et al., 2016; Djath et al., 2018; Platis et al., 2018, 2020, 2021; Siedersleben et al., 2018; Djath and Schulz-Stellenfleh, 2019; Cañadillas et al., 2020). The measurements demonstrated a strong correlation between atmospheric stability and the dimension of wakes. Wind speed deficits propagate much further under stable conditions and were detected up to 70 km downstream of the respective wind farms (Djath et al., 2018; Cañadillas et al., 2020). At the same time, the superposition of wind farm wakes is a decisive factor for the wake dimension (Djath et al., 2018). The magnitudes of wind speed deficits depend for the most part on the mean wind speeds at wind farms and the wind farm drag by the wind turbines.

The impact of energy extraction by wind turbines cascades down to the sea surface and reduces the wind stress at the sea surface boundary. Although the strongest wind speed reductions emerge at hub height [$\sim 20\text{--}30\%$, Cañadillas et al. (2020) and Platis et al. (2020)], the SAR measurements showed that the wind speed at 10 m height is still reduced by about 10% (Christiansen and Hasager, 2005; Djath et al., 2018). Since, not only residual currents but also mixing of the surface mixed layer are primarily shear-driven (Kantha and Clayson, 2015), anomalies in the wind field can have severe consequences for the upper ocean dynamics. This applies particularly to the shallow North Sea, where the general circulation is significantly controlled by the atmosphere (Sündermann and Pohlmann, 2011). In addition, thermodynamic processes in marginal seas, like the North Sea, are strongly sensitive to variations in atmospheric forcing (Schrum and Backhaus, 1999; Skogen et al., 2011; Schrum, 2017). Turbulent processes near the sea surface boundary determine vertical fluxes (e.g., heat, water, and momentum) between atmosphere and ocean (Kantha and Clayson, 2015). Thus, a reduction of shear-driven turbulent mixing can result in changes of the heat content in the upper ocean and associated surface heating or cooling.

Earlier studies started to investigate the oceanic response to wind stress anomalies in idealized model approaches (Broström, 2008; Paskyabi and Fer, 2012; Paskyabi, 2015). The studies demonstrated the occurrence of an elevation pattern and corresponding up- and downwelling at the sea surface, which results from the adjustment of wind-driven Ekman transport along the wake-impacted area (Ludewig, 2015). For the case of an idealized stratified water column, Ludewig (2015) showed that the convergence and divergence of surface water masses trigger dipole-related vertical transport and results in perturbations of the pycnocline. At this, Ludewig (2015) found associated vertical velocities of several meters per day in a German Bight scenario, which induced anomalies in the temperature and salinity distribution.

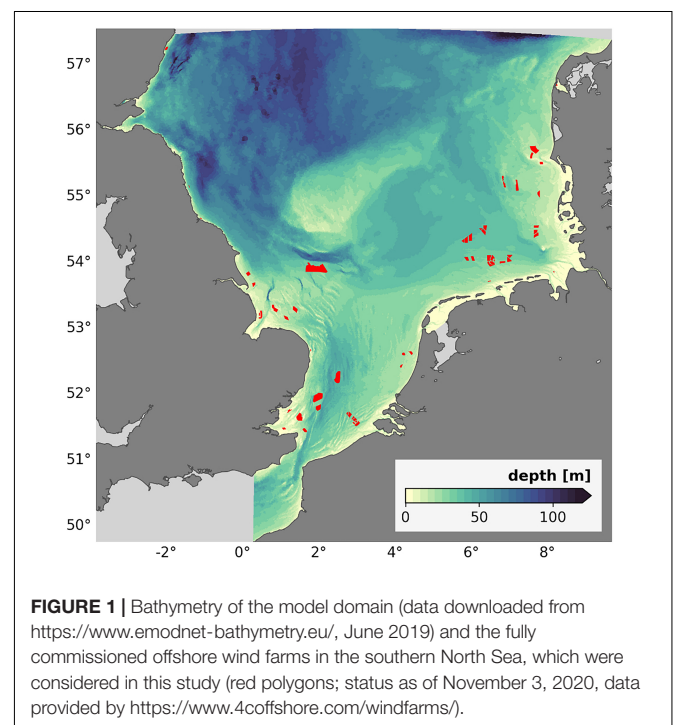
The latest results of recent studies on potential thermo- and hydrodynamic effects by wind farm wakes raise concerns about substantial changes to the hydrodynamics of the North Sea. In particular, since the offshore development in the North

Sea is growing continuously, questions about environmental consequences of offshore wind farming become crucial for prospective research. Broström (2008) already discussed the impact of the wake-induced dipoles on the marine temperature field and related regional nutrient availability and stated the need for more realistic investigations of the wake-induced forcing mechanisms.

In this manuscript, we address the potential mean impact of atmospheric wakes on the hydrodynamic system of the southern North Sea in consideration of the current state of fully commissioned offshore wind farms (**Figure 1**). For this purpose, we developed a new cross-scale hydrodynamic model setup, which allows high model resolution in areas of offshore wind farm production. In order to investigate the effect of wake-associated wind speed deficits, we introduce a top-down wake formulation build upon former wake models and SAR observational data. By implementing the simplified wake parameterization into the hydrodynamic model, we aim to expand the results of existing studies and complement missing knowledge about large-scale and long-lasting effects in a realistic North Sea scenario. In particular, we answer questions about the magnitude and the dimension of hydrodynamic changes and provide a first overview about the spatial perturbations due to offshore wind farm wakes.

ATMOSPHERIC WAKE PARAMETERIZATION

Over the years, several empirical and analytical models have been developed to parameterize the downstream wake effects



in the atmosphere (Jensen, 1983; Frandsen, 1992; Emeis and Frandsen, 1993; Frandsen et al., 2006; Emeis, 2010; Peña and Rathmann, 2014; Shapiro et al., 2019). While trying to describe wake deficit and wake length, most formulations focused on the relative difference between wind speed along the lee side of wind farms and the undisturbed wind flow. For instance, the analytical model proposed by Emeis (2010) considers wind turbines as additional roughness and is based on the equilibrium between momentum extraction by wind turbines and the replenishment of momentum through turbulent fluxes from above. At this, the change in roughness is assumed proportional to the wind turbine drag coefficient and the wind speed at hub height. However, existing wake models, with regard to wind speed reduction, have so far only been developed for the processes at hub height. Due to the vertical changes of the wake pattern (Frandsen et al., 2006; Emeis, 2010; Fitch et al., 2012; Akhtar et al., 2021), the former models can thus not directly be used for processes near the sea surface boundary. For this reason, we adjusted former model assumptions based on SAR measurements so that they become applicable for numerical ocean modeling.

In a strongly simplified first order approximation, which neglects dependencies arising from specific wind farm characteristics, we parameterized the wind speed deficits resulting from operating wind farms and reduced the mean wind speed in dependence of the respective wind direction. Other impacts, such as turbulence changes or effects on local weather conditions remain unconsidered.

$$u(x, y) = u_0 (1 - \Delta u) \quad (1)$$

The parameterization for the downstream wind speed reduction [Eq. (1)] is based on earlier studies (Frandsen, 1992; Frandsen et al., 2006) and alters the undisturbed wind field u_0 by the wind speed deficit Δu . The parameterization is applied in a reference coordinate system, where x is the downstream distance aligned to the prevailing wind direction and y defines the distance from the central wake axis. Accordingly, the deficit $\Delta u(x, y)$ consist of two components describing the downstream wake recovery and the width of the wake structure.

Wake Recovery

The formulation of the downstream velocity deficit is based on the concept of the model by Emeis (2010) (E10 model). The model is a top-down approach model, meaning that the wind farms are considered as one unit of additional roughness, and describes the wake recovery by an exponential decay function. The E10 model was validated in recent studies, which showed that the exponential approach is able to reproduce airborne measurements of atmospheric wakes appropriately (Cañadillas et al., 2020; Platis et al., 2020, 2021). Similar to recent studies, we use the exponential approach of the E10 model to describe the wind speed deficits on the lee side of wind farms. Here, however, we apply the wake formulation in the spatial domain. At this, the wind speed magnitude is prescribed to decrease the strongest close to the offshore wind farms and recovers exponentially over

the downstream distance. In summary, the velocity deficit Δu along the downstream distance x is given by:

$$\Delta u(x) = \alpha e^{-x/\sigma} \quad (2)$$

with α as the maximum relative deficit and σ as the exponential decay constant.

Given that the E10 model is established for turbine wakes at hub height, some adjustments are required for the determination of the wake deficit α and the decay constant σ . The individual values for α and σ , in particular near the sea surface, depend on complex relations between multiple aspects, such as the wind field, atmospheric stability, vertical momentum fluxes and wind farm density as well as the wind turbine drag. By the knowledge of the authors of this manuscript, there is so far no empirical or analytical formulation, which either considers these aspects or provides respective values for wind deficit and wake length. Thus, we selected typical mean values for α and σ based on measurements of recent studies (Table 1) and computed SAR data statistics (Figure 2). Thereby, the decay constant σ is defined by the wake length.

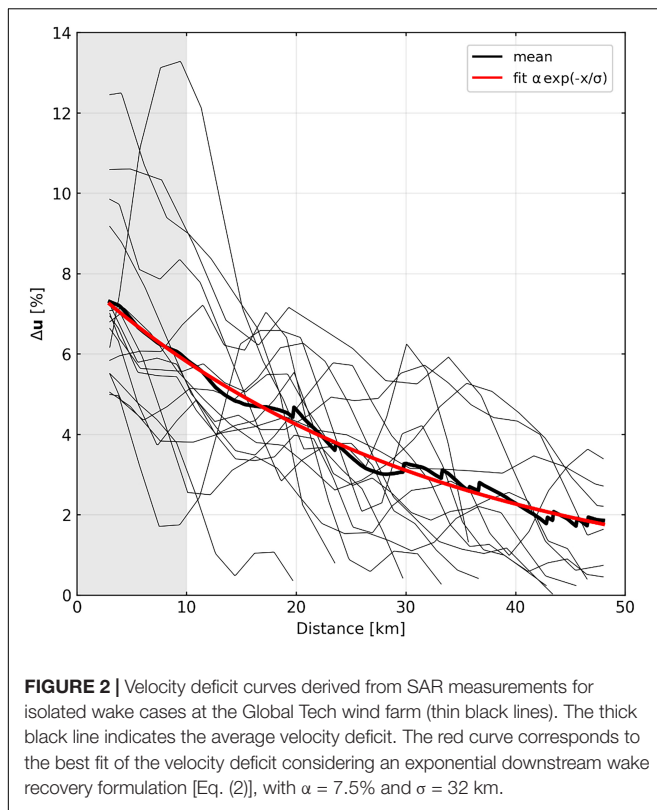
For the SAR data statistics, we utilized latest data sets from Copernicus Sentinel 1 (downloaded April 2019)¹, which consisted of satellite SAR Sentinel1-A and Sentinel1-B data from the period June 2016 to March 2019. We focused on the wind farm Global Tech in the German Bight, which is composed of 80 turbines, and considered wakes from all wind directions, except for cases of superposition of wakes from neighboring wind farms. The velocity deficits were computed using the 10-m wind field from the Synthetic Aperture Radar (SAR). Indeed, SAR technology demonstrated its ability of measuring the surface winds at fine resolution. Thereby, the changes in surface roughness caused by the perturbation of wind speed are captured by the SAR system and modify the Normalized Radar Cross Section (NRCS), which is measured by the satellite. With this, the 10-m surface wind speed is derived from the surface roughness using a geophysical model function *CMOD5N* (Hersbach et al., 2007) and velocity deficits can be calculated relative to the undisturbed wind field. A detailed description of how to obtain wind speed deficits from satellite SAR data can be found in Djath et al. (2018); Djath and Schulz-Stellenfleth (2019).

¹https://www.esa.int/Applications/Observing_the_Earth/Copernicus/

TABLE 1 | Compilation of wind speed deficit α and wake length σ observations of satellite SAR and airborne measurements.

	Wake deficit [%]	Wake length [km]
Cañadillas et al. (2020)	–	14 – 70
Christiansen and Hasager (2005, 2006)	8 – 9	5 – 20
Djath et al. (2018) and Djath and Schulz-Stellenfleth (2019)	5 – 10	30 – 60
Hasager et al. (2015)	–	15 – 70
Mean value	8.0	35.5

Bold notations were used to highlight the final mean values calculated from the listed values in each column.



In total, the SAR data set resulted in 16 undisturbed wake cases exceeding 15 km length, which are shown in **Figure 2**. The wake measurements show the highest deficits in the first kilometers behind the wind farm, which decrease over the downstream distance. For the set of profiles, the mean velocity deficit was calculated and fitted to the exponential wake recovery function [Eq. (2)] using the least square method. The exponential fit led to values for α and σ of 7.5% and 32 km, respectively. However, the estimated values for the wake dimension apply primarily for the offshore wind farm Global Tech and might vary due to different wind farm arrays or atmospheric conditions. Thus, we ultimately selected reasonable values of $\alpha = 8\%$ and $\sigma = 30$ km for the simplified wake parameterization of an undisturbed wake structure. This assumption is supported by earlier studies (**Table 1**), as the estimated wake deficit and length agree with the mean of previous sea surface wake observations.

Wake Cross-Sectional Shape

The cross-sectional shape of an atmospheric wake can be described by a symmetric exponential function, which is scaled by the characteristic wind farm width L . This assumption was validated in recent airborne measurements, where several wind speed profiles were measured perpendicular to the wake at hub height and fitted to a Gaussian function (Cañadillas et al., 2020). However, Djath and Schulz-Stellenfleth (2019) indicated that the cross-sectional shape of a wake at 10-m height is likely more distinct toward the wake edges. Hence, we chose an exponential decay constant of $\gamma = L/3$, in order to narrow the wake cross

section at sea surface height in comparison to the hub height assumption. As for the former studies, L describes the wind farm width with respect to the respective wind direction and is calculated for each wind farm individually.

$$\Delta u(y) = e^{-(y/\gamma)^2} \quad (3)$$

The adjusted Gaussian function [Eq. (3)] produces similar cross-sectional shapes to the Kaiser window function, proposed by Djath and Schulz-Stellenfleth (2019), and strikes a balance between the recent cross shape proposals.

MODEL DESCRIPTION

Model Setup

Due to their spatial extension, atmospheric wakes affect both the small-scale processes near the wind farms and the larger-scale processes in the vicinity of the wind farms. In order to model the cross-scale wake effects, we developed a model setup, which enables the simultaneous resolution of large-scale ocean dynamics and smaller-scale processes near offshore wind farms. For this purpose, we used the Semi-implicit Cross-scale Hydroscience Integrated System Model [SCHISM, Zhang et al. (2016b)]. The SCHISM model is a hydrostatic model grounded on unstructured horizontal grids, which uses Reynolds-averaged Navier-Stokes equations based on the Boussinesq approximation. The model solves transport equations with a second-order Total Variation Diminishing (TVD) advection scheme and applies a higher-order Eulerian-Lagrangian method for momentum advection. At this, it uses semi-implicit time stepping and a hybrid finite-element/finite-volume formulation. A more detailed description of the SCHISM model and its capacities can be found in Zhang et al. (2016a,b).

Our model region covers the North Sea extending laterally from the British Channel in the South to the Norwegian trench in the North and thereby includes the major areas of current offshore wind energy production in the North Sea (**Figure 1**). The model setup includes the highly resolved coastlines as well as major islands and river estuaries of the surrounding mainland. We used a depth-dependent horizontal grid cell resolution for the triangular unstructured grid, ranging from 500 m in shallow coastal areas to 5,000 m in the deep open sea. In total, the grid has approximately 161 K nodes and 311 K triangles. In the vertical direction, we applied a flexible LSC² [Localized Sigma Coordinates with Shaved Cells, Zhang et al. (2015)] grid, which is composed of a depth-dependent number of localized sigma coordinates and considers in total 40 depth levels. The layer thickness increases gradually from about 2 m in the surface layers to 10 m in levels below 100 m depth.

At the open boundaries, the model was forced by the North-West European shelf ocean physics reanalysis data from the Copernicus Marine Service (downloaded July 2019)², which we interpolated for time series of elevation, velocity, temperature, and salinity. Additionally, we prescribed tidal amplitudes and

²<https://marine.copernicus.eu/>

phases of eight tidal constituents (M_2 , S_2 , K_2 , N_2 , K_1 , O_1 , Q_1 , and P_1) from the data-assimilative HAMTIDE model (Taguchi et al., 2014). For the atmospheric forcing, the coastDat-3 COSMO-CLM ERA interim atmospheric reconstruction (HZG, 2017) was applied, while daily river discharge values were provided by the mesoscale Hydrologic Model [mHM, Samaniego et al. (2010), Kumar et al. (2013)] using the E-OBS18 temperature and precipitation data set (Cornes et al., 2018). Werner et al. (in prep.) will provide a more detailed description of the discharge data. Bottom roughness was set to 0.1 mm and we used a vertical background diffusivity of 10^{-6} m²/s. Initial conditions were interpolated from the same data sets as the boundary forcing data.

Model Simulation

After an initial spin-up simulation of two and a half years, we simulated offshore wind farm operation for the summer period of 2013 (May to September) in a subsequent model run. As the characteristic “flushing time” of the North Sea is about one year (Otto et al., 1990), the short spin-up period can be deemed sufficient for the model area. While the period of the simulations was generally chosen based on data availability, the simulation period for the wind farm simulations was chosen to ensure mostly stable atmospheric conditions, which enable the formation of large-scale wake structures. Thus, the simulations allow the investigation of the impact of wind farm wakes on the summer stratification. For all simulations, an implicit time step of 120 s was used and the daily mean was calculated for the output data.

The wind farm simulation took into account the recent state of offshore wind farm production within the model domain (see **Figure 1**). However, the wind farms were only considered via the implemented wake parameterization and were not represented physically in the horizontal grid. For the simulation, we applied the wake parameterization to the wind field interpolated onto the horizontal model grid and reduced the horizontal components of the wind speed respectively. Specifically, the wind speed on downstream grid points was iteratively reduced for each wind farm. While the parameterization modified the downstream wind field at each time step of the simulation, we considered a wind speed limitation (cut-in and cut-out speed) for wind farm operation in the wake model. For this, we used a typical wind speed range of 3–25 m/s at hub height, which inhibits wake generation for too weak and too strong wind speeds.

We enhanced the horizontal grid cell resolution in the wind farm simulation to resolve hydrodynamic processes near the offshore wind farms sufficiently and to provide highly resolved wake effects. The grid optimization involved a boundary layer of 30 km around each wind farm polygon with a grid cell size of 1,000 m (see **Figure 3**). In addition, a high-resolution zone with a grid cell size of 500 m was defined in the first five kilometers around each wind farm, where the wind deficits are most pronounced. In total, the adjusted horizontal grid of the wind farm simulation resulted in approximately 278 K nodes and 544 K triangles.

In order to compare differences between the wake-exposed North Sea and the reference case we ran the summer period twice,

with and without wind farm parameterization. For both cases, the enhanced grid cell resolution was applied.

Model Validation

In order to validate the model simulations, temperature and salinity values were downloaded from the ICES database (downloaded March 2020)³ for the period from January 2012 to December 2013. The observational data set consists of about 3,250 stations, at which temperature and salinity samples were collected at different water levels. For the validation, we calculated the depth-averaged data to avoid uncertainties in depth levels and compared it to the respective daily-mean values of the spin-up simulation, which forms the basis of the wind farm scenarios.

We utilized a Taylor diagram (Taylor, 2001) to display the statistics of our model simulations. The diagram is based on the law of cosine and quantifies differences between observation and model by the centered root mean square difference E' and the correlation coefficient R . The root mean square difference and the correlation coefficient are calculated as:

$$E' = \left(\frac{1}{N} \sum_{n=1}^N ((O_n - \bar{O}) - (M_n - \bar{M}))^2 \right)^{\frac{1}{2}} \quad (4)$$

and

$$R = \frac{\frac{1}{N} \sum_{n=1}^N (M_n - \bar{M}_n) (O_n - \bar{O}_n)}{\sigma_M \sigma_O} \quad (5)$$

with $\sigma_X = \sqrt{\frac{1}{N} \sum_{n=1}^N (X - \bar{X})^2}$ as the standard deviation, M as model data and O as observation data.

Similar to Daewel and Schrum (2013), we subdivided our model domain into different validation areas based on their physical characteristics (**Figure 4A**). Here, we focused on five main characteristic regions: The Atlantic inflow area (D), the British coast (E), the shallow tidal-impacted coastal areas connected to the Wadden Sea (F&G), the Baltic in- and outflow area (H) and the seasonally stratified central North Sea (K&L). For the statistics, we treated each region individually.

The calculated Taylor diagram (**Figure 4B**) shows high correlation ($R > 0.9$) between the spin-up simulation and the observations for sea surface temperatures. Seven out of eight subareas exhibit correlation coefficients above 0.95, from which the areas connected to the Wadden Sea (F&G) show the highest values ($R > 0.99$). Only region K, the deep central North Sea area, shows a slightly lower correlation, which is probably due to the influence of the large northern open boundary of the model domain. Surface salinity has a lower, but still decent, overall agreement between the model and the observational data. Most coefficients range between 0.8 and 0.9, whereas only region E, the British coast region, and again region K show lower correlations. Generally, the lower correlation in salinity likely results from the comparison of daily-mean model data and instantaneous observational data, as we observe strong fluctuations in the fresh

³<http://www.ices.dk>

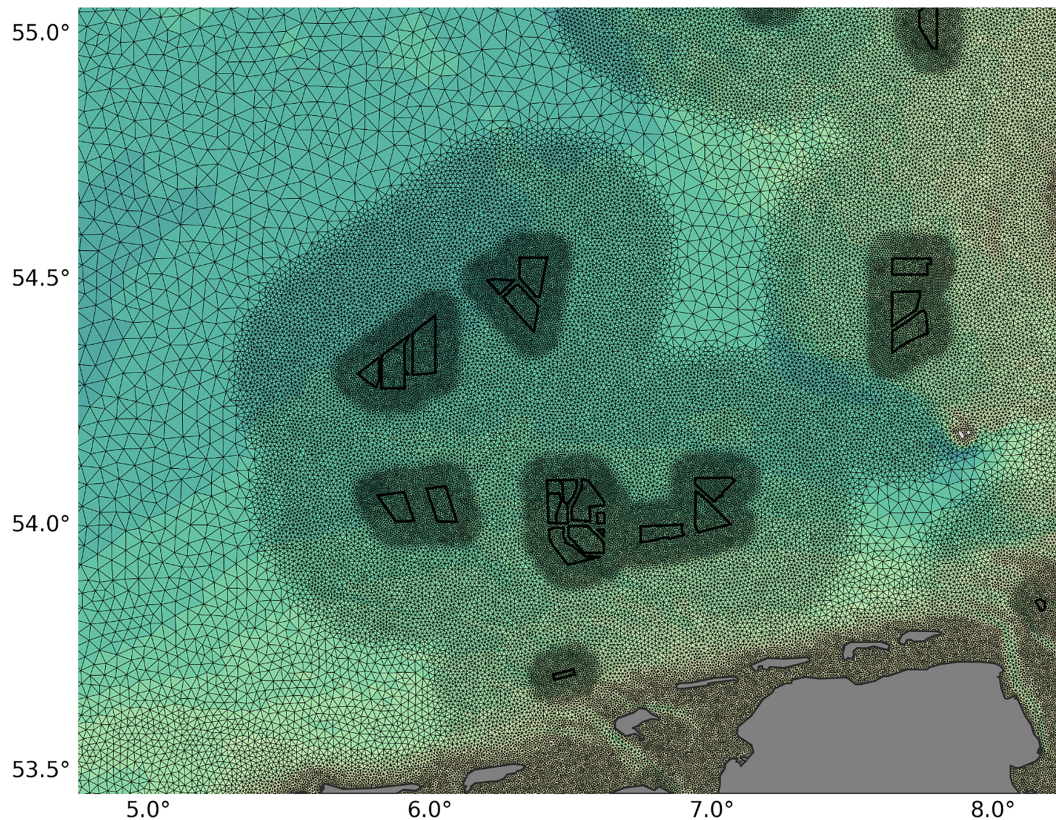


FIGURE 3 | Example of the horizontal grid cell resolution at wind farm polygons (black) for the wind farm simulations.

water inflow due to the tidal signal. Averaging the model data results in attenuated tidal fluctuations and thus lower correlation to the instantaneous values of the observational data. The British coastal area in particular, has strong tidal amplitudes, which could explain the particularly low correlation in region E.

In general, the model proves a sufficient correlation to the in-situ measurements and is able to reproduce seasonal stratification in the southern North Sea (**Figure 4A**). The pattern of the mean potential energy anomaly, which is a gravitational-based measure of stratification strength of the water column (Simpson and Bowers, 1981), shows expected characteristics, such as strong stratification in the deep central North Sea as well as mixing fronts around the shallow Dogger Bank and along the tidal-impacted Wadden Sea area. Thereby, the stratification patterns (exemplarily shown for August, **Figure 4A**) agree well with results of former North Sea studies (Schrum et al., 2003; Holt and Proctor, 2008) considering that magnitude and spatial dimension of summer stratification vary between years (Schrum et al., 2003).

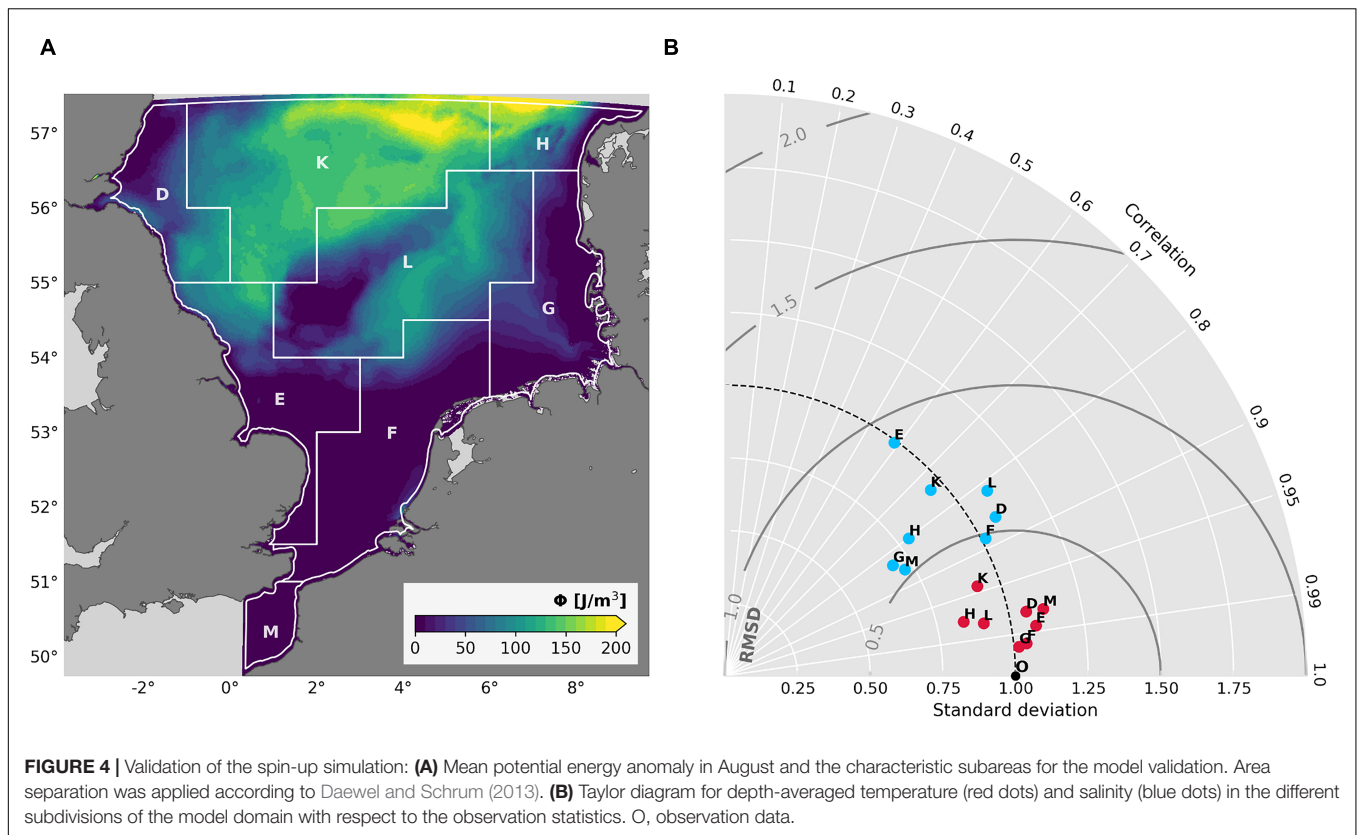
RESULTS AND DISCUSSION

The analysis of wake effects in this manuscript concentrates on general processes related to the transfer of atmospheric momentum into the water column and associated mean changes in horizontal currents and stratification. In order to emphasize

the induced changes during the summer period of 2013, wake effects are shown as the differences between the case of wind farm operation and the case without offshore wind farms in the southern North Sea. In the following, the data is primarily depicted as monthly means, while only a selection of figures is depicted in the analysis. For further insights on the monthly means, see **Supplementary Figures A1–A6**.

Spatial and Temporal Variability in Hydrodynamics

The implemented wake parameterization iteratively generates leeward wind speed reductions at each time step of the simulation. Despite the constant values for the wake deficit and wake length prescribed by the wake model, the resulting wake structures vary individually in size and intensity due to the different sizes of the respective wind farm arrays and due to superposition of neighboring wakes. A snapshot of a strong wind event during the simulation and an example of the associated downstream velocity deficits are depicted in **Figure 5A**. The emerging wakes extend along the present wind field and show comparable patterns to recent satellite SAR wake observations (Djath et al., 2018; Siedersleben et al., 2018). At this, the simulated wakes exhibit relative deficits around 10% in short downstream distances, which agrees with the observations of recent satellite SAR data (**Table 1**). The strongest reductions in wind speed are



observed in densely built areas of the domain, in particular in the German Bight. Although the wake model prescribed a constant deficit of 8%, superposition of neighboring wakes in densely built areas results in even higher velocity deficits of up to 15%, as multiple wind farms affect the wind speed.

As a result of constantly changing wind directions, pronounced wake patterns disappear when averaging over time and shape continuous zones of reduced wind speed around the respective wind farms. Thereby, the German Bight is the most affected region of the model domain, as a large number of current offshore wind farms is located off the Danish, German and Dutch coast. The mean deficits in wind speed of the 5 months of simulation are shown in **Figure 5B**. The deficits were calculated for the absolute values of the wind vectors. **Figure 5B** shows that the mean wind speed deficits primarily adapt to the predominant wind field during the simulation period, which here points into eastward direction. Furthermore, strong wind events, which might differ from the mean wind directions, can influence the shape of the wind speed anomalies particularly in areas of weaker winds (e.g., the British coast). Between May and September, the total absolute mean changes in wind speed range on average around 1–2% relative to the mean undisturbed wind field and can reach even beyond 5% in areas of clustered wind farms, like the Southern Bight or German Bight. Compared to the mean undisturbed wind speeds, which are between 5.0 and 7.0 m/s, the deficits account for an order of magnitude of about 0.1 m/s and range between 0.1 and 0.4 m/s. The order of magnitude is in agreement with recent atmospheric

modeling results of Akhtar et al. (2021), where deficits near the sea surface range around 0.5 m/s during the summer months, considering that Akhtar et al. (2021) applied more influential future wind farm scenarios. Nevertheless, here, with regard to the interpretation of the magnitude of mean wind speed perturbations, the supposed over- and underestimation of the wake dimension due to the prescribed constant wake parameters should be taken into account.

The wake-induced anomalies in wind speed cover large areas around the actual wind farm locations. Consequently, wide areas are affected by reduced shear forcing and reduced vertical momentum fluxes at the sea surface boundary. This becomes particularly apparent looking at a cross section through the strongly influenced southeastern part of the German Bight (**Figure 5C**). Along the cross section the percentage change in wind speed and wind stress is shown relative to the undisturbed values from the scenario without wind farm operation. Both, wind speed and wind stress, exhibit continuous deficits over several tens of kilometers, which do not fully recover in between adjacent wind farms and are particularly strong in the case of superimposed wakes. Thereby, the impact on the wind stress, which is the decisive factor for vertical air-sea exchange, is about twice as high in percentage as for the mean wind speed. Within the wind farm areas deficits slightly recover, since the wake parameterization reduces wind speed only downstream of wind farms. A similar pattern of the continuous influence arising from superimposed wakes was also shown by recent high-resolution atmospheric modeling

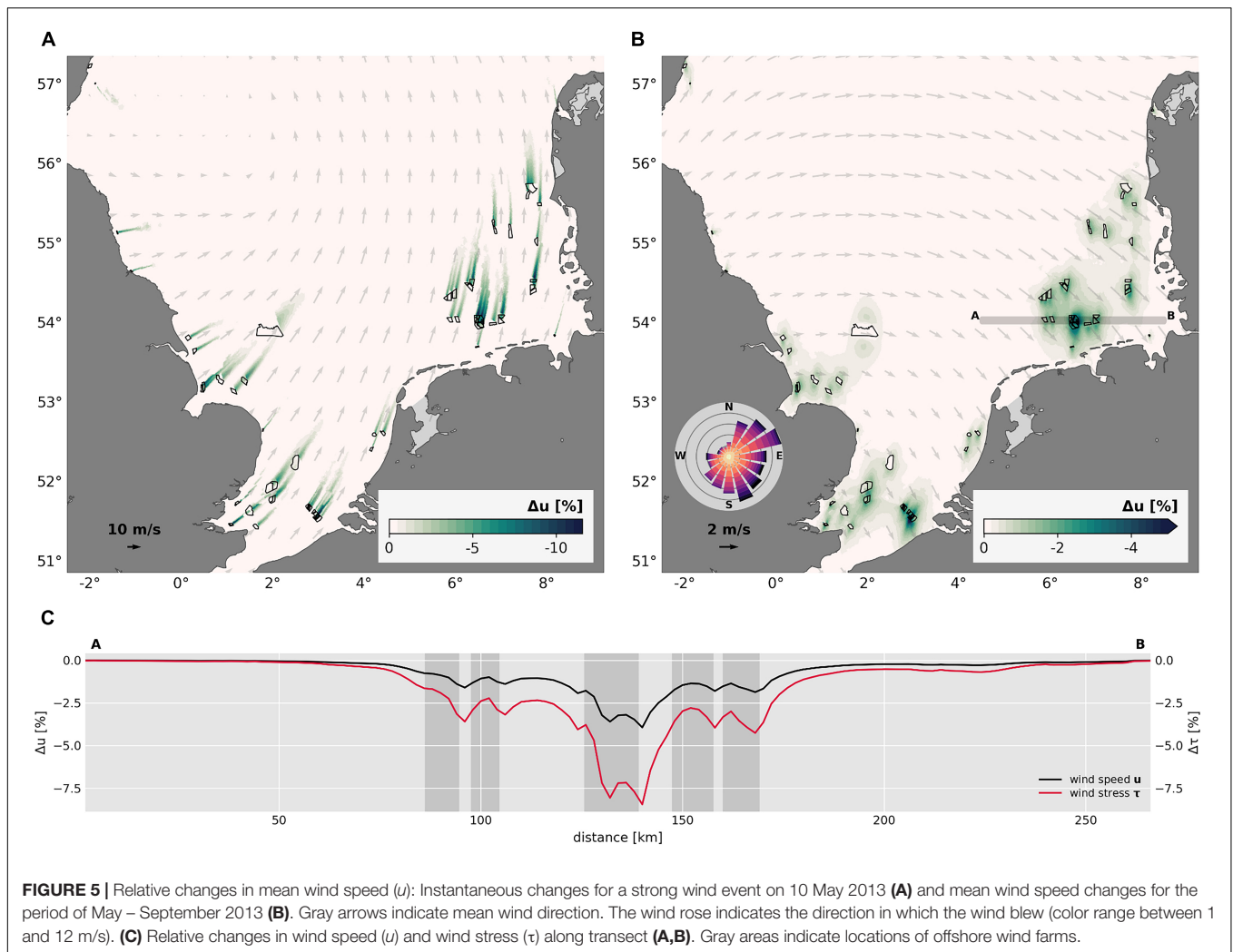


FIGURE 5 | Relative changes in mean wind speed (u): Instantaneous changes for a strong wind event on 10 May 2013 **(A)** and mean wind speed changes for the period of May–September 2013 **(B)**. Gray arrows indicate mean wind direction. The wind rose indicates the direction in which the wind blew (color range between 1 and 12 m/s). **(C)** Relative changes in wind speed (u) and wind stress (τ) along transect **(A,B)**. Gray areas indicate locations of offshore wind farms.

of offshore wind farm effects (Akhtar et al., 2021), where moreover the effect on offshore wind energy production itself was addressed.

In this study, the focus is on the large regions of attenuated wind forcing and related impact on the marine environment. In the shallow southern North Sea, where for the most part wind determines the general circulation (Sündermann and Pohlmann, 2011), the reduction of wind speed and associated wind stress results in substantial changes of the residual circulation. As less shear force is acting on the sea surface in areas around the wind farms, vertical momentum fluxes become attenuated and less momentum is transferred from the atmosphere into the ocean. This entails potential changes in wave formation and horizontal surface velocity but also potentially reduces turbulence within the surface mixed layer and impacts stratification.

Figure 6A depicts the mean changes in horizontal surface velocity after the first month of wind farm operation. The pattern shows expected lateral gradients in the horizontal currents as a result of the reduced wind stress behind offshore wind farms. At this, negative anomalies arise at wind farms in direct correlation

to the downstream wind speed deficits of the predominant mean wind field (**Supplementary Figure A1**). In consideration of the prescribed wake intensity (8% deficit, 30 km length) and the prevailing wind speeds, the deficits in surface current speed range around -0.0025 m/s and exhibit peak values beyond -0.005 m/s. While the order of magnitude agrees with former wind farm studies (Ludewig, 2015), the velocity changes account for up to 5% compared to the mean surface residual velocity in May (about 0.1 m/s). The induced changes are up to 10–25% of the interannual and decadal surface velocity variability, as the mean surface velocity in the southern North Sea ranges between 0.11 and 0.13 m/s (Daewel and Schrum, 2017). Consequently, wake-induced anomalies in surface velocity can be quite substantial, considering that instantaneous changes are generally even stronger, and might affect the horizontal transport and eventually the residual currents in areas of wind farm operation significantly.

In order to evaluate the impact of the wind stress reduction on the vertical structure of the horizontal momentum, mean vertical profiles at the wind farm locations are depicted in **Figures 6B–D**. For the vertical profiles, we used grid points only located within

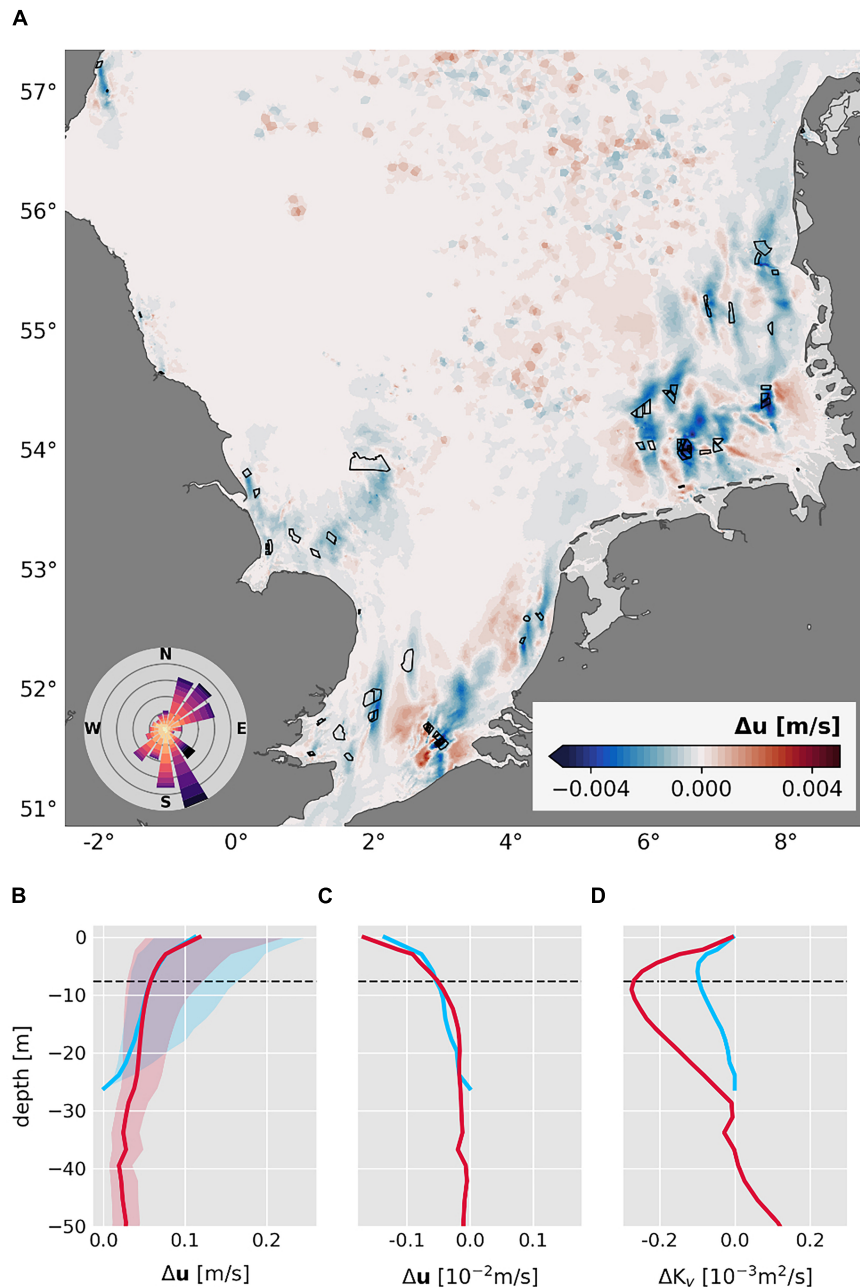


FIGURE 6 | Mean changes in horizontal velocity (u) and mixing rate (K_v). **(A)** Mean changes in horizontal sea surface velocity for daily mean data in the month of May. Black polygons indicate offshore wind farms. The wind rose indicates the direction in which the wind blew (color range between 1 and 12 m/s). Mean vertical profiles for the mean horizontal velocity **(B)**, the mean changes in horizontal velocity **(C)**, and the mean changes in mixing rate **(D)** at wind farms for the month of May 2013. Filled envelopes in panel **(B)** demonstrate the temporal variability during May. Dashed lines indicate location of the mixed layer depth. For the profiles, grid points within 5 km around each wind farm were considered. Profiles are divided into deep ($z \geq 25$ m, red lines) and shallow ($z < 25$ m, blue lines) water depths.

a radius of about 5 km around each wind farm and calculated the average monthly mean changes within the water column. Thereby, shallow ($z < 25$ m) and deep ($z \geq 25$ m) waters were treated separately, as they show different dynamics related to the wind shear.

Figure 6B shows the average horizontal velocity profile at the offshore wind farm locations and the temporal variability during

the month of May. As for the entire southern North Sea, the mean surface velocity at the wind farm locations is about 0.12 m/s, which agrees with the results of Daewel and Schrum (2017). However, the variability of surface velocity itself reaches up to 0.15 m/s within May and is much stronger than the interannual variability. In terms of wake-induced alterations in the horizontal velocity, the wind farm profiles show the strongest changes

occurring at the sea surface boundary, where the impact by the wind speed reduction is most powerful (**Figure 6C**). Here, the maximum values range around -0.002 m/s at the sea surface, which is lower than the maximum changes in **Figure 6A**, since the wind farm locations are less affected by wakes than the areas in downstream direction. The order of magnitude of the changes accounts for about 2% of the mean horizontal velocity profiles at the wind farms as well as of the velocity variability over the month of May (**Figure 6B**). The wake-induced changes in horizontal velocity are more pronounced in deeper waters than in shallow coastal areas. Thereby, deep waters exhibit a strong vertical gradient between the surface and deeper layers, which emphasizes that particularly the wind-driven surface mixed layer is affected by the wind stress deficits. Nevertheless, the impact of the momentum deficit also cascades downward into deeper layers and diminishes toward the sea floor.

In addition to the perturbations in velocity, the attenuation of vertical momentum fluxes results in the associated reduction of turbulent mixing inside the surface mixed layer (**Figure 6D**). Here, as a measure for the mixing rate, we depict the vertical eddy diffusivity K_v . The profiles exhibit a reduced mixing rate over the entire water column. As for the horizontal velocity, the deficits in mixing are more pronounced in deep waters than in well-mixed shallow waters, which is likely favored by influence of the bottom mixed layer in shallow depths. In both cases, the strongest deficits occur near the pycnocline depth. While, in general, the apparent decrease in mean turbulent mixing implies a less turbulent water column, the maximum deficits near the mixed layer depth indicate a shallower surface mixed layer at offshore wind farms. This implies that the wind wakes counteract to the recently identified effects of Kármán vortices and turbulent wakes created by the pile structures of wind turbines, which are responsible for additional mixing in downstream direction (Carpenter et al., 2016; Grashorn and Stanev, 2016; Schultze et al., 2020). Thus, offshore wind farms induce counteracting processes, namely the reduction of horizontal momentum and the generation of turbulence, due to the wind turbine rotors and wind turbine foundations, respectively. However, the counteracting processes emerge on different spatial scales, since the pile effects remain primarily within the wind farm areas (Schultze et al., 2020).

Earlier studies showed the impact of the wind stress reduction on the sea surface elevation at offshore wind farms (Broström, 2008; Paskyabi and Fer, 2012; Ludewig, 2015). The studies demonstrated the formation of up- and downwelling dipoles under constant wind directions, which extend several kilometers around the wind farms. In a realistic model setup, such as we used, however, the wind field changes continuously over time and individual dipole patterns are expected to superimpose or mitigate, depending on the respective wind field. **Figure 7A** depicts the resulting mean surface pattern in August. Indeed, the changes in elevation superimpose into large coherent patterns of positive and negative anomalies, which smoothly merge into each other. Thereby, large-scale dipoles with spatial dimensions of up to hundreds of kilometers emerge in the wind farm regions and in particular in the German Bight area, where superposition and thus amplification of wake effects occurs most frequently. Compared to the mean wind field in August, which points into

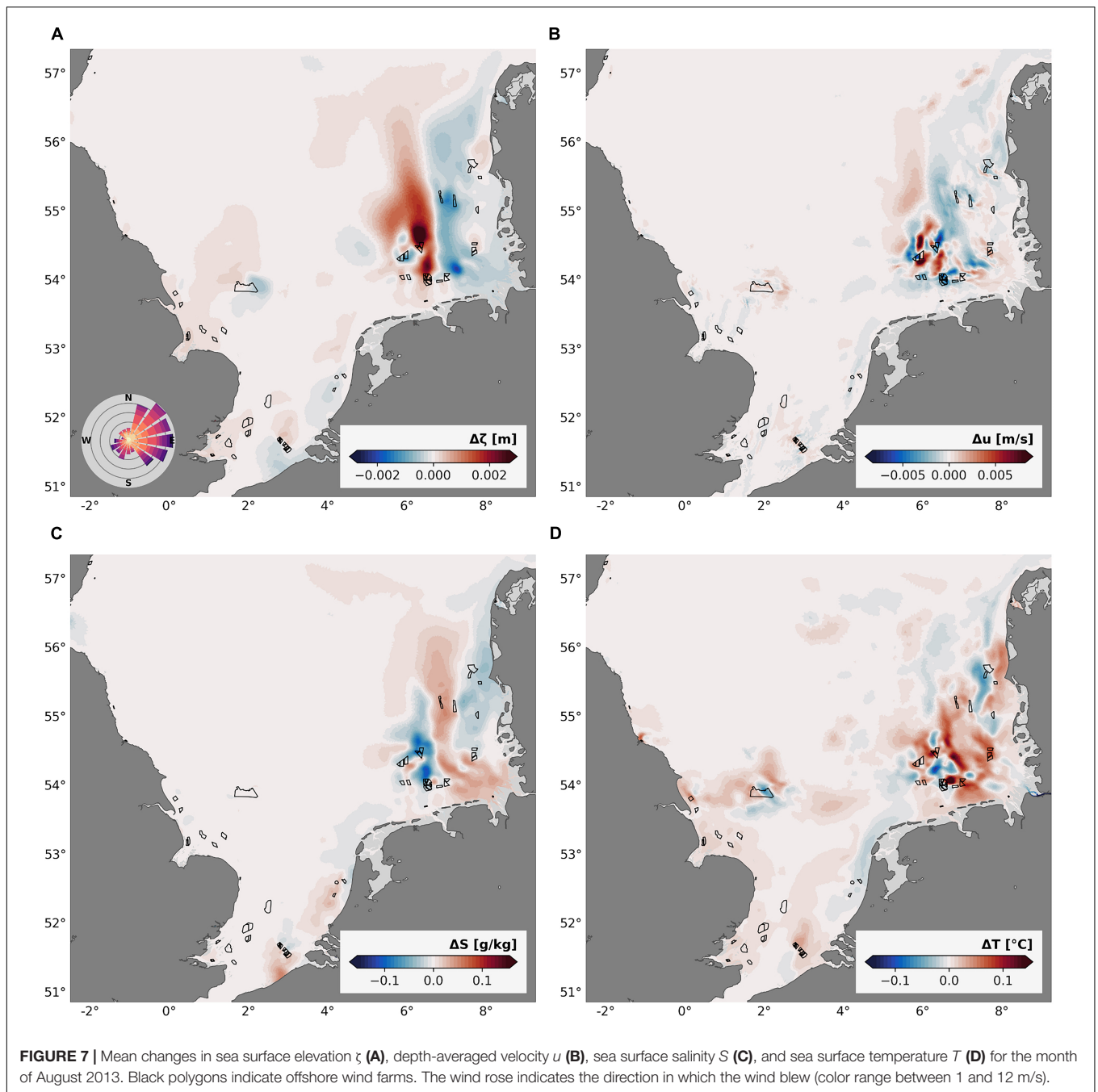
eastward direction (see **Supplementary Figure A1D**), the surface elevation dipoles exhibit their positive amplitude roughly on the windward side of wind farm areas and their negative amplitudes to the lee side. This might indicate a damming effect of wind-driven horizontal flow by the offshore wind farms.

The changes in sea surface elevation show a clear correlation to the anomalies in mean depth-averaged velocity, which resemble the dipole pattern in the German Bight in August (**Figure 7B**). At this, the mean depth-averaged velocity changes range between ± 0.001 and 0.005 m/s and reach on maximum nearly 0.01 m/s. These changes are up to twice as strong as the wind stress related velocity changes at the sea surface in May (**Figure 6A**) and account for up to 10% of the mean horizontal flow velocity in the German Bight. In percentage terms, such perturbations of the flow pattern are quite significant, as they are comparable to the potential changes due to climate change (Mathis and Pohlmann, 2014; Schrum et al., 2016) and may affect the residual currents as well as the gradients of the mean sea surface elevation in the German Bight area.

The relation between horizontal flow perturbations and sea level anomalies becomes more apparent by zooming in on the dipole structure in the German Bight specifically (**Figures 8A,B**). The figures illustrate the vector field of the mean depth-averaged horizontal velocity changes, in addition to the mean sea level and velocity changes in August. **Figure 8A** shows that the positive and negative mean sea level anomalies are clearly related to attenuated or enhanced horizontal flow velocities. At this, the sea level sinks in regions of increased flow velocity, while the sea level rises due to damming in regions of reduced flow velocities. This applies specifically to the large-scale dipole pattern. In the center of the German Bight, where the perturbations are most pronounced, the mean changes in sea surface elevation reach orders of magnitude of around ± 2 mm and result in spatial gradients of up to 4 mm over a distance of several tens of kilometers. These magnitudes are weak, compared to the local tidal variability and account for about 1–10% of the mean surface elevation variability in the German Bight, which varies by around 0.05 – 0.10 m over the respective spatial scales. However, the occurrence of such strong sea level gradients can in turn affect the geostrophic balance in the German Bight. Considering the apparent sea level differences of 2 – 4 mm, the resulting horizontal pressure gradients would affect the predominant circulation pattern by an order of magnitude of about 10^{-3} m/s, which is similar to the wake-related changes in horizontal velocity. In fact, these secondary induced perturbations of the geostrophic flow can be seen in the changes of the mean horizontal flow pattern (**Figure 8B**), where eddy-like structures with associated magnitudes of ± 0.006 m/s emerge in the center of the German Bight. However, these eddy-like structures might also be the result of mean depth-averaged circulation changes, which in turn favor the emergence of up- and downwelling cells.

Impact on Stratification

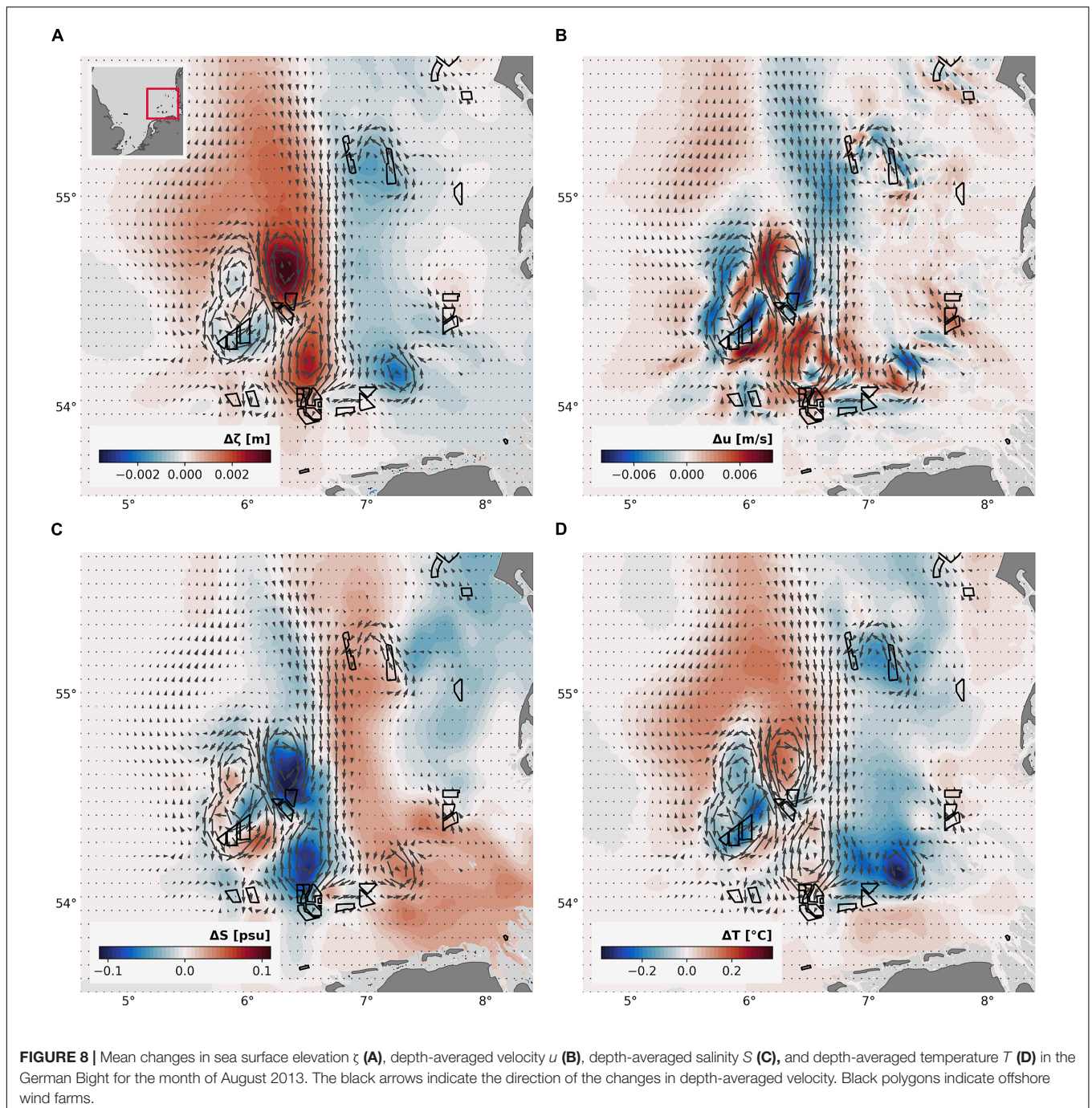
The alterations of the sea level and the horizontal transport suggest changes in the lateral and vertical density fields. In a previous modelling study, Ludewig (2015) observed the occurrence of vertical upward and downward currents at offshore



wind farms, which were inversely correlated to the displacements of the sea surface dipole. With sufficient temperature and salinity stratification, the induced vertical flow is expected to result on the one hand in advection of colder and saltier toward the surface and on the other hand in the downward advection of warmer and fresher water within the dipole area. Consequently, the changes in sea surface elevation are accompanied by changes in the vertical temperature and salinity distribution.

Figure 7C depicts the mean sea surface salinity changes in August, where the magnitudes on average range between ± 0.05 g/kg. In the Southern Bight, the presumed

correlation between the surface elevation anomalies and the surface salinity changes becomes most apparent. Positive and negative changes in surface salinity agree with the locations of the sea level perturbations and extend several tens of kilometers around the wind farms. At this, saltier surface water occurs in regions of lowered sea level, while surface salinity decreases in regions of elevated sea surface height. In the German Bight however, the large-scale pattern is more complex and does not clearly resemble the specific pattern of the mean sea surface elevation. Here, mean surface salinity decreases within the center of the large sea level dipole and along the shallow Jutland coast.



Between the two negative salinity anomalies, salinity increases and the positive anomaly spreads along the fresh water plume from the Elbe estuary.

The mean surface temperature changes show much less agreement to the anomalies in sea surface height (Figure 7D). Instead, it appears that the surface temperature primarily increases in the vicinity of offshore wind farms, which confirms earlier simulations by Ludwig (2015). The apparent surface heating presumably results from the reduction in mixing and is hence directly related to the large-scale wind speed reduction

in the atmospheric forcing. Over time, advection and lateral transport likely cause the temperature anomalies to spread over a large scale in the affected areas. Therefore, coherent patterns of increasing mean sea surface temperature are present in areas of wind farm development. At this, mean changes in sea surface temperature are on average around $\pm 0.02\text{--}0.05^\circ\text{C}$, whereas changes in the German Bight reach even beyond 0.1°C . The large-scale surface heating of up to 0.1°C imitates the effects of climate change, in which an increase in sea surface temperature is also to be expected as a result of the warming

of the earth's atmosphere (Schrum et al., 2016). However, the wake-related changes are about one order of magnitude smaller than the average perturbations due to climatic changes (Schrum et al., 2016). Furthermore, the changes account for a maximum of 10% of the annual and interannual variability of surface temperature in the southern North Sea, which are at least 1.0–1.5°C (Daewel and Schrum, 2017).

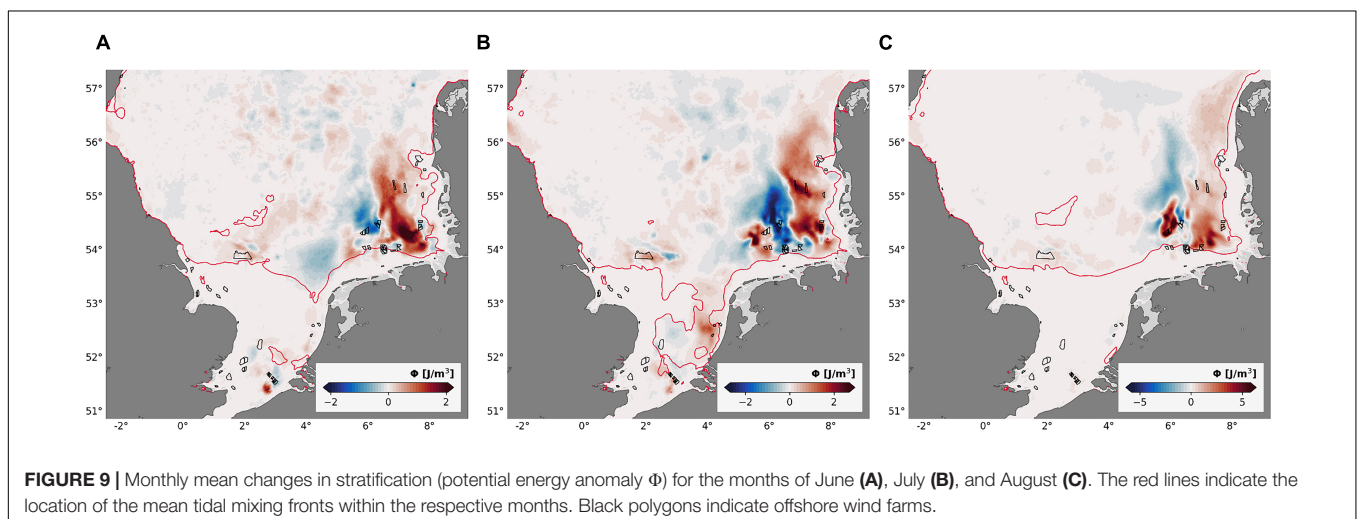
Despite the deviations in the surface anomalies, the mean depth-averaged changes in temperature and salinity confirm the assumed correlation between the sea level changes and the changes in the density field in the German Bight (Figures 8C,D). The figures show again the vector plot of the mean depth-averaged horizontal velocity changes, in addition to the mean depth-averaged changes in temperature and salinity in August. For the depth-averaged data, salinity and particularly temperature exhibit stronger changes than for the sea surface with up to ± 0.1 g/kg and $\pm 0.3^\circ\text{C}$, respectively. At this, the anomalies show a clear agreement with the vector plot of the depth-averaged velocity changes and with the mean sea level anomalies (see Figure 8A). In particular, the mean temperature changes strongly resemble the sea level alterations (Figure 8D). Nevertheless, for both, temperature and salinity, a notable amplification of the changes occurs due to the eddy-like structures in the horizontal flow anomalies and hence due to the amplified changes in sea level. These changes agree with the presumed correlation between the sea level anomalies and changes in the vertical density distribution and thus with the results of Ludewig (2015). However, associated changes in the mean vertical velocity field are not detectable.

The identified changes in temperature and salinity suggest an impact on the seasonal summer stratification in the southern North Sea. In order to investigate the impact, we calculated the potential energy anomaly as a measure for the stratification strength. Figure 9 depicts monthly mean changes in potential energy anomaly and the position of the tidal mixing fronts for the months of June to August 2013. For the tidal mixing fronts, the transition from mixed to stratified waters was defined by a surface-to-bottom temperature difference of 0.5°C , similar to

Skogen et al. (2011). Alterations in the potential energy anomaly can be seen in all summer months, which occur most strongly in the German Bight (Figure 9). The coherent changes show again large dipole patterns, which are related to the anomalies in sea surface elevation and consequently to temperature and salinity anomalies. What is notable here is that the changes in potential energy anomaly primarily occur in stratified waters. The apparent sensitivity of the wake effects to stratification was already seen in the influence on the mixing (Figure 6C), where the impact was much stronger in deeper and hence likely stratified waters.

The comparison of the monthly means shows a seasonal trend in the intensity of the impact on the potential energy anomaly (Figure 9). Initially, as the summer stratification evolves (Figures 9A,B), the patterns have a strong correlation to the spatial changes in the sea surface temperature and salinity (see Supplementary Figures A4, A5). At this, the changes in potential energy anomaly range on average around $\pm 2 \text{ Jm}^{-3}$. However, during the decline of stratification toward autumn (Figure 9C), strong magnitudes of beyond $\pm 6 \text{ Jm}^{-3}$ arise in the German Bight, which account for about 10–20% of the actual mean stratification strength (Figure 4A). Thereby, the strongest changes in the potential energy anomaly arise in the center of the surface elevation dipole and in regions of declining stratification toward the Frisian coast. While the alterations within the dipole are expected to result from the dipole-related processes, changes near the tidal mixing fronts are presumably associated to the reduction of wind stress and hence of the reduction of mixing in regions of declining stratification. As the mixing reduces, the wake effects sustain stratification in areas of wind speed reduction and thus lead to the amplification of stratification.

Figure 10 depicts the vertical profiles at wind farms, similar to Figures 6B–D, for the mean mixing rate K_v for the months of June to September. The vertical profiles support the assumption about the impact of the mixing alterations on the development of the summer stratification. As seen for the month of May (Figure 6B), the mixing at wind farms generally decreases in all months of the simulation as a result of the wind speed reduction. Thereby, the most pronounced changes occur around



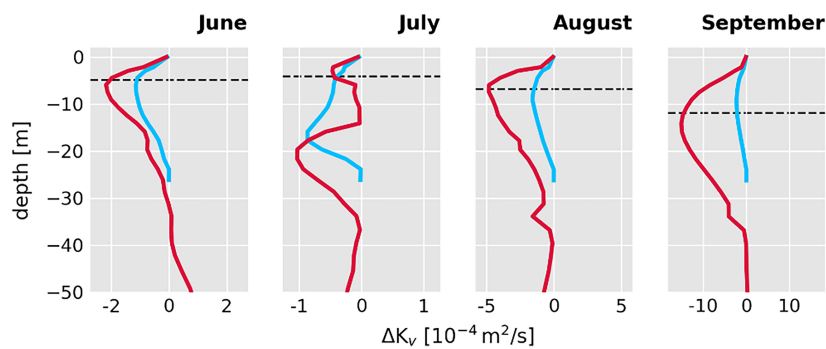


FIGURE 10 | Monthly mean profiles in mixing rate for the period of June to September. The dashed lines indicate the location of the mixed layer depth. For the profiles, grid points within 5 km around each wind farm were considered. Profiles are divided into deep ($z \geq 25$ m, red lines) and shallow ($z < 25$ m, blue lines) water depths.

the mixed layer depth and in deep waters. In comparison of the different months, however, it is notable that the strongest reductions in mixing occur during the formation (May and June) and the breakdown (August and September) of the summer stratification. Especially toward autumn, the changes are up to five to ten times stronger than in the other months. At this, the maximum deficits generally occur near the mixed layer depth, which emphasizes the enhancement of stratification and the shallowing of the surface mixed layer at offshore wind farms due to atmospheric wake effects.

CONCLUSION

As wind turbines extract kinetic energy from the wind field, atmospheric wakes result on the leeward side of offshore wind farms and affect the far field wind speed near the sea surface boundary. However, wind farm wakes and their impact on the hydrodynamic system represent a multivariate system, which is highly sensitive to external influences in atmosphere and ocean. In this study, we developed an empirical approach to describe the wake-related wind speed deficits in a hydrodynamic model. With this, we provided first insights about the interference of single wake effects due to the recent offshore wind energy production and resulting larger-scale disturbances in hydro- and thermodynamics in the southern and central North Sea. The implemented wake model generated wakes with constant dimensions, which, in terms of the different wind farm properties (e.g., the number of turbines and turbine density) or the changing atmospheric conditions, lead to over- and underestimation of the actual wake dimensions. Although the actual wake dimensions might vary in reality, the basic impact of wind farms, namely the downstream reduction in wind speed, is sufficiently considered to investigate the general consequences of wind speed deficits due to offshore wind farms. However, a more specific and realistic formulation will be important for more detailed future studies, since the wake dimensions determine the intensity of the associated impacts.

Over time, the extraction of energy by offshore wind farms results in extensive areas of reduced wind speed and

subsequently the decrease of the shear-driven forcing at the sea surface boundary. As this reduces the momentum transfer from the atmosphere into the ocean, horizontal velocities and turbulent mixing initially decrease several tens of kilometers around offshore wind farms. Thereby the induced perturbations imply significant changes for the residual currents in the respective areas. Furthermore, convergence and divergence of water masses lead to the formation of sea surface elevation dipoles, which over time merge into large coherent structures. As shown here, these large-scale anomalies in the sea surface elevation are one of the main drivers of wake-related processes in the ocean. In addition to the general reduction of turbulent mixing, the large-scale sea level alterations trigger lateral and vertical changes in the temperature and salinity distribution and affect the hydrodynamics in areas covered by offshore wind farms. However, the magnitude of these changes is rather small compared to the long-term variability of temperature and salinity and can hardly be distinguished from the interannual variability. A severe overall impact by the wake effects on the ocean's thermodynamic properties is thus not expected but rather large-scale structural change in the stratification strength and unanticipated mesoscale spatial variability in the mean current field. Nevertheless, further investigations are necessary to assess possible feedback on the air-sea exchange and thus potential impact on the regional atmospheric conditions, since surface heating along with the reduction in turbulent mixing influences the upward heat and momentum fluxes from the ocean into the atmosphere.

In this study, the structural changes in stratification become noticeable in a couple of ways. Firstly, we observed large dipole-related changes in the potential energy anomaly, as the geostrophic and baroclinic changes alter the temperature and salinity distribution. Secondly, the reduction of mixing at offshore wind farms results in the enhancement of the stratification strength, in particular, during the decline of the summer stratification. While the structural changes in stratification are minor in shallow mixed waters, the pronounced alterations in stratified waters can translate to the mixed layer depth, which likely increases or decreases depending on the

respective stratification changes. This, in turn, might be crucial for marine ecosystem processes (Sverdrup, 1953). During the stratified summer months, the mixed layer depth is acting as barrier for nutrients and phytoplankton and plays a major role for the ecosystem dynamics. Therefore, induced fluctuations of the mixed layer depth can entail the intrusion of nutrients from the pycnocline into the surface mixed layer or the spreading of the nutrient-poor surface layer, respectively. The alterations in the nutrient availability, in turn, might affect local primary production and the nutrient balance. Thus, further studies are required to elucidate the impact on marine ecosystems and organisms in the North Sea, with regard to current and future wind farm scenarios.

Although the simulation was limited by the summer season of the year 2013, this study provides already important knowledge about the magnitude of implications of extensive offshore wind farming in the marine environment. Ultimately, the results showed that, in addition to the initial large-scale reduction in dynamics, wake effects cause internal processes, which affect the lateral and vertical transport of heat and salt even far beyond the associated wind farms. At this, changing wind directions inhibit severe local impact, as the varying internal processes mitigate each other. For the current state of wind energy production in the southern North Sea, the impact by the offshore wind farms entails structural changes in stratification strength and perturbations of the residual currents. Thereby, the cascading hydrodynamic processes particularly affect areas of clustered wind farms, like the German Bight. However, future wind energy development includes large installations in the Southern Bight and especially near the Dogger Bank, which will increase number of wind farms and hence possibly the impact in those areas (see Akhtar et al., 2021). Therefore, further investigations and improvements of the wake model are crucial, in order to assess the actual impact of future wind farm development in the North Sea environment. Especially since stratification anomalies entail perturbations of the pycnocline, assessment of potential biogeochemical impacts is of major interest.

DATA AVAILABILITY STATEMENT

The original contributions presented in the study are included in the article/**Supplementary Material**, further inquiries can be directed to the corresponding author.

REFERENCES

- Akhtar, N., Geyer, B., Rockel, B., Sommer, P. S., and Schrum, C. (2021). Accelerating deployment of offshore wind energy alter wind climate and reduce future power generation potentials. *Sci. Rep.* 11:11826. doi: 10.1038/s41598-021-91283-3
- Broström, G. (2008). On the influence of large wind farms on the upper ocean circulation. *J. Mar. Syst.* 74, 585–591. doi: 10.1016/j.jmarsys.2008.05.001
- Cañadillas, B., Foreman, R., Barth, V., Siedersleben, S., Lampert, A., and Platis, A. (2020). Offshore wind farm wake recovery: Airborne measurements and its representation in engineering models. *Wind Energy* 23, 1249–1265. doi: 10.1002/we.2484

AUTHOR CONTRIBUTIONS

NC generated the data set, performed the data analysis, and wrote the manuscript. BD performed statistical analysis and contributed to the parameterization section of the manuscript. UD and CS provided essential background knowledge and advised to the study. CS initiated the idea of the study. All authors contributed to conception and design of the study, manuscript revision, read, and approved the submitted version.

ACKNOWLEDGMENTS

We would like to acknowledge the contribution by Johannes Schulz-Stellenfleth to the development of the wake parameterization. We would like to thank Jeffrey R. Carpenter and Thomas Pohlmann for helpful advice and appreciate the help by Johannes Pein regarding the SCHISM model. We appreciate the use of the mHM river discharge data generated by Rohini Kumar and Oldrich Rakovec and mapped onto the SCHISM grid by Stefan Hagemann. The data originate from a collaborative effort led by Sabine Attinger (Umweltforschungszentrum Leipzig) and Corinna Schrum (Helmholtz-Zentrum Hereon) that was supported by funding from the Initiative and Networking Fund of the Helmholtz Association through the project “Advanced Earth System Modelling Capacity (ESM).” This project is a contribution to theme “C3: Sustainable Adaption Scenarios for Coastal Systems” of the Cluster of Excellence EXC 2037 “CLICCS – Climate, Climatic Change, and Society” – Project Number: 390683824 funded by the Deutsche Forschungsgemeinschaft (DFG, German Research Foundation) under Germany’s Excellence Strategy and to the CLICCS-HGF networking project funded by the Helmholtz-Gemeinschaft Deutscher Forschungszentren (HGF).

SUPPLEMENTARY MATERIAL

The Supplementary Material for this article can be found online at: <https://www.frontiersin.org/articles/10.3389/fmars.2022.818501/full#supplementary-material>

- Carpenter, J. R., Merckelbach, L., Callies, U., Clark, S., Gaslikova, L., and Baschek, B. (2016). Potential Impacts of Offshore Wind Farms on North Sea Stratification. *PLoS One* 11:e0160830. doi: 10.1371/journal.pone.0160830
- Christiansen, M. B., and Hasager, C. B. (2005). Wake effects of large offshore wind farms identified from satellite SAR. *Remote Sens. Env.* 98, 251–268. doi: 10.1016/j.rse.2005.07.009
- Christiansen, M. B., and Hasager, C. B. (2006). Using airborne and satellite SAR for wake mapping offshore. *Wind Energy* 9, 437–455. doi: 10.1002/we.196
- Cornes, R. C., van der Schrier, G., van den Besselaar, E. J. M., and Jones, P. D. (2018). An Ensemble Version of the E-OBS Temperature and Precipitation Data Sets. *J. Geophys. Res. Atmos.* 123, 9391–9409. doi: 10.1029/2017JD028200

- Daewel, U., and Schrum, C. (2013). Simulating long-term dynamics of the coupled North Sea and Baltic Sea ecosystem with ECOSMO II: Model description and validation. *J. Mar. Syst.* 119–120, 30–49. doi: 10.1016/j.jmarsys.2013.03.008
- Daewel, U., and Schrum, C. (2017). Low-frequency variability in North Sea and Baltic Sea identified through simulations with the 3-D coupled physical-biogeochemical model ECOSMO. *Earth Syst. Dynam.* 8, 801–815. doi: 10.5194/esd-8-801-2017
- Djath, B., and Schulz-Stellenfleth, J. (2019). Wind speed deficits downstream offshore wind parks? A new automatised estimation technique based on satellite synthetic aperture radar data. *Meteorologische Zeitschrift* 28, 499–515. doi: 10.1127/metz/2019/0992
- Djath, B., Schulz-Stellenfleth, J., and Cañadillas, B. (2018). Impact of atmospheric stability on X-band and C-band synthetic aperture radar imagery of offshore windpark wakes. *J. Renew. Sust. Energy* 10:43301. doi: 10.1063/1.5020437
- Emeis, S. (2010). A simple analytical wind park model considering atmospheric stability. *Wind Energ.* 13, 459–469. doi: 10.1002/we.367
- Emeis, S., and Frandsen, S. (1993). Reduction of horizontal wind speed in a boundary layer with obstacles. *Bound. Layer Meteorol.* 64, 297–305. doi: 10.1007/BF00708968
- Emeis, S., Siedersleben, S., Lampert, A., Platis, A., Bange, J., and Djath, B. (2016). Exploring the wakes of large offshore wind farms. *J. Phys.* 753:92014. doi: 10.1088/1742-6596/753/9/092014
- Fitch, A. C., Lundquist, J. K., and Olson, J. B. (2013). Mesoscale Influences of Wind Farms throughout a Diurnal Cycle. *Monthly Weather Rev.* 141, 2173–2198. doi: 10.1175/MWR-D-12-00185.1
- Fitch, A. C., Olson, J. B., Lundquist, J. K., Dudhia, J., Gupta, A. K., and Michalakes, J. (2012). Local and Mesoscale Impacts of Wind Farms as Parameterized in a Mesoscale NWP Model. *Monthly Weather Rev.* 140, 3017–3038. doi: 10.1175/MWR-D-11-00352.1
- Frandsen, S. (1992). On the wind speed reduction in the center of large clusters of wind turbines. *J. Wind Eng. Indust. Aerodynam.* 39, 251–265. doi: 10.1016/0167-6105(92)90551-K
- Frandsen, S., Barthelmie, R., Pryor, S., Rathmann, O., Larsen, S., and Højstrup, J. (2006). Analytical modelling of wind speed deficit in large offshore wind farms. *Wind Energ.* 9, 39–53. doi: 10.1002/we.189
- Grashorn, S., and Stanev, E. V. (2016). Kármán vortex and turbulent wake generation by wind park piles. *Ocean Dyn.* 66, 1543–1557. doi: 10.1007/s10236-016-0995-2
- Hasager, C. B., Vincent, P., Badger, J., Badger, M., Di Bella, A., and Peña, A. (2015). Using Satellite SAR to Characterize the Wind Flow around Offshore Wind Farms. *Energies* 8, 5413–5439. doi: 10.3390/en8065413
- Hersbach, H., Stoffelen, A., and Haan, S. (2007). An improved C-band scatterometer ocean geophysical model function: CMOD5. *J. Geophys. Res.* 112:3743. doi: 10.1029/2006JC003743
- Holt, J., and Proctor, R. (2008). The seasonal circulation and volume transport on the northwest European continental shelf: A fine-resolution model study. *J. Geophys. Res.* 113:4034. doi: 10.1029/2006JC004034
- HZG (2017). *coastDat-3_COSMO-CLM_ERAI*. World Data Center for Climate (WDCC) at DKRZ. Available online at: http://cera-www.dkrz.de/WDCC/ui/Compact.jsp?acronym=coastDat-3_COSMO-CLM_ERAI (accessed date 2017-11-02)
- Jensen, N. O. (1983). *A note on wind generator interaction*. Roskilde: Risø National Laboratory.
- Kantha, L., and Clayson, C. A. (2015). “BOUNDARY LAYER (ATMOSPHERIC) AND AIR POLLUTION | Ocean Mixed Layer,” in *Encyclopedia of Atmospheric Sciences (Second Edition)*, Vol. 2015, eds G. R. North, J. Pyle, and F. Zhang (Oxford: Academic Press), 290–298.
- Kumar, R., Samaniego, L., and Attinger, S. (2013). Implications of distributed hydrologic model parameterization on water fluxes at multiple scales and locations. *Water Resour. Res.* 49, 360–379. doi: 10.1029/2012WR012195
- Li, X., and Lehner, S. (2013). Observation of TerraSAR-X for Studies on Offshore Wind Turbine Wake in Near and Far Fields. *IEEE J. Sel. Top. Appl. Earth Observ. Rem. Sens.* 6, 1757–1768. doi: 10.1109/JSTARS.2013.2263577
- Lissaman, P. B. S. (1979). Energy Effectiveness of Arbitrary Arrays of Wind Turbines. *J. Energy* 3, 323–328. doi: 10.2514/3.62441
- Ludewig, E. (2015). *On the Effect of Offshore Wind Farms on the Atmosphere and Ocean Dynamics*. Cham: Springer International Publishing.
- Mathis, M., and Pohlmann, T. (2014). Projection of physical conditions in the North Sea for the 21st century. *Clim. Res.* 61, 1–17. doi: 10.3354/cr01232
- Otto, L., Zimmerman, J. T. F., Furnes, G. K., Mork, M., Saetre, R., and Becker, G. (1990). Review of the physical oceanography of the North Sea. *Neth. J. Sea Res.* 26, 161–238. doi: 10.1016/0077-7579(90)90091-T
- Paskyabi, M. B. (2015). “Offshore Wind Farm Wake Effect on Stratification and Coastal Upwelling,” in *12th Deep Sea Offshore Wind R&D Conference, EERA DeepWind2015*, Vol. 80, (Trondheim), 131–140. doi: 10.1016/j.egypro.2015.11.415
- Paskyabi, M. B., and Fer, I. (2012). “Upper Ocean Response to Large Wind Farm Effect in the Presence of Surface Gravity Waves,” in *Selected papers from Deep Sea Offshore Wind R&D Conference*, Vol. 24, (Trondheim), 245–254. doi: 10.1016/j.egypro.2012.06.106
- Peña, A., and Rathmann, O. (2014). Atmospheric stability-dependent infinite wind-farm models and the wake-decay coefficient. *Wind Energ.* 17, 1269–1285. doi: 10.1002/we.1632
- Platis, A., Bange, J., Bärfuss, K., Cañadillas, B., Hundhausen, M., and Djath, B. (2020). Long-range modifications of the wind field by offshore wind parks? Results of the project WIPAFF. *Meteorologische Zeitschrift* 29, 355–376. doi: 10.1127/metz/2020/1023
- Platis, A., Hundhausen, M., Mauz, M., Siedersleben, S., Lampert, A., and Bärfuss, K. (2021). Evaluation of a simple analytical model for offshore wind farm wake recovery by in situ data and Weather Research and Forecasting simulations. *Wind Energ.* 24, 212–228. doi: 10.1002/we.2568
- Platis, A., Siedersleben, S. K., Bange, J., Lampert, A., Bärfuss, K., and Hankers, R. (2018). First in situ evidence of wakes in the far field behind offshore wind farms. *Sci. Rep.* 8:2163. doi: 10.1038/s41598-018-20389-y
- Samaniego, L., Kumar, R., and Attinger, S. (2010). Multiscale parameter regionalization of a grid-based hydrologic model at the mesoscale. *Water Resour. Res.* 46:7327. doi: 10.1029/2008WR007327
- Schrum, C. (2017). Regional Climate Modeling and Air-Sea Coupling. *Oxford Res. Encyclop. Clim. Sci.* 2017:3. doi: 10.1093/acrefore/9780190228620.013.3
- Schrum, C., and Backhaus, J. O. (1999). Sensitivity of atmosphere-ocean heat exchange and heat content in the North Sea and the Baltic Sea. *Tellus A* 51, 526–549. doi: 10.1034/j.1600-0870.1992.00006.x
- Schrum, C., Lowe, J., Meier, H. E. M., Grabemann, I., Holt, J., and Mathis, M. (2016). “Projected Change - North Sea,” in *North Sea Region Climate Change Assessment*, eds M. Quante and F. Colijn (Cham: Springer International Publishing), 175–217.
- Schrum, C., Siegmund, F., and St. John, M. (2003). Decadal variations in the stratification and circulation patterns of the North Sea; are the 90’s unusual? *ICES Mar. Sci. Symp.* 219, 121–131.
- Schultze, L. K. P., Merckelbach, L. M., Horstmann, J., Raasch, S., and Carpenter, J. R. (2020). Increased Mixing and Turbulence in the Wake of Offshore Wind Farm Foundations. *J. Geophys. Res. Oceans* 125:e2019JC015858. doi: 10.1029/2019JC015858
- Shapiro, C. R., Starke, G. M., Meneveau, C., and Gayme, D. F. (2019). A Wake Modeling Paradigm for Wind Farm Design and Control. *Energies* 12:12152956. doi: 10.3390/en12152956
- Siedersleben, S. K., Platis, A., Lundquist, J. K., Lampert, A., Bärfuss, K., and Cañadillas, B. (2018). Evaluation of a Wind Farm Parameterization for Mesoscale Atmospheric Flow Models with Aircraft Measurements. *Meteorologische Zeitschrift* 27, 401–415. doi: 10.1127/metz/2018/0900
- Simpson, J. H., and Bowers, D. (1981). Models of stratification and frontal movement in shelf seas. Deep Sea Research Part A. *Oceanogr. Res. Papers* 28, 727–738. doi: 10.1016/0198-0149(81)90132-1
- Skogen, M. D., Drinkwater, K., Hjøllø, S. S., and Schrum, C. (2011). North Sea sensitivity to atmospheric forcing. *J. Mar. Syst.* 85, 106–114. doi: 10.1016/j.jmarsys.2010.12.008
- Stündermann, J., and Pohlmann, T. (2011). A brief analysis of North Sea physics. *Oceanologia* 53, 663–689. doi: 10.5697/oc.53-3.663
- Sverdrup, H. U. (1953). On Conditions for the Vernal Blooming of Phytoplankton. *ICES J. Mar. Sci.* 18, 287–295. doi: 10.1093/icesjms/18.3.287

- Taguchi, E., Stammer, D., and Zahel, W. (2014). Inferring deep ocean tidal energy dissipation from the global high-resolution data-assimilative HAMTIDE model. *J. Geophys. Res. Oceans* 119, 4573–4592. doi: 10.1002/2013JC009766
- Taylor, K. E. (2001). Summarizing multiple aspects of model performance in a single diagram. *J. Geophys. Res.* 106, 7183–7192. doi: 10.1029/2000JD900719
- Volker, P. J. H., Badger, J., Hahmann, A. N., and Ott, S. (2015). The Explicit Wake Parametrisation V1.0: a wind farm parametrisation in the mesoscale model WRF. *Geosci. Mod. Dev.* 8, 3715–3731. doi: 10.5194/gmd-8-3715-2015
- Zhang, Y. J., Ateljevich, E., Yu, H.-C., Wu, C. H., and Yu, J. C. (2015). A new vertical coordinate system for a 3D unstructured-grid model. *Ocean Modelling* 85, 16–31. doi: 10.1016/j.ocemod.2014.10.003
- Zhang, Y. J., Stanev, E. V., and Grashorn, S. (2016a). Unstructured-grid model for the North Sea and Baltic Sea: Validation against observations. *Ocean Model.* 97, 91–108. doi: 10.1016/j.ocemod.2015.11.009
- Zhang, Y. J., Ye, F., Stanev, E. V., and Grashorn, S. (2016b). Seamless cross-scale modeling with SCHISM. *Ocean Model.* 102, 64–81. doi: 10.1016/j.ocemod.2016.05.002

Conflict of Interest: The authors declare that the research was conducted in the absence of any commercial or financial relationships that could be construed as a potential conflict of interest.

Publisher's Note: All claims expressed in this article are solely those of the authors and do not necessarily represent those of their affiliated organizations, or those of the publisher, the editors and the reviewers. Any product that may be evaluated in this article, or claim that may be made by its manufacturer, is not guaranteed or endorsed by the publisher.

Copyright © 2022 Christiansen, Daewel, Djath and Schrum. This is an open-access article distributed under the terms of the Creative Commons Attribution License (CC BY). The use, distribution or reproduction in other forums is permitted, provided the original author(s) and the copyright owner(s) are credited and that the original publication in this journal is cited, in accordance with accepted academic practice. No use, distribution or reproduction is permitted which does not comply with these terms.

Supplementary Figures

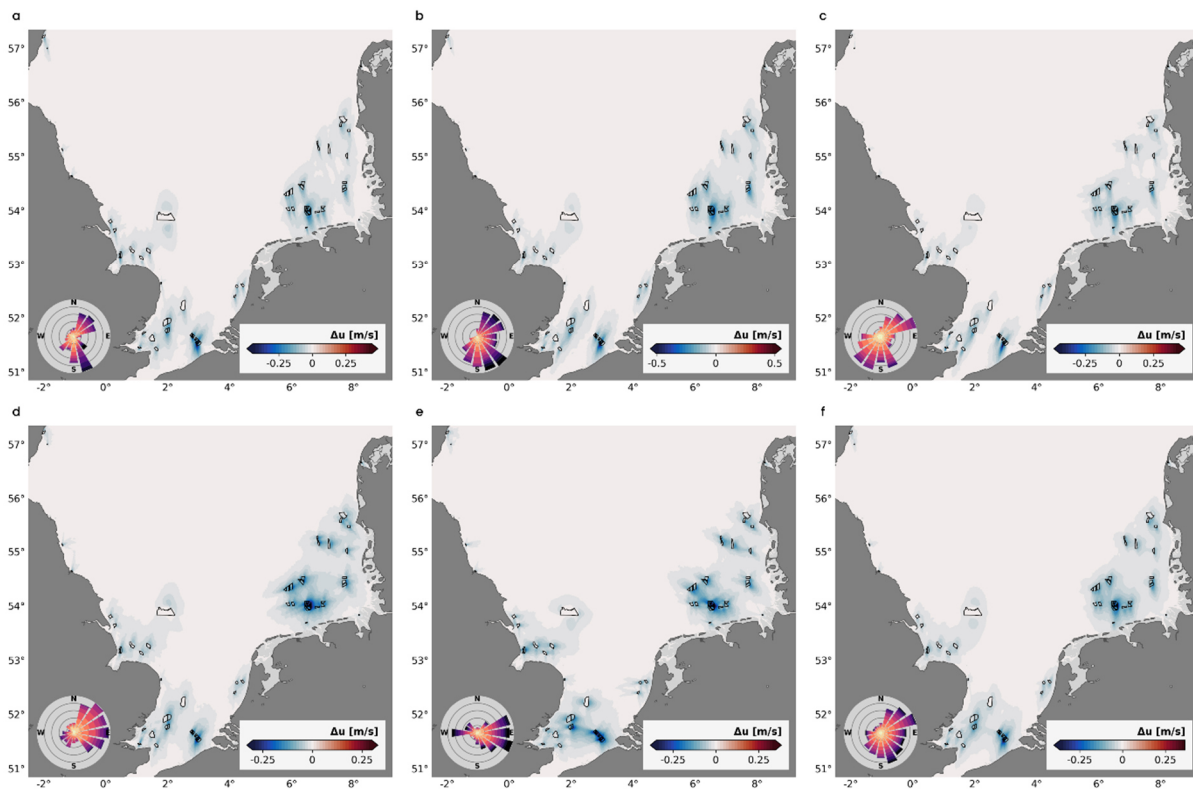


Figure 1: Monthly mean changes in wind speed (u): May (a), June (b), July (c), August (d), September (e) and total mean from May to September 2013 (f). The wind roses indicate the direction in which the wind blew (color range between 1-12 m/s). Black polygons indicate offshore wind farms.

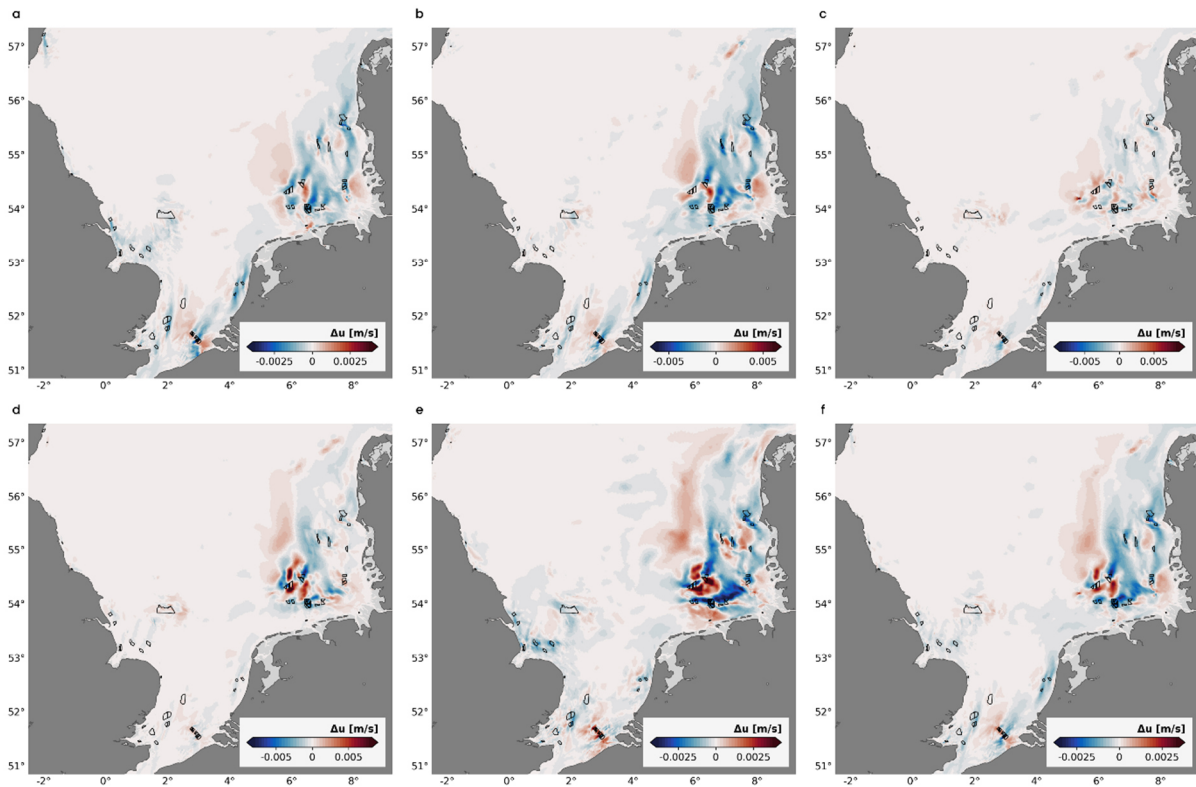


Figure 2: Monthly mean changes in depth-averaged horizontal velocity (u): May (a), June (b), July (c), August (d), September (e) and total mean from May to September 2013 (f). Black polygons indicate offshore wind farms.

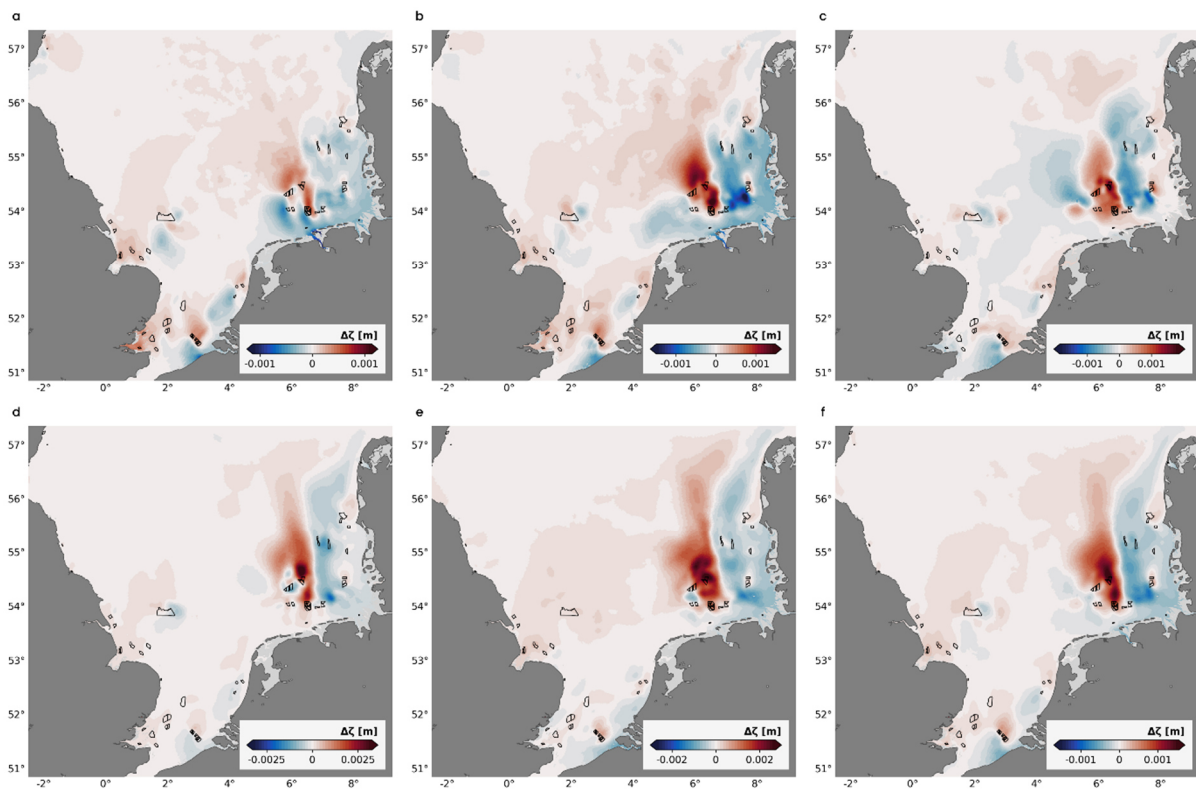


Figure 3: Monthly mean changes in surface elevation (ζ): May (a), June (b), July (c), August (d), September (e) and total mean from May to September 2013 (f). Black polygons indicate offshore wind farms.

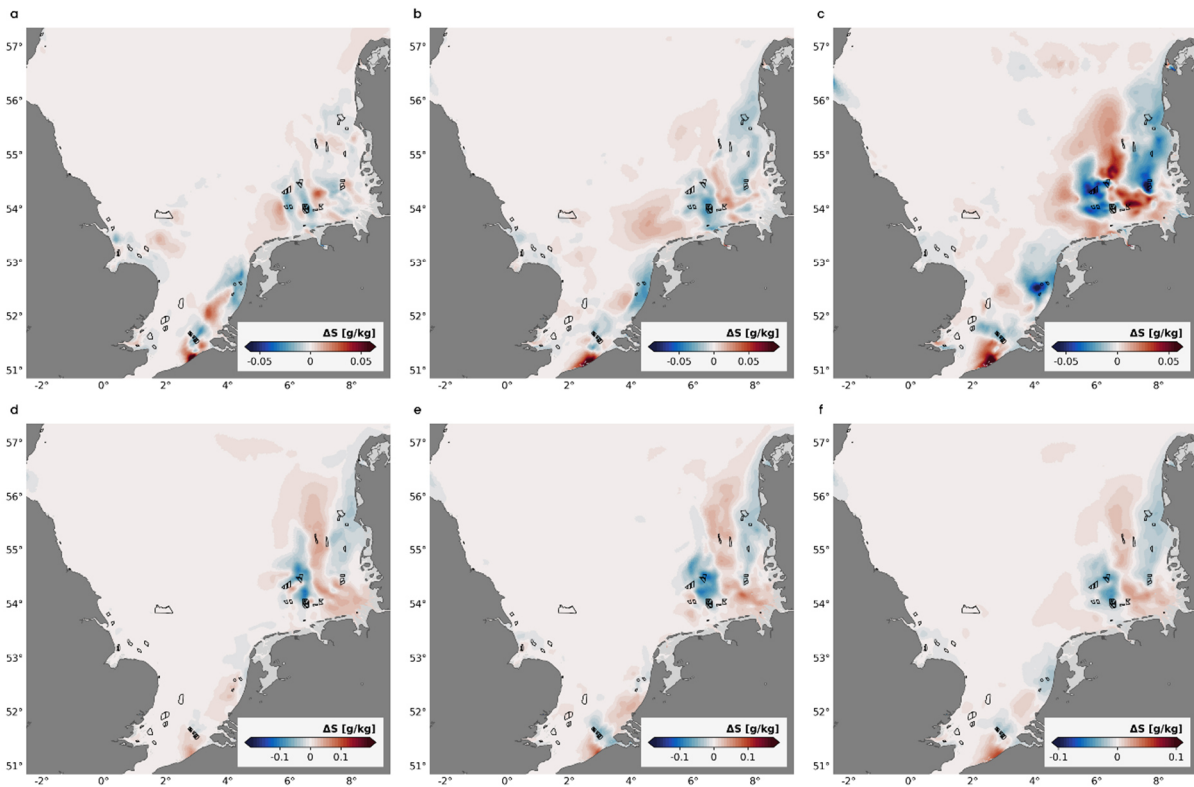


Figure 4: Monthly mean changes in surface salinity (S): May (a), June (b), July (c), August (d), September (e) and total mean from May to September 2013 (f). Black polygons indicate offshore wind farms.

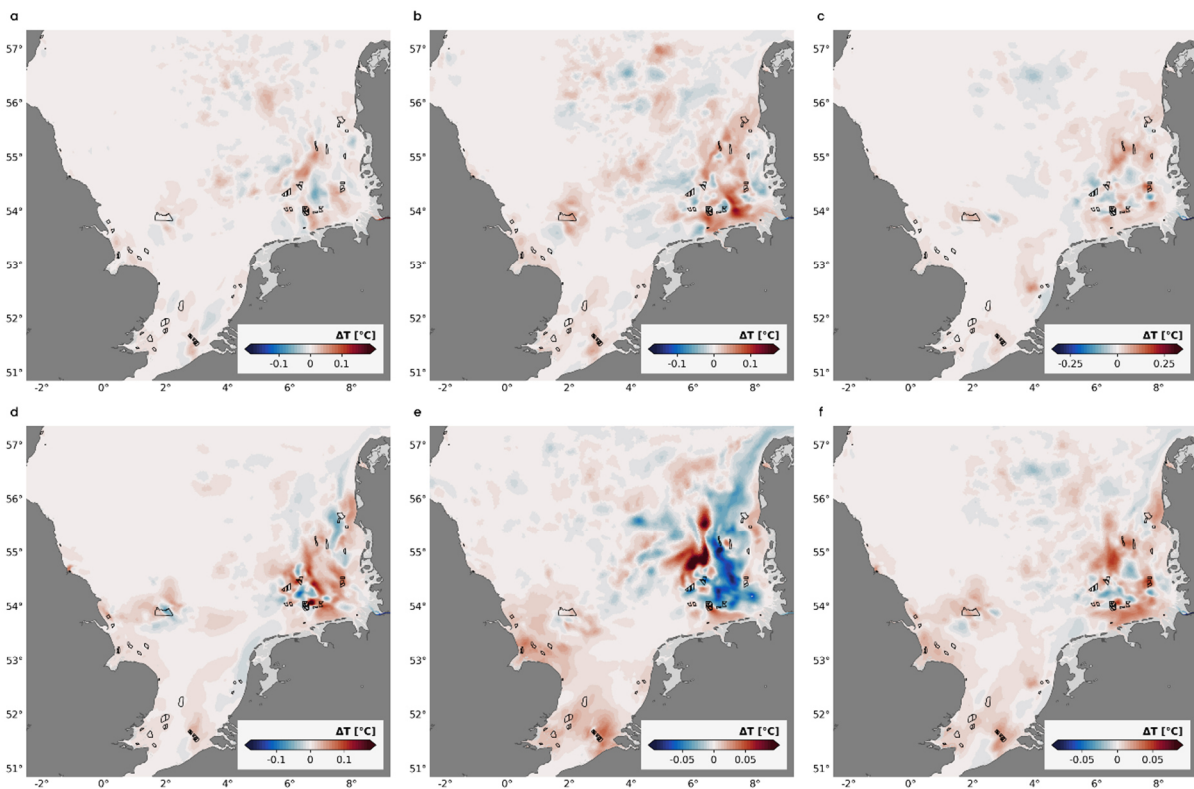


Figure 5: Monthly mean changes in surface temperature (T): May (a), June (b), July (c), August (d), September (e) and total mean from May to September 2013 (f). Black polygons indicate offshore wind farms.

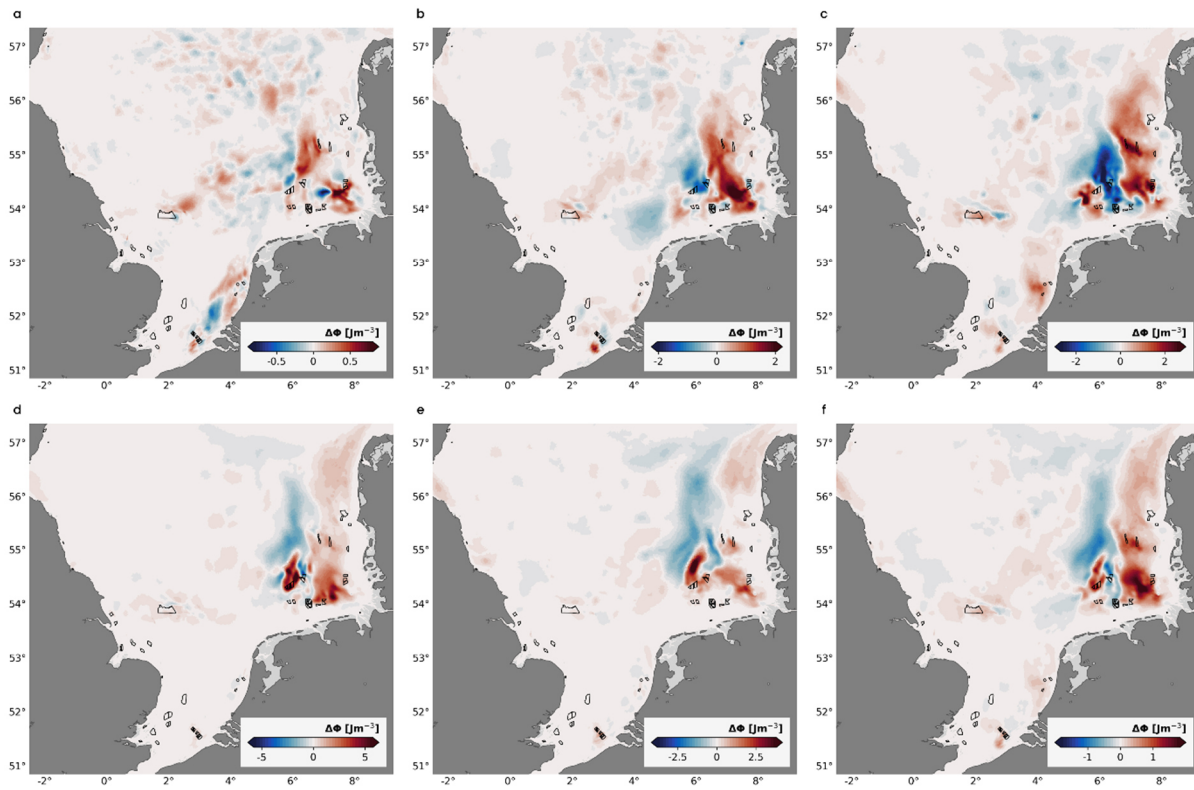


Figure 6: Monthly mean changes in potential energy anomaly (Φ): May (a), June (b), July (c), August (d), September (e) and total mean from May to September 2013 (f). Black polygons indicate offshore wind farms.

3 Study II – Tidal Mitigation of Wake Effects

This chapter contains the second paper, published in *Frontiers in Marine Science – Coastal Ocean Processes*:

Christiansen, N., Daewel, U. and Schrum, C. (2022). **Tidal mitigation of offshore wind wake effects in coastal seas**. *Front. Mar. Sci.* 9:1006647. doi: 10.3389/fmars.2022.1006647

Author Contributions:

NC generated the data sets, performed the data analysis and wrote the manuscript with input from all authors. UD and CS contributed to the data analysis and discussion. All authors conceived the study, revised and approved the manuscript.





OPEN ACCESS

EDITED BY

Alejandro Jose Souza,
Center for Research and Advanced
Studies - Mérida Unit, Mexico

REVIEWED BY

Robert Dorrell,
University of Hull, United Kingdom
Thomas Pohlmann,
University of Hamburg, Germany

*CORRESPONDENCE

Nils Christiansen
nils.christiansen@hereon.de

SPECIALTY SECTION

This article was submitted to
Coastal Ocean Processes,
a section of the journal
Frontiers in Marine Science

RECEIVED 29 July 2022

ACCEPTED 20 September 2022

PUBLISHED 03 October 2022

CITATION

Christiansen N, Daewel U and
Schrum C (2022) Tidal mitigation of
offshore wind wake effects in
coastal seas.
Front. Mar. Sci. 9:1006647.
doi: 10.3389/fmars.2022.1006647

COPYRIGHT

© 2022 Christiansen, Daewel and
Schrum. This is an open-access article
distributed under the terms of the
[Creative Commons Attribution License
\(CC BY\)](https://creativecommons.org/licenses/by/4.0/). The use, distribution or
reproduction in other forums is
permitted, provided the original
author(s) and the copyright owner(s)
are credited and that the original
publication in this journal is cited, in
accordance with accepted academic
practice. No use, distribution or
reproduction is permitted which does
not comply with these terms.

Tidal mitigation of offshore wind wake effects in coastal seas

Nils Christiansen^{1*}, Ute Daewel¹ and Corinna Schrum^{1,2}

¹Institute of Coastal Systems – Analysis and Modeling, Helmholtz-Zentrum Hereon, Geesthacht, Germany, ²Institute of Oceanography, Center for Earth System Research and Sustainability, Universität Hamburg, Hamburg, Germany

With increasing offshore wind development, more and more marine environments are confronted with the effects of atmospheric wind farm wakes on hydrodynamic processes. Recent studies have highlighted the impact of the wind wakes on ocean circulation and stratification. In this context, however, previous studies indicated that wake effects appear to be attenuated in areas strongly determined by tidal energy. In this study, we therefore determine the role of tides in wake-induced hydrodynamic perturbations and assess the importance of the local hydrodynamic conditions on the magnitude of the emerging wake effects on hydrodynamics. By using an existing high-resolution model setup for the southern North Sea, we performed different scenario simulations to identify the tidal impact. The results show the impact of the alignment between wind and ocean currents in relation to the hydrodynamic changes that occur. In this regard, tidal currents can deflect emerging changes in horizontal surface currents and even mitigate the mean changes in horizontal flow due to periodic perturbations of wake signals. We identified that, particularly in shallower waters, tidal stirring influences how wind wake effects translate to changes in vertical transport and density stratification. In this context, tidal mixing fronts can serve as a natural indicator of the expected magnitude of stratification changes due to atmospheric wakes. Ultimately, tide-related hydrodynamic features, like periodic currents and mixing fronts, influence the development of wake effects in the coastal ocean. Our results provide important insights into the role of hydrodynamic conditions in the impact of atmospheric wake effects, which are essential for assessing the consequences of offshore wind farms in different marine environments.

KEYWORDS

tides, mitigation, offshore, wind farms, wakes, North Sea

Introduction

Aerodynamic drag from wind turbine rotors creates wake structures in the atmosphere associated with decreasing wind speed and increasing turbulence downstream of wind turbines (Lissaman, 1979; Wilson, 1980). The atmospheric wakes propagate downstream both laterally and vertically, reaching the surface at a distance of

about 10 rotor diameters (Christiansen and Hasager, 2005; Frandsen et al., 2006). In marine environments, the atmospheric wakes imply wind speed deficits near the sea surface boundary, resulting in attenuated shear forcing extending several tens of kilometers in lee of offshore wind farms (see Christiansen and Hasager, 2005; Christiansen and Hasager, 2006; Li and Lehner, 2013; Emeis et al., 2016; Djath et al., 2018; Platis et al., 2018; Siedersleben et al., 2018; Djath and Schulz-Stellenfleth, 2019; Cañadillas et al., 2020; Platis et al., 2020; Platis et al., 2021). As a consequence, wind-driven circulation becomes affected by the atmospheric wind farm wakes, changing the regional hydrodynamic conditions (Ludewig, 2015; Christiansen et al., 2022). Earlier idealized studies showed that, on the one hand, less wind stress at the sea surface causes decreasing horizontal surface currents behind offshore wind farms, which are in the order of centimeters per second (Ludewig, 2015). On the other hand, changes in wind-driven Ekman transport lead to convergence and divergence of surface waters and associated up- and downwelling dipoles along the wake axis (Broström, 2008; Paskyabi and Fer, 2012; Ludewig, 2015). At this, the resulting vertical transport can influence the temperature and salinity distribution in a stratified water column, with vertical velocities in the order of meters per day (Broström, 2008; Ludewig, 2015).

As offshore wind development increases rapidly to increase renewable energy generation, research on wake effects and their potential impact on the marine environment becomes increasingly important. In 2020, the European offshore wind energy development reached a total of 116 offshore wind farms, corresponding to 5402 offshore wind turbines installed in European waters (WindEurope, 2021). With currently 79% of the total European offshore wind energy production, the majority of European offshore wind farms is located in the southern and central North Sea. In a recent study, we thus demonstrated how wake-induced wind speed reductions caused by the current-state offshore wind farms affect the hydrodynamics of the southern North Sea (Christiansen et al., 2022). The accumulation of wind farms in the coastal areas led to superposition of wind wake effects and, over time, in large-scale structural changes of hydrodynamic processes. As a result of the reduction in wind stress, the wakes influenced horizontal surface currents and shear-induced turbulence in the wind-driven surface mixed layer. The changes in lateral transport and accompanying sea surface elevation and pressure changes affected the vertical transport and density distribution at wind farms, which ultimately altered the development of summer stratification along the tidal mixing fronts (see Christiansen et al., 2022). However, spatial differences in the magnitude of wake effects occurred, despite similar changes in wind forcing, which appeared to be related to the local hydrodynamic conditions. Specifically, in well-mixed shallow waters the impact of wake effects on the density distribution appeared weaker, as tidal mixing fronts formed a boundary between

more pronounced and weaker anomalies in density stratification (see Christiansen et al., 2022), which was not investigated further.

The southern North Sea is characterized by tidal energy, shallow bathymetry and continental influences (e.g. ROFI), all determining the dynamics and stratification development in the shallow coastal waters (Sündermann and Pohlmann, 2011). Wind stress and bottom friction create turbulence in the surface and bottom layers that destroy stratification (Simpson and Sharples, 2012), resulting in different regimes of well-mixed waters, frontal areas and seasonally stratified regions in the southern North Sea (Otto et al., 1990; van Leeuwen et al., 2015), depending on the bathymetry. As the physical regimes are characterized by different hydrodynamic conditions, they can be expected to respond differently to wind speed reduction, and thus magnitude and impact of wind wake effects might vary by location.

Understanding the various factors that lead to the mitigation or enhancement of hydrodynamic disturbances from offshore wind farms is essential for impact analysis. In this paper, we aim to further explore the mitigation and amplification processes and assess the influence of the tides and tide-related hydrodynamic features on emerging wake effects to enable a better assessment of atmospheric wake effects in different marine environments. Here, we focus on direct impacts of tidal currents on the wind stress reduction at the sea surface, as well as on impacts of mixed waters from tidal stirring on the development of induced wake effects. This is done by performing realistic case studies simulating the southern North Sea under the influence of recently installed offshore wind farms, considering realistic tidal forcing compared to imaginary cases without tidal forcing. For this purpose, we used the model setup by Christiansen et al. (2022) and compared the conducted scenarios, to address the differences in the emerging wake effects and highlight the impact of tidal currents.

Methods

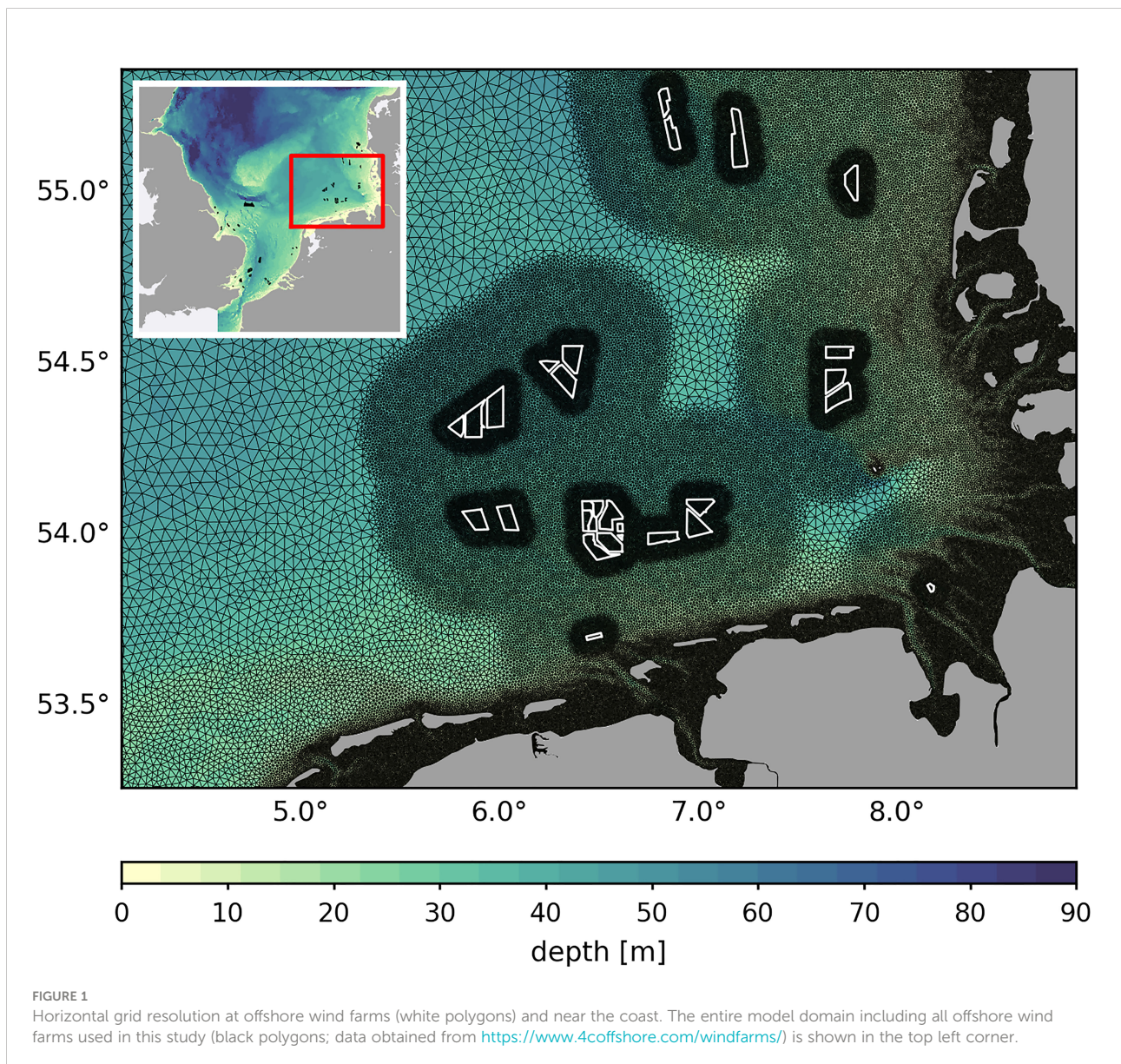
Model description

We utilized the Semi-implicit Cross-scale Hydroscience Integrated System Model (Zhang et al., 2016), which is a three-dimensional hydrostatic model using Reynolds-averaged Navier-Stokes equations based on the Boussinesq approximation. As the SCHISM model is grounded on unstructured horizontal grids, it enables seamless transition between large-scale ocean dynamics and smaller-scale processes near offshore wind farms. For the simulations presented here, we used the model setup presented in Christiansen et al. (2022). The setup covers the southern North Sea extending laterally from the British Channel in the South to the Norwegian trench in the North. Both, the horizontal and vertical grid resolution are a function of the water depth. The

horizontal grid cells vary in size between 500 m in shallow coastal waters and 5000 m in the deep central North Sea, while the vertical grid consists of a maximum of 40 localized sigma coordinates. Additionally, the resolution of the horizontal grid cells is refined at and around the respective wind farm locations, considering only fully commissioned offshore wind farms in the North Sea (status as of November 3rd, 2020; see Christiansen et al., 2022). Specifically, the grid cell resolution increased to 500 m in the first five kilometers and to 1000 m in the following 25 km around each wind farm, to ensure high resolution of wake-related hydrodynamic processes within a radius of 30 km around wind farms (Figure 1). Wind farms are not physically integrated into the grid. In total, the horizontal grid results in approximately 278 K nodes and 544 K triangles. Wind turbines and associated

turbulent hydrodynamic wakes (e.g. Dorrell et al., 2022) are not considered in this study, to emphasize and elaborate on processes related to the wind wake effects.

At the lateral boundaries in the north and the southwest, horizontally and vertically interpolated daily means were prescribed for surface elevation, horizontal velocity, temperature and salinity from the North-West European shelf ocean physics reanalysis data from the Copernicus Marine Service (<https://marine.copernicus.eu/>, downloaded July 2019). In addition, tidal amplitudes and phases for eight tidal constituents (M_2 , S_2 , K_2 , N_2 , K_1 , O_1 , Q_1 , P_1) from the HAMTIDE model (Taguchi et al., 2014) were applied at each time step of the simulation. For the atmospheric forcing, we used the coastDat-3 COSMO-CLM ERAinterim atmospheric



reconstruction (HZG, 2017) and daily river discharge was provided by the mesoscale Hydrodynamic Model (mHM; Rakovec and Kumar, 2022). For more details about the model forcing and the model validation, see Christiansen et al. (2022).

Wake parameterization

The utilized model setup includes an empirical atmospheric wake parameterization based on satellite Synthetic Aperture Radar (SAR) data statistics and former wake models (Frandsen, 1992; Emeis and Frandsen, 1993; Frandsen et al., 2006; Emeis, 2010), which enables to reduce the surface wind speed u_0 on the lee side of offshore wind farms (Eq. (1)). The parameterization is defined as the wind speed recovery function u_r , describing the deficit in wind speed downstream of a wind farm. At this, the parameterization corresponds to a top-down approach, i.e. a wind farm is considered as a single unit.

$$u_r(x, y) = u_0 \left(1 - \alpha \cdot e^{-\left(\frac{x}{\sigma} + \frac{y^2}{\gamma^2}\right)} \right) \quad (1)$$

The wakes are described by an exponential function in a reference coordinate system oriented along the prevailing wind direction. Here, x and y define the wind-aligned downstream distance and the distance from the central wake axis, respectively. The exponential function is determined by constant values describing the maximum percentage wind speed reduction (α), the scaling factor for the wake length (σ) and the scaling factor for the cross-sectional wake shape (γ). Values for α and σ were derived from SAR measurements at the offshore wind farm Global Tech and balanced by mean values of previous sea surface wake observations (Christiansen and Hasager, 2005; Christiansen and Hasager, 2006; Hasager et al., 2015; Djath et al., 2018; Djath and Schulz-Stellenfleth, 2019; Cañadillas et al., 2020). Although, magnitude and length of atmospheric wakes can vary strongly, depending on atmospheric conditions and wind farm configuration (Djath et al., 2018), the observation-based parameters give a sufficient estimate for the general impact of wind wakes, namely the downstream reduction in wind speed (see Christiansen et al., 2022). For α we used a constant value of 8%, whereas σ was set to 30 km. On the other hand, the scaling factor for the cross-sectional shape was calculated for each wind farm individually and is defined as $\gamma = L/3$, with L as the wind farm width with respect to the wind direction. The wake parameterization is applied to the wind field interpolated onto the model grid and reduces the wind speed at each time step of the model simulation. In this process, the horizontal velocity components at the downstream grid points of each wind farm are modified in the reference coordinate system, accordingly. A detailed description of the atmospheric wake parameterization is provided by Christiansen et al. (2022).

Model simulations

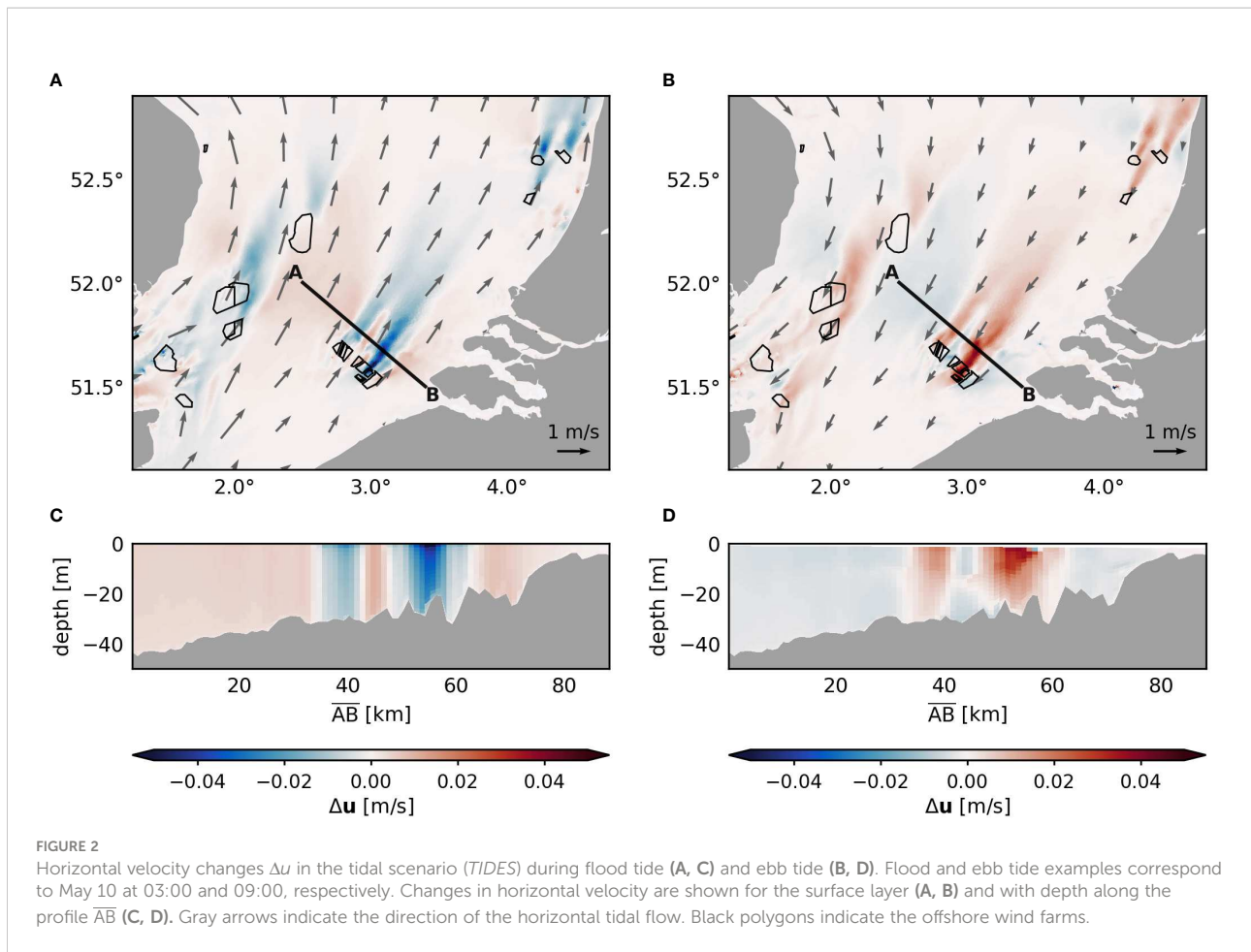
For the investigations of the tidal influence on wake-related processes, we applied four different simulations split into two scenarios: a tidal scenario (*TIDES*) and a tide-free scenario (*NOTIDES*). For each of the scenarios, we generated one reference simulation without wake parameterization (*REF*) and one simulation including the wake parameterization (*OWF*). Each simulation was calculated with an implicit time step of 120 seconds and produced hourly, instantaneous output data for the period of May to September 2013. The simulation period during the summer season was chosen to ensure mostly stable atmospheric conditions and to match the seasonal time span of the utilized satellite SAR measurements. For daily and monthly means, the absolute velocities were averaged over time. The *NOTIDES* scenario was generated using the same forcing data as for the *TIDES*, but without prescribing the amplitudes and phases of the different tidal constituents at the boundary nodes. For the wind farm simulations, the recent status (as of November 3, 2020) of offshore wind farm development in the North Sea was taken into account *via* the wake parameterization (data obtained from <https://www.4coffshore.com/windfarms/>). To illustrate the wake effects, the differences between the wind farm simulations to the reference simulations were used (*OWF-REF*).

Results and discussion

Primary wake effects

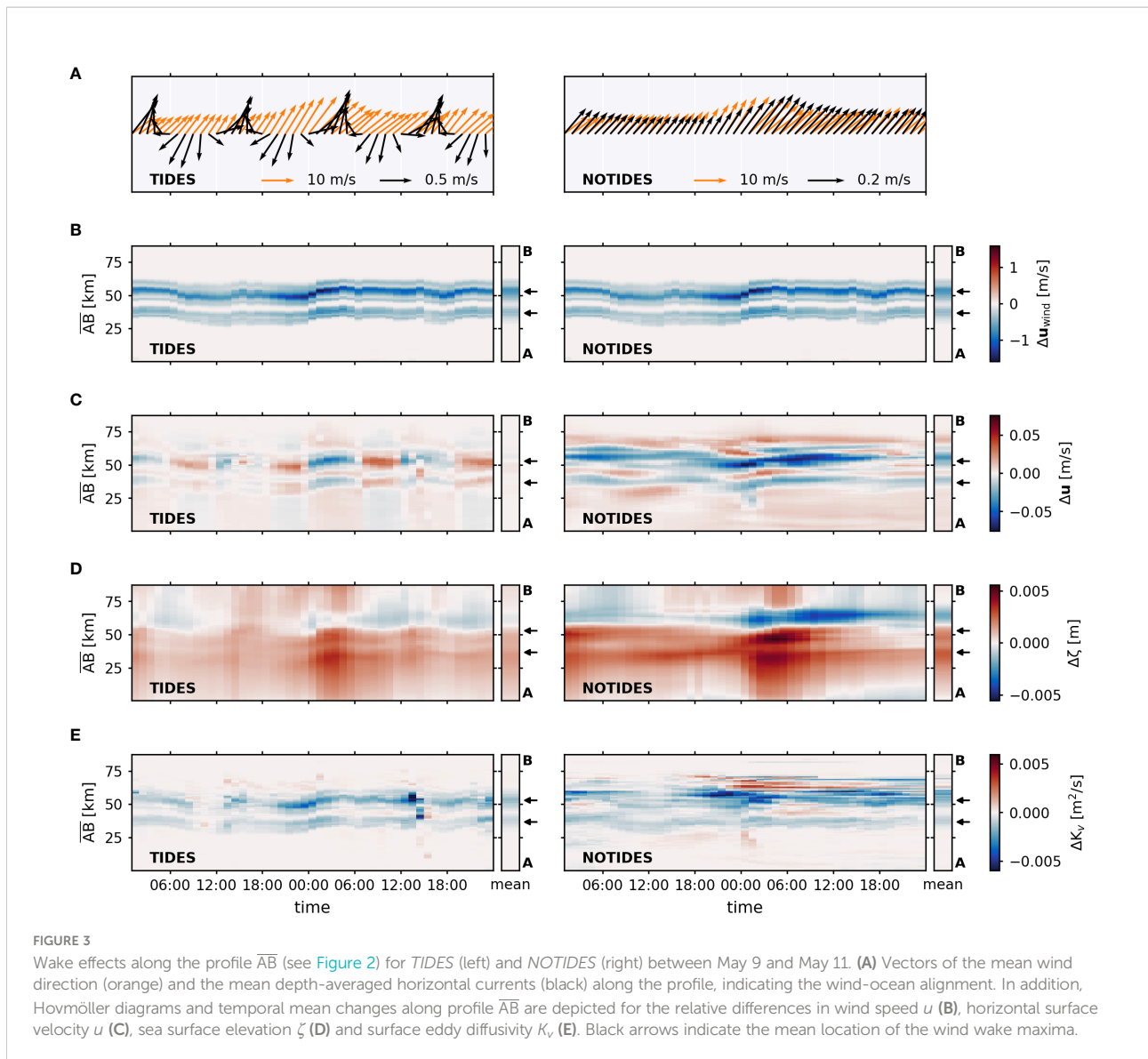
To investigate the impact of tides on processes related to the atmospheric wake effect, constant wind direction over at least one tidal period is beneficial, resulting in stable wake patterns. Here, we therefore focus on emerging wind wakes at offshore wind farms located in the Southern Bight, where the wind blows in northeasterly direction over a period of 48 hours between May 9 and May 11, 2013, nearly parallel to the local flood and ebb tide currents. As a result, stable wind speed reductions develop downwind, affecting the wind stress at the sea surface boundary and thus the horizontal surface velocity (Figure 2). In this context, wind speeds are on the order of about 10 m/s, whereas the tidal velocities range around 1 m/s, an order of magnitude lower. As the wind-driven horizontal currents are directly affected by the wind speed reduction, we define the induced changes in momentum and horizontal velocity as the primary wake effects. These effects do occur not only in the surface layer (Figures 2A, B), but are transferred to the entire water column (Figures 2C, D).

Figure 2A shows the absolute changes in surface velocity during flood tide, where the tidal current flows in similar direction as the surface wind speed. As the reduced shear



forcing leads to weaker wind-driven transport in the direction of the tidal current, the horizontal velocity decreases in the wake area, which is consistent with previous modeling studies (Ludewig, 2015; Christiansen et al., 2022). This process, however, cannot be generalized for the primary wake effects, as the induced changes in horizontal velocity appear to depend on the characteristics of the tidal flow. When the tidal cycle turns to ebb tide, wind field and tidal flow align in opposite directions (Figure 2B). In this case, the reduced shear forcing results in less countercurrents to the tidal current and thus the net transport along the wake area increases. Consequently, positive absolute changes develop in the wake area, contrary to the effects for aligned currents. Regardless of the alignment between wind and tides, the magnitudes of the wake-related horizontal velocity changes range between ± 0.05 m/s, which accounts for about 5% of the maximum prevailing tidal velocities at the profile \overline{AB} , which range between 0.8–1.1 m/s during the selected time steps. As already mentioned by Christiansen et al. (2022), such strong velocity anomalies are substantial for the horizontal transport and persistent velocity perturbations due to the wind farms can influence the residual currents and the horizontal circulation.

In order to investigate how the relation between the wind direction and tidal flow determines the impact of atmospheric wind wakes, processes occurring over the entire tidal cycle of the example case are compared for the *TIDES* and *NOTIDES* scenarios. Figure 3 shows the temporal development of the absolute changes in wind speed and horizontal surface velocity as well as surface elevation and surface mixing between May 9 and May 11 along the profile \overline{AB} roughly perpendicular to the mean wind direction (see Figure 2). During the two days, wind blows relatively constant from southwestern direction with an average wind speed of 10 m/s and a maximum of 15 m/s at the beginning of May 10 (Figure 3A). In the *TIDES* scenario, the average tidal flow along the profile changes with time according to its tidal ellipse, resulting in parallel and opposite flow directions between air and sea for flood and ebb tide, respectively (Figure 3A). The instantaneous tidal-driven surface currents averaged along profile \overline{AB} are around 0.5 m/s. On the other hand, in the *NOTIDES* scenario horizontal currents are primarily wind-driven and therefore roughly parallel to the wind field over the selected period. Here, instantaneous surface currents range around 0.2 m/s. Opposing current directions, e.g.



due to density-driven transport, are not evident during the selected period in the tide-free scenario.

Figure 3C shows the response of the horizontal surface current to the wind speed reduction, i.e., the primary wake effect, and the role of the tidal flow on the emerging velocity anomalies. In *TIDES*, the horizontal velocity changes show the periodic change in amplitude and direction, which result from the periodic inversion of the tidal current. In this context, positive and negative velocity changes are directly related to the identified flow changes depicted in Figure 3A. The horizontal velocity changes in *TIDES* range between ± 0.04 m/s, with the largest changes occurring on May 10 following the strong wind speed event and an average absolute change of about 0.025 m/s. While these changes account for about 1–5% of horizontal surface currents during

tidal rise and fall (velocities between 0.6–1.2 m/s), they can account for more than 10% of horizontal surface currents at high and low tide (velocities between 0.1–0.3 m/s). However, the induced velocity changes do not affect the direction of the tidal flow or the tidal ellipses respectively. Due to the opposing effects, the mean changes over the 48-hour period are very small and show little effect on the mean horizontal flow compared to *NOTIDES*. Apparently, positive velocity changes due to countercurrents counteract the negative changes due to aligned currents and therefore prevent the development of consistent surface velocity reduction in *TIDES*. Consequently, the countercurrents attenuate the magnitude of the mean velocity anomalies along profile \overline{AB} . In this regard, mitigation depends on the consistency of the wind field and the ratio of the flood and ebb tide currents. In

contrast, the *NOTIDES* scenario shows consistent reductions in surface velocity in the wake areas, which are also clearly visible on the 48-hour mean. Here, the instantaneous velocity changes are almost twice as strong as in *TIDES* with up to ± 0.08 m/s and even account for about 50% of the actual horizontal wind-driven flow, implying significant changes in the tide-free scenario. The mean velocity changes reach up to ± 0.025 m/s.

Secondary wake effects

Besides primary wake effects, atmospheric wakes trigger secondary effects associated to the primary changes in horizontal momentum and turbulence. Secondary wake effects involve, for instance, the reduction in wind-driven mixing of the surface layer due to weaker shear at the surface boundary (Christiansen et al., 2022) or the development of upwelling/downwelling dipoles due to changes in the Ekman dynamics (Broström, 2008; Paskyabi and Fer, 2012; Ludewig, 2015). Since primary and secondary wake effects are closely linked, the secondary effects are also expected to be attenuated by the inversion of the horizontal surface currents in *TIDES*.

Emerging sea level dipoles for both scenarios are shown in Figure 3D. In *NOTIDES*, the consistent changes in horizontal surface velocity result in a pronounced dipole pattern along profile \overline{AB} , with magnitudes of induced sea level changes of about ± 0.006 m. Mean changes are between ± 0.0025 m. In contrast, the instantaneous and mean sea level changes in *TIDES* are again only half as strong as in *NOTIDES*, similarly to the horizontal velocity changes. Compared to the local tidal variability, the changes in sea surface elevation due to the wind speed reductions are insignificant for the tidal scenario. Here, the attenuation of the surface elevation dipoles results from the advection of the Ekman-related anomalies due to the variable tidal currents. The elliptical water parcel movement due to changing current directions continuously shifts the emerging anomalies around the actual location of the wind speed reduction, leading to a constant adjustment of the Ekman dynamics (see Supplementary Figure 1). Therefore, the periodic advection hinders the development of pronounced dipole maxima, causing an overall weaker dipole pattern along the wake axis compared to constant current direction. Periodic shifting of the surface elevation dipole can also be seen in Figure 3D. Nevertheless, a dipole pattern, albeit weaker, does still occur in *TIDES* for both instantaneous and mean sea surface height changes. Previous studies have shown that the wake-induced sea level dipoles are associated with changes in vertical transport and perturbations of the pycnocline (Broström, 2008; Paskyabi and Fer, 2012; Ludewig, 2015). Thus, attenuation of the sea level changes implies weaker changes in vertical velocities and density stratification. However, changes in vertical velocity are not clearly visible along profile \overline{AB} , since bathymetric

features and strong tidal mixing impede the development of distinct wake-induced changes in the vertical velocity here. In addition to the sea surface elevation, changes in horizontal surface currents also affect the generation of turbulent kinetic energy and thus the turbulent mixing of the surface mixed layer. As the horizontal shear at the surface layer decreases with lower wind speeds, the vertical mixing rate decreases in the wake areas in both scenarios (Figure 3E). Here, we used the vertical eddy diffusivity K_v as a measure for the vertical mixing rate. Again, changes in the tidal scenario appear weaker over the 48-hour period. Particularly, during strong winds at the beginning of May 10, where the tidal direction is opposite to the wind direction, changes in mixing are clearly stronger in *NOTIDES*. Nevertheless, the order of magnitude of changes in eddy diffusivity is similar in *TIDES* and *NOTIDES* over time, especially along the wake at about 30 km of profile \overline{AB} , as the surface mixing is primarily determined by the wind stress. The magnitudes in *TIDES* are slightly lower on average due to the influence of tidal mixing. In both scenarios, the surface eddy diffusivity is reduced along the wind wakes by up to -0.006 m²/s and about -0.002 m²/s on average, indicating an enhancement of stratification in the surface layers along the wake areas. Temporarily, these changes can influence the actual eddy diffusivity in the surface layer (0.01–0.03 m²/s) significantly, especially in *NOTIDES*. However, compared to the depth-averaged eddy diffusivity, i.e., the tidal mixing in *TIDES*, the induced surface mixing reductions account for less than 10%.

Christiansen et al. (2022) showed that the magnitude of wake-induced stratification changes due to sea level dipoles or mixing reduction depend on the stratification conditions, suggesting a distinction between processes in stratified and well-mixed waters. To investigate this further, we analyze changes in vertical velocity and density gradients along profile \overline{CD} northwards of the West and East Frisian Islands (Figure 4). Here, wake effects occur simultaneously in both stratified and mixed water. Again, we focus on a simulation period in which the wind remains stable over at least one tidal cycle. On May 2, winds blow constantly in southwesterly direction over a 12-hour period with mean wind speeds around 7 m/s (Figure 4A). During the period, the M2 tidal ellipses are mainly oriented in the direction of the wind field, but with deviations of up to 45 degrees. Three wake areas occur along the profile \overline{CD} , resulting from offshore wind farms in the German Bight. The strongest wake-induced anomalies occur at a profile distance of about 80 km due to superposition of several emerging wakes behind the large wind farm cluster located at 54.0° N and 6.5° E (see Figure 4A). Another dominant wake pattern occurs at about 20 km. As shown before for profile \overline{AB} , constant wind direction and the periodic change of the tidal currents along profile \overline{CD} result in opposing alterations of the horizontal surface currents and thus to perturbations of the secondary wake effects (see Figure 4D, C).

Secondary wake effects influence the vertical velocity and density distribution through dipole-related vertical transport

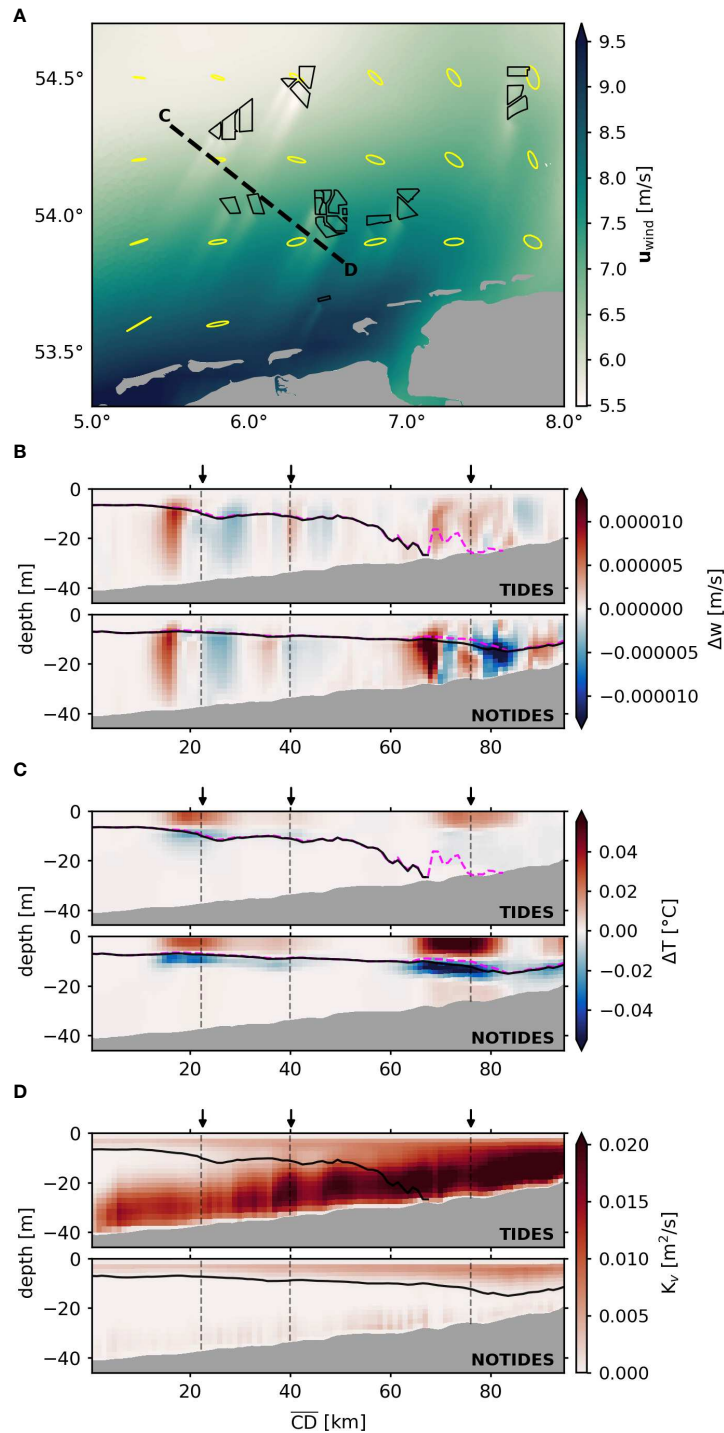


FIGURE 4

Mean wake effects along profile \overline{CD} for *TIDES* and *NOTIDES* on May 2 between 06:00 and 18:00. (A) Mean wind speed u over the 12-hour period, illustrating the stable wake patterns in the example region. M2 tidal ellipses are indicated in yellow. Black polygons indicate the offshore wind farms. (B) Vertical profiles of the mean vertical velocity changes Δw over the 12-hour period in *TIDES* (top) and *NOTIDES* (bottom). Solid black line and dashed purple line show the mixed layer depth in the reference run (REF) and the wind farm run (OWF), respectively. Here, the mixed layer depth is defined by the density threshold criterion of $\Delta\rho = 0.03 \text{ kg/m}^3$ (de Boyer Montégut et al., 2004). Arrows and black and gray dashed lines indicate mean location of wind wake maxima. (C) Vertical profiles of the mean temperature changes ΔT over the 12-hour period in *TIDES* (top) and *NOTIDES* (bottom). (D) Vertical profiles of the vertical eddy diffusivity K_v in the reference simulation (REF), indicating the mean vertical surface and bottom mixing rates in *TIDES* (top) and *NOTIDES* (bottom) over the 12-hour period.

and the reduction of surface layer mixing. In this context, on the one hand, the latter results from the reduction in wind stress and leads to a general relaxation of the surface layers, which elevates the mean mixed layer depth and increases stratification strength in wake-affected areas (Figure 4B). The elevation of the mixed layer under the influence of wind wakes compared to the reference run is apparent in both *TIDES* and *NOTIDES*, affecting the temperature stratification near the surface mixed layer (Figure 4C). On the other hand, the sea level dipoles are associated with inverse changes in vertical transport, resulting in upwelling and downwelling patterns in the vertical velocity and stratification (Paskyabi and Fer, 2012; Ludewig, 2015). This is also shown here for the mean vertical velocity changes over the 12-hour period (Figure 4B). While these patterns can also lead to perturbations of the pycnocline, the upwelling/downwelling can affect the density distribution in the wake areas (Ludewig, 2015), which contributes to the occurring changes in mean temperature (Figure 4C).

In stratified deeper waters, distinct dipoles in the vertical velocity changes related to changes in Ekman transport are visible in regions influenced by wind speed reduction (Figure 4B). These dipoles occur similarly in *TIDES* and *NOTIDES* due to comparable stratification conditions and exhibit changes in mean vertical velocity of about $\pm 7 \cdot 10^{-6}$ m/s. Consequently, similar changes in temperature stratification of about $\pm 0.03^\circ\text{C}$ occur in deeper waters (Figure 4C). In shallower regions, in contrast, induced changes differ significantly between *TIDES* and *NOTIDES*. In *NOTIDES*, the pycnocline persists in the shallow waters, allowing upwelling and downwelling patterns to continue to develop. The mean changes in the shallow waters exceed $\pm 1 \cdot 10^{-5}$ m/s corresponding to approximately 1 meter per day, which agrees with the findings by Broström (2008) and Ludewig (2015). The vertical velocities as well as the reduced surface layer mixing result in distinct mean temperature changes of more than $\pm 0.05^\circ\text{C}$. At this, magnitudes in velocity and temperature changes show a clear correlation with the magnitudes of the wind speed reduction.

In *TIDES*, however, the tidal mixing mitigates the secondary wake effects in shallow waters. Here, the strong vertical mixing rates from the bottom layers, which originate from tidal currents, overlap and dominate the wind-driven mixing from the surface layers (Figure 4D). As a result, the shallow waters in *TIDES* are well mixed and governed by tidal stirring. Consequently, Ekman dynamics are dominated by the strong tidal mixing rates and thus upwelling/downwelling is not visible in the vertical velocity changes along profile \overline{CD} (Figure 4B). Besides, uniform vertical density distributions inhibit vertical transport in temperature and salinity. Instead, the induced changes in mean temperature stratification are primarily driven by the reduction of surface layer mixing, exhibiting magnitudes more than 50% weaker compared to *NOTIDES* (Figure 4C). At this, magnitudes do not appear related to the wind speed reductions, but to the extent of tidal influence.

Hence, tidal mixing determines the impact of secondary wake effects on shallow coastal waters. In deeper waters, however, where the bottom shear and thus tidal mixing rates become less dominant, the secondary wake effects develop similarly in the tidal and non-tidal environment, particularly for increasing stratification strength.

Regional impact of tidal mitigation

According to the results of profiles \overline{AB} and \overline{CD} , tides influence the wake effects on the hydrodynamics directly and indirectly through periodic currents and tidal mixing, respectively. The different tidal influences as well as primary and secondary wake effects are illustrated in Figure 5. On the one hand, the tidal currents have a direct impact on the surface velocity changes caused by the wind wakes, with frequently changing flow directions leading to deviations and inversions of the horizontal velocity changes (Figures 5A, B). In this context, both positive and negative instantaneous velocity changes can occur along the wake areas, as the reduction of wind stress reduces either the thrust of surface currents in tidal direction or the counterforce to the opposing tidal flow, depending on the alignment between wind and ocean current (see Figure 6A). Thus, direct tidal influences are related to the changes in vertical shear and affect particularly the wake-induced changes in the wind-driven flow and the mean horizontal circulation. With constant wind direction aligned with the tidal ellipses, the opposing changes in horizontal velocity at flood and ebb tide may even result in an attenuation of the mean velocity changes. Thus, the direct tidal influence can result in minor mean changes in horizontal velocity despite possibly strong instantaneous changes during the tidal cycle. This, however, requires equally strong flood and ebb currents and a constant wind field over the tidal cycle.

Regardless of the alignment between wind and tidal currents, the reduction in wind stress results in decreasing surface mixing and Ekman-driven vertical transport, ultimately affecting the pycnocline (Figure 5C). However, tidal mixing and stratification strength determine the magnitude of the secondary wake effects. This indirect impact of the tides occurs particularly in shallow waters where strong tidal stirring superimposes the surface layer mixing, hindering the development of Ekman-related vertical transport. In tidally dominated regions, therefore, secondary wake effects are limited to the reduction of surface layer mixing. Overall, wake-related changes in stratification appear as a function of the local stratification strength (see Figure 6B), which is governed by tidal mixing. In weakly stratified waters, secondary wake effects occur much weaker, whereas the mitigation effects diminish in more stratified deeper waters. Thus, local stratification strength can help to evaluate the expected impact of secondary wake effects.

It has been shown that the hydrodynamic effects of atmospheric wind farm wakes are not limited to local processes but involve large-scale structural changes in the hydrodynamic

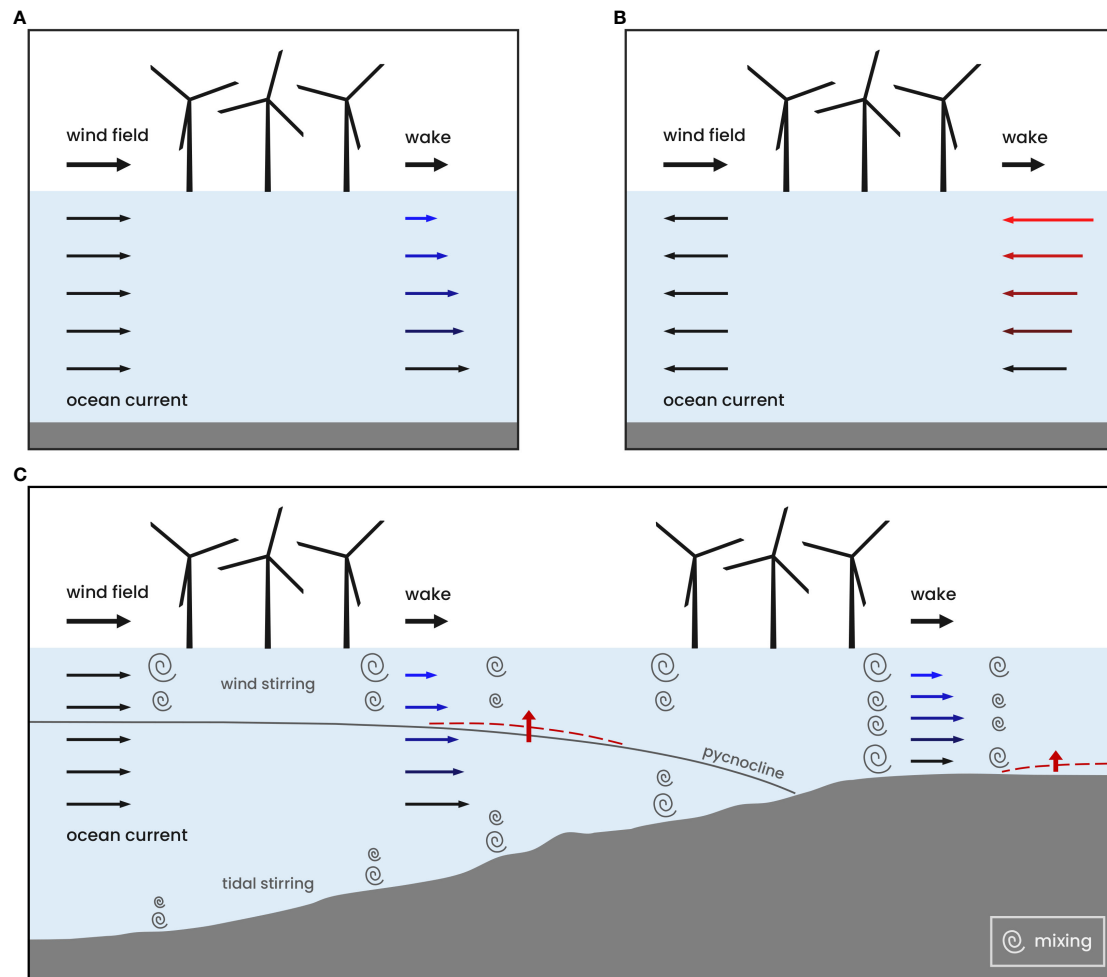
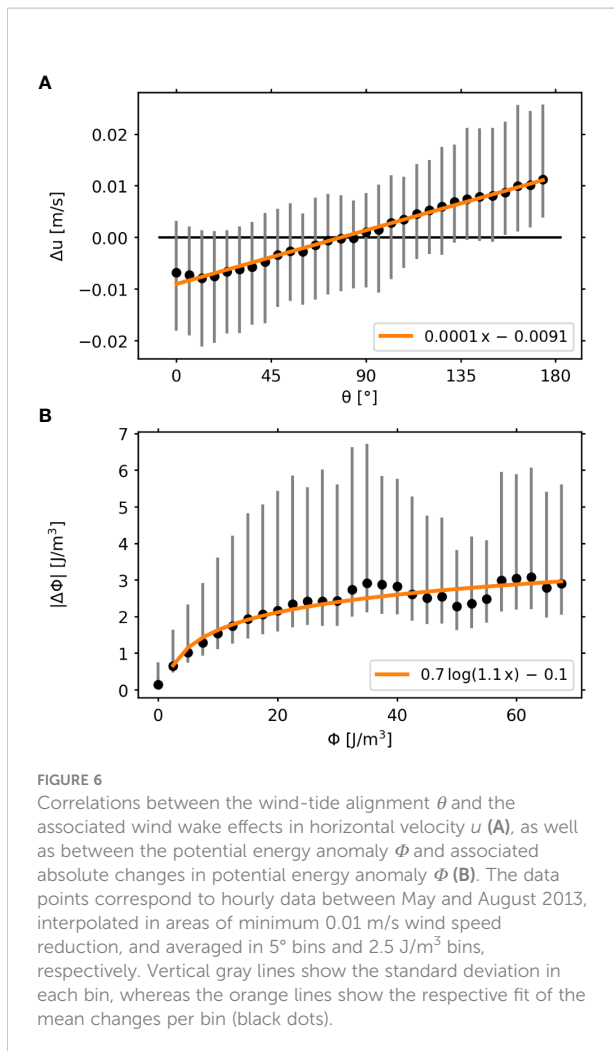


FIGURE 5
Schematic illustrations of tide-related hydrodynamic features (direct: periodic currents, indirect: mixing fronts) on the primary and secondary wake effects. **(A)** Primary wake effects, namely the reduction of the wind-driven ocean current, in the case of aligned wind and ocean currents. **(B)** Primary wake effects in the case of opposing wind and ocean currents. **(C)** Secondary wake effects, namely the mixing reductions and stratification increase, in stratified (left) and mixed (right) waters. Red dashed lines and arrows indicate the doming of the pycnocline in stratified waters and the development of a pycnocline in mixed waters, respectively.

system (Christiansen et al., 2022). Thus, the influence of the tides must also be considered on regional scales. Figure 7 shows the regional mean changes in horizontal surface velocity and stratification strength over the entire simulation period between May and September. Both the changes for the scenario with (Figures 7A, C) and without tidal forcing (Figures 7B, D) are depicted. In *TIDES*, the changes in the mean surface currents show an inhomogeneous pattern with both positive and negative amplitudes around the wind farms (Figure 7A). This inhomogeneous pattern is related to the tidal influence during varying wind speeds and directions and unequal flood and ebb currents, resulting in positive, negative and deflected velocity changes over the period of five months. The velocity changes in the tidal scenario range between ± 0.002 m/s. These changes are

relatively small as they account for only about 0.5-1.0% of the actual mean horizontal surface velocities, which are between 0.2-0.5 m/s in the reference simulation. In contrast, the mean changes in *NOTIDES* are much larger (Figure 7B). Here, the changes are between ± 0.01 m/s, which is an order of magnitude larger than in *TIDES* and accounts for about 5-10% of the mean horizontal velocities in the tide-free reference simulation, which are about 0.1-0.2 m/s. In addition, there are large-scale reductions in surface velocity around the wind farms, forming coherent patterns. Compared to *TIDES*, both the patterns and the magnitudes of the changes in *NOTIDES* clearly demonstrate the impact of the tidal currents on the primary wake effects. It shows that in highly tidal-driven environments, such as the southern North Sea, the mean changes in horizontal currents due to atmospheric wakes



are attenuated and weaker than in the absence of tides. Nevertheless, we found that strong instantaneous changes, both positive and negative, still occur in the wake areas downstream of wind farms even in the tidal-driven environment, which can affect tidal stream transport and generation of turbulent mixing in the surface and bottom mixed layers. This becomes potentially important with regard to nutrient intrusion into the nutrient-depleted surface mixed layers (Schrum et al., 2006; Simpson and Sharples, 2012) or the larvae transport and fish migration (Gibson, 2003; van Berkel et al., 2020). In particular, the reduction of wind-driven surface layer mixing is not mitigated by the periodic flow reversals and thus can still affect stratification in the tidal environment.

Despite impact on stratification in both scenarios, the influence of tides on secondary wake effects, specifically the changes in mean stratification, can be observed at the regional scale (Figures 7C, D). Here, changes in stratification are shown by changes in the potential energy anomaly, which is a gravitational-based measure of stratification strength (Simpson and Bowers, 1981). In *TIDES*, stratification changes occur mainly in the seasonally stratified

regions and near the frontal areas of the southern North Sea, bounded by the location of the tidal mixing fronts (Figure 7C). Impact on weakly stratified waters is attenuated by strong tidal mixing rates. The changes in mean stratification strength range between $\pm 2 \text{ J/m}^3$, with a clear dipole pattern observed in the German Bight. This dipole pattern was shown to be related to the baroclinic changes and indicates an enhancement of the summer stratification towards the coastal waters (Christiansen et al., 2022). The *NOTIDES* scenario also shows a dipole pattern in the German Bight, indicating baroclinic changes (Figure 7D). In general, however, the changes in *NOTIDES* are more than twice as strong as in *TIDES* with values between $\pm 5 \text{ J/m}^3$, which is related to the overall stronger stratification in *NOTIDES*. At this, induced perturbations occur in all regions covered by wind farms, including significant stratification changes in the Southern Bight and regimes, which are characterized by strong mixing in the tidal environment. This clearly shows the influence of the tidal mixing on the development of the secondary wake effects.

With respect to the physical regimes of the southern North Sea, secondary wake effects appear to emerge primarily in seasonally and intermittently stratified regions, as tidal stirring in well-mixed regions mitigates the development of the wake effects. This becomes important regarding future expansion of offshore wind energy into deeper waters of the North Sea (WindEurope, 2022b). Based on the results, tidal mitigation will be minor in these regions and therefore the impact of the wind wakes on stratification will be more substantial. As Dorrell et al. (2022) noted, the effects of offshore wind farms in yet undeveloped areas have still to be investigated and could involve significant influence on the seasonal stratification. In terms of the wind farm effects, reduced surface layer mixing could further increase the stratification in wind farm areas. However, counteracting processes due to additional mixing from wind turbine foundations (see Carpenter et al., 2016; Schultze et al., 2020; Dorrell et al., 2022) could affect and even dominate the processes related to wind wakes. This leads to uncertainties about possible consequences in stratified waters, as the interaction of wind wake effects and additional turbulence inside the wind farm has yet to be determined. Furthermore, as shown by Christiansen et al. (2022), wake-related stratification changes also depend largely on induced sea level dipoles and could thus have both positive and negative amplitudes due to significant upwelling/downwelling patterns.

The tidal attenuation of vertical density stratification may mitigate not only the impact on the hydrodynamics in the southern North Sea but also impact on important ecological processes. Vertical mixing and stratification in the pycnocline are decisive factors in nutrient availability, primary production, and sediment resuspension (Sverdrup, 1953; Simpson and Sharples, 2012). Consequently, fluctuations of the mixed layer due to wake-related stratification changes are assumed to affect the nutrient balance in the system and thus primary production (Christiansen et al., 2022). van der Molen et al. (2014) simulated

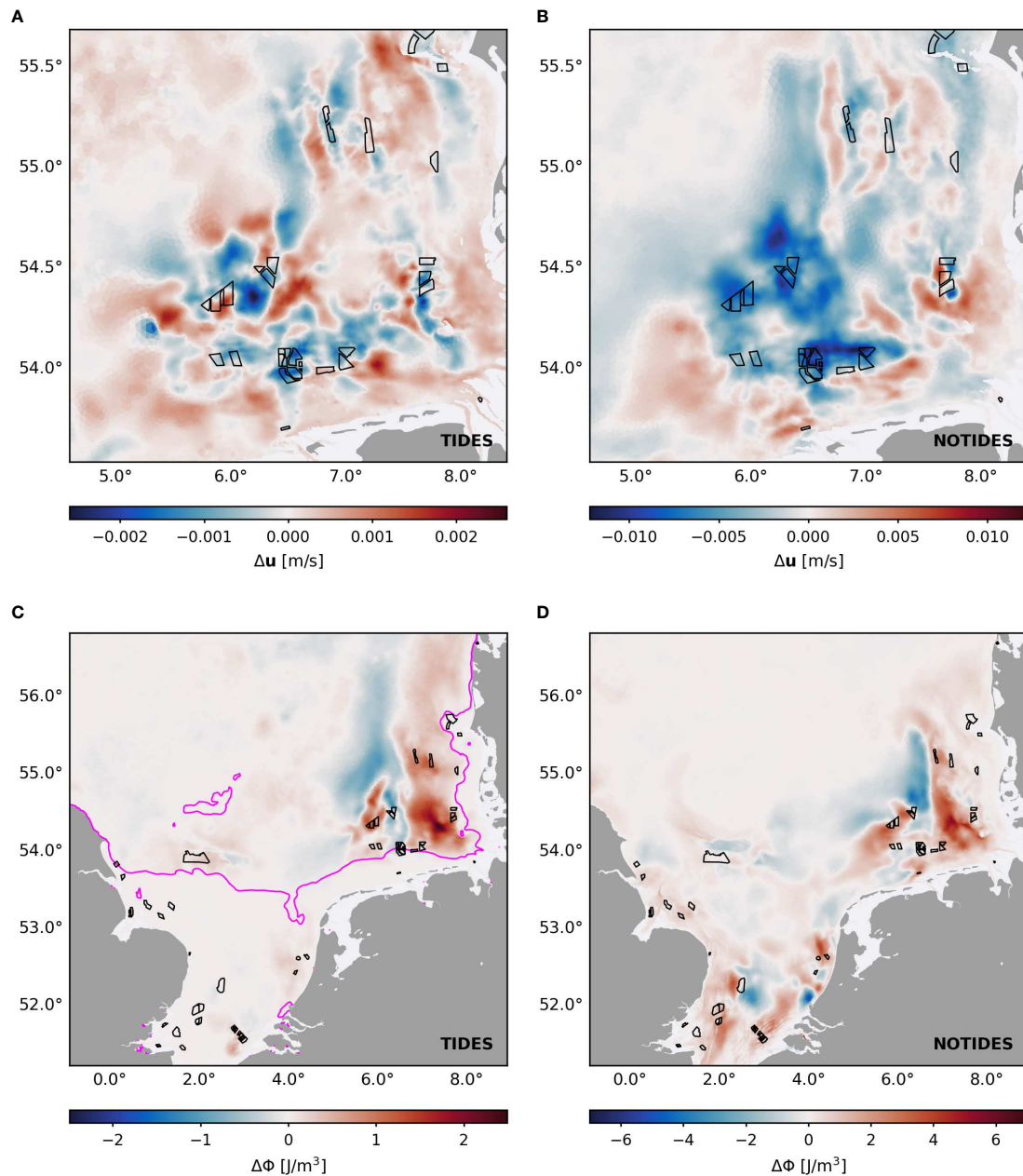


FIGURE 7

Regional mean wake effects on surface velocity u (A, B) and potential energy anomaly ϕ (C, D) in *TIDES* (left) and *NOTIDES* (right). Monthly mean changes are depicted for the simulation period between May and September 2013. Magenta line in (C) indicates the mean tidal mixing fronts in *TIDES*. Black polygons indicate the offshore wind farms.

the effect of hypothetical wind speed reduction on biogeochemistry and, in fact, showed that the anomaly in wind speed resulted in higher ecosystem productivity and lower turbidity. With tidal mitigation, however, wind wake effects are much weaker and thus the potential impact on ecosystem dynamics. Nevertheless, van der Molen et al. also pointed out the counteracting processes of wind wakes and turbulent pile wakes and the need for further investigations, in

order to evaluate the impact on the marine environment and determine the dominant processes.

Conclusion

Tides play an important role in the changes in hydrodynamics caused by atmospheric wind farm wakes. As our analysis showed,

tides have both direct and indirect influences on the wake effects, altering the induced processes due to periodic tidal currents and tide-induced stratification conditions, respectively. While the tidal currents determine how the hydrodynamics respond to the wind speed reductions, stratification conditions and tidal mixing rates determine the impact on vertical transport and density stratification. In previous studies (Ludewig, 2015; Christiansen et al., 2022), the reduction of surface wind speed due to offshore wind farms has been associated to the reduction of the horizontal surface current. Here, however, we showed that tidal currents can deflect and even inverse wake-induced processes. Specifically, the alignment between wind and ocean currents determines the magnitudes of the wake effects. The periodic tidal currents can mitigate the impact of the wind speed reduction over time due to opposing changes in the horizontal flow, resulting in hydrodynamic changes only half as strong as those without tides. This mitigation can translate to secondary wake effects, like the development of sea level dipoles. However, we found that the degree of mixing in the water column is critical for the development of secondary wake effects, such as changes in vertical transport and density distribution. In this regard, induced changes are much more pronounced in stratified waters, whereas in well-mixed waters tidal stirring can influence the effects on vertical transport and attenuate the impact on temperature and salinity stratification.

In the southern North Sea, a tidal-driven environment, the strong tidal currents and the mixing induced by the tides appear to affect the wind wake effects on the hydrodynamics and even attenuate the induced mean changes. In this regard, our simulations suggest that the regional mean impacts in the southern North Sea would be more significant without tides. However, as the impact on the environment depends on the tidal and stratification conditions, the demonstrated attenuation of wake effects does not apply to all regions affected by offshore wind farm wakes. The Esbjerg Declaration 2022 (WindEurope, 2022a) as well as the EU's renewable energy target of 40% by 2030 (WindEurope, 2022b) imply a significant expansion of offshore wind energy in European waters. These include the North Sea but also other marine environments characterized by different tidal regimes, water depths or stratification conditions. In the North Sea, an expansion of wind energy means development into seasonally stratified deeper waters with much lower tidal velocities (see Otto et al., 1990), such as the central or northeastern North Sea. In these regions, tidal mitigation effects will be weaker and wake effects, particularly the secondary wake effects that depend on stratification strength, may develop more strongly, suggesting stronger impact on vertical mixing and density stratification. On the other hand, primary wake effects might be much stronger in marine environments with almost no tidal energy, such as the Baltic Sea, where wind-driven processes are hardly affected by opposing ocean currents. The Baltic Sea, in particular, might be especially vulnerable to instantaneous and mean wind wake effects, as, in addition to

mainly wind-driven and density-driven currents, salinity stratification persists throughout the year, complemented by seasonal temperature stratification (Leppäranta and Myrberg, 2009), and thus favors secondary wake effects. However, regional model simulations are needed to determine the actual response to wind wakes in these environments. Ultimately, we can say it is not only atmospheric conditions that determine the impact of atmospheric offshore wind farm wakes on the ocean, but also the regional hydrodynamic conditions in the respective environment. With this study, we emphasize the importance of the wind-tide interaction on the impact of wake effects on hydrodynamics and provide a guideline for wake effects in different marine environments.

Data availability statement

The raw data supporting the conclusions of this article will be made available by the authors on request.

Author contributions

NC generated the data set, performed the data analysis, and wrote the manuscript with input from all authors. UD and CS contributed to the data analysis and provided critical feedback. All authors contributed to the article and approved the submitted version.

Funding

This project is a contribution to the EXC 2037 'Climate, Climatic Change, and Society (CLICCS)' (Project Number: 390683824) funded by the German Research Foundation (DFG), to the CLICCS-HGF networking project funded by the Helmholtz Association of German Research Centers (HGF), and to the Helmholtz Research Program "Changing Earth – Sustaining our Future", Topic 4.

Conflict of interest

The authors declare that the research was conducted in the absence of any commercial or financial relationships that could be construed as a potential conflict of interest.

The reviewer TP declared a shared affiliation with the author CS to the handling editor at the time of review.

Publisher's note

All claims expressed in this article are solely those of the authors and do not necessarily represent those of their

affiliated organizations, or those of the publisher, the editors and the reviewers. Any product that may be evaluated in this article, or claim that may be made by its manufacturer, is not guaranteed or endorsed by the publisher.

References

- Broström, G. (2008). On the influence of large wind farms on the upper ocean circulation. *J. Mar. Syst.* 74, 585–591. doi: 10.1016/j.jmarsys.2008.05.001
- Cañadillas, B., Foreman, R., Barth, V., Siedersleben, S., Lampert, A., Platis, A., et al. (2020). Offshore wind farm wake recovery: Airborne measurements and its representation in engineering models. *Wind Energy* 23, 1249–1265. doi: 10.1002/we.2484
- Carpenter, J. R., Merckelbach, L., Callies, U., Clark, S., Gaslikova, L., and Baschek, B. (2016). Potential impacts of offshore wind farms on north Sea stratification. *PLoS One* 11, e0160830. doi: 10.1371/journal.pone.0160830
- Christiansen, N., Daewel, U., Djath, B., and Schrum, C. (2022). Emergence of Large-scale hydrodynamic structures due to atmospheric offshore wind farm wakes. *Front. Mar. Sci.* 9. doi: 10.3389/fmars.2022.818501
- Christiansen, M. B., and Hasager, C. B. (2005). Wake effects of large offshore wind farms identified from satellite SAR. *Remote Sens. Environ.* 98, 251–268. doi: 10.1016/j.rse.2005.07.009
- Christiansen, M. B., and Hasager, C. B. (2006). Using airborne and satellite SAR for wake mapping offshore. *Wind Energy* 9, 437–455. doi: 10.1002/we.196
- de Boyer Montégut, C., Madec, G., Fischer, A. S., Lazar, A., and Iudicone, D. (2004). Mixed layer depth over the global ocean: An examination of profile data and a profile-based climatology. *J. Geophys. Res.* 109, C12003. doi: 10.1029/2004JC002378
- Djath, B., and Schulz-Stellenfleth, J. (2019). Wind speed deficits downstream offshore wind parks? A new automated estimation technique based on satellite synthetic aperture radar data. *Meteorologische Z.* 28, 499–515. doi: 10.1127/metz/2019/0992
- Djath, B., Schulz-Stellenfleth, J., and Cañadillas, B. (2018). Impact of atmospheric stability on X-band and c-band synthetic aperture radar imagery of offshore windpark wakes. *J. Renewable Sustain. Energy* 10, 43301. doi: 10.1063/1.5020437
- Dorrell, R. M., Lloyd, C. J., Lincoln, B. J., Rippeth, T. P., Taylor, J. R., Caulfield, C.-c. P., et al. (2022). Anthropogenic mixing in seasonally stratified shelf seas by offshore wind farm infrastructure. *Front. Mar. Sci.* 9. doi: 10.3389/fmars.2022.830927
- Emeis, S. (2010). A simple analytical wind park model considering atmospheric stability. *Wind Energy* 13, 459–469. doi: 10.1002/we.367
- Emeis, S., and Frandsen, S. (1993). Reduction of horizontal wind speed in a boundary layer with obstacles. *Boundary-Layer Meteorology* 64, 297–305. doi: 10.1007/BF00708968
- Emeis, S., Siedersleben, S., Lampert, A., Platis, A., Bange, J., Djath, B., et al. (2016). Exploring the wakes of large offshore wind farms. *J. Physics: Conf. Ser.* 753, 92014. doi: 10.1088/1742-6596/753/9/092014
- Frandsen, S. (1992). On the wind speed reduction in the center of large clusters of wind turbines. *J. Wind Eng. Ind. Aerodynamics* 39, 251–265. doi: 10.1016/0167-6105(92)90551-K
- Frandsen, S., Barthelmie, R., Pryor, S., Rathmann, O., Larsen, S., Højstrup, J., et al. (2006). Analytical modelling of wind speed deficit in large offshore wind farms. *Wind Energy* 9, 39–53. doi: 10.1002/we.189
- Gibson, R. (2003). Go with the flow: tidal migration in marine animals. *Hydrobiologia* 503, 153–161. doi: 10.1023/B:HYDR.0000008488.33614.62
- Hasager, C. B., Vincent, P., Badger, J., Badger, M., Di Bella, A., Peña, A., et al. (2015). Using satellite SAR to characterize the wind flow around offshore wind farms. *Energies* 8, 5413–5439. doi: 10.3390/en8065413
- HZG (2017). “coastDat-3_COSMO-CLM_ERAI,” in *World data center for climate (WDCC) at DKRZ*. Available at: http://cera-www.dkrz.de/WDCC/ui/Compact.jsp?acronym=coastDat-3_COSMO-CLM_ERAI.
- Leppäranta, M., and Myrberg, K. (2009). *Physical oceanography of the Baltic Sea* (Berlin, Heidelberg: Springer). doi: 10.1007/978-3-540-79703-6_3
- Li, X., and Lehner, S. (2013). Observation of TerraSAR-X for studies on offshore wind turbine wake in near and far fields. *IEEE J. Selected Topics Appl. Earth Observations Remote Sens.* 6, 1757–1768. doi: 10.1109/JSTARS.2013.2263577
- Lissaman, P. B. S. (1979). Energy effectiveness of arbitrary arrays of wind turbines. *J. Energy* 3, 323–328. doi: 10.2514/3.62441
- Ludewig, E. (2015). *On the effect of offshore wind farms on the atmosphere and ocean dynamics* (Springer International Publishing: Cham). doi: 10.1007/978-3-319-08641-5
- Otto, L., Zimmerman, J., Furnes, G. K., Mork, M., Saetre, R., and Becker, G. (1990). Review of the physical oceanography of the north Sea. *Netherlands J. Sea Res.* 26, 161–238. doi: 10.1016/0077-7579(90)90091-T
- Paskyabi, M. B., and Fer, I. (2012). “Upper ocean response to Large wind farm effect in the presence of surface gravity waves,” in *Selected papers from Deep Sea Offshore Wind R&D Conference*. (Trondheim, Norway) 24, 245–254. doi: 10.1016/j.egypro.2012.06.106
- Platis, A., Bange, J., Bärfuss, K., Cañadillas, B., Hundhausen, M., Djath, B., et al. (2020). Long-range modifications of the wind field by offshore wind parks? Results of the project WIPAFF. *Meteorologische Z.* 29, 355–376. doi: 10.1127/metz/2020/1023
- Platis, A., Hundhausen, M., Mauz, M., Siedersleben, S., Lampert, A., Bärfuss, K., et al. (2021). Evaluation of a simple analytical model for offshore wind farm wake recovery by *in situ* data and weather research and forecasting simulations. *Wind Energy* 24, 212–228. doi: 10.1002/we.2568
- Platis, A., Siedersleben, S. K., Bange, J., Lampert, A., Bärfuss, K., Hankers, R., et al. (2018). First *in situ* evidence of wakes in the far field behind offshore wind farms. *Sci. Rep.* 8, 2163. doi: 10.1038/s41598-018-20389-y
- Rakovec, O., and Kumar, R. (2022). “Mesoscale hydrologic model based historical streamflow simulation over Europe at 1/16 degree,” in *World data center for climate (WDCC) at DKRZ*. doi: 10.26050/WDCC/mHMBassimEur
- Schrum, C., Alekseeva, I., and St. John, M. (2006). Development of a coupled physical-biological ecosystem model ECOSMO part I: model description and validation for the north Sea. *J. Mar. Syst.* 61, 79–99. doi: 10.1016/j.jmarsys.2006.01.005
- Schultze, L. K. P., Merckelbach, L. M., Horstmann, J., Raasch, S., and Carpenter, J. R. (2020). Increased mixing and turbulence in the wake of offshore wind farm foundations. *J. Geophys. Res. Oceans* 125, e2019JC015858. doi: 10.1029/2019JC015858
- Siedersleben, S. K., Platis, A., Lundquist, J. K., Lampert, A., Bärfuss, K., Cañadillas, B., et al. (2018). Evaluation of a wind farm parametrization for mesoscale atmospheric flow models with aircraft measurements. *Meteorologische Z.* 27, 401–415. doi: 10.1127/metz/2018/0900
- Simpson, J. H., and Bowers, D. (1981). Models of stratification and frontal movement in shelf seas. deep Sea research part a. *Oceanographic Res. Papers* 28, 727–738. doi: 10.1016/0198-0149(81)90132-1
- Simpson, J. H., and Sharples, J. (2012). *Introduction to the physical and biological oceanography of shelf seas* (Cambridge: Cambridge University Press). doi: 10.1017/CBO9781139034098
- Sündermann, J., and Pohlmann, T. (2011). A brief analysis of north Sea physics. *Oceanologia* 53, 663–689. doi: 10.5697/oc.53-3.663
- Sverdrup, H. U. (1953). On conditions for the vernal blooming of phytoplankton. *ICES J. Mar. Sci.* 18, 287–295. doi: 10.1093/icesjms/18.3.287
- Taguchi, E., Stammer, D., and Zahel, W. (2014). Inferring deep ocean tidal energy dissipation from the global high-resolution data-assimilative HAMTIDE model. *J. Geophys. Res. Oceans* 119, 4573–4592. doi: 10.1002/2013JC009766
- van Berkel, J., Burchard, H., Christensen, A., Mortensen, L. O., Svenstrup Petersen, O., and Thomsen, F. (2020). The effects of offshore wind farms on hydrodynamics and implications for fishes. *Oceanography* 33, 108–117. doi: 10.5670/oceanog.2020.410
- van der Molen, J., Smith, H. C., Lepper, P., Limpenny, S., and Rees, J. (2014). Predicting the large-scale consequences of offshore wind turbine array development on a north Sea ecosystem. *Continental Shelf Res.* 85, 60–72. doi: 10.1016/j.csr.2014.05.018

Supplementary material

The Supplementary Material for this article can be found online at: <https://www.frontiersin.org/articles/10.3389/fmars.2022.1006647/full#supplementary-material>

van Leeuwen, S., Tett, P., Mills, D., and van der Molen, J. (2015). Stratified and nonstratified areas in the north Sea: Long-term variability and biological and policy implications. *J. Geophys. Res. Oceans* 120, 4670–4686. doi: 10.1002/2014JC010485

Wilson, R. E. (1980). Wind-turbine aerodynamics. *Wind Energy Conversion Syst.* 5, 357–372. doi: 10.1016/0167-6105(80)90042-2

WindEurope. (2021). *Offshore wind in Europe: Key trends and statistics in 2020*. Available at: <https://windeurope.org/intelligence-platform/product/offshore-wind-in-europe-key-trends-and-statistics-2020/>.

WindEurope (2022a) *The esbjerg offshore wind declaration: The north Sea as a green power plant of Europe*. Available at: <https://windeurope.org/policy/joint-statements/the-esbjerg-offshore-wind-declaration/>.

WindEurope (2022b) *Wind energy in Europe: 2021 statistics and the outlook for 2022-2026*. Available at: <https://windeurope.org/intelligence-platform/product/wind-energy-in-europe-2021-statistics-and-the-outlook-for-2022-2026/>.

Zhang, Y. J., Ye, F., Stanev, E. V., and Grashorn, S. (2016). Seamless cross-scale modeling with SCHISM. *Ocean Model.* 102, 64–81. doi: 10.1016/j.ocemod.2016.05.002

Supplementary Figures

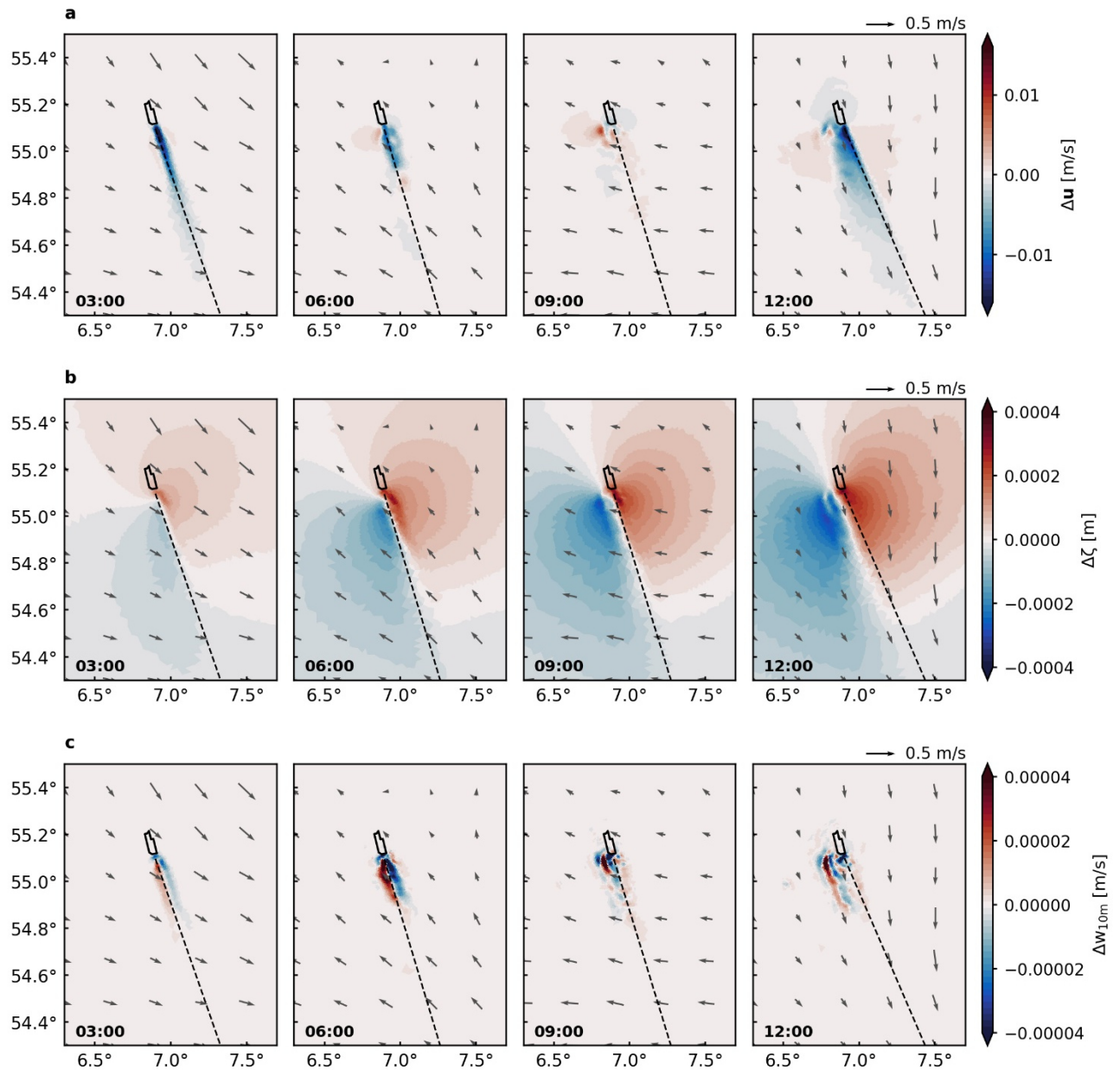


Figure 1: Example of the advection of wake-induced anomalies in horizontal surface velocity u (a), sea surface elevation ζ (b), and vertical velocity w at 10 m depth (c) due to the changing tidal currents. Differences between the simulations with and without wind wakes (*OWF-REF*) are depicted for June 1, 2013. The dashed lines indicate the wind wake axis at each time step. Gray arrows indicate the direction of depth-integrated horizontal currents. Note that for this example only one wind farm, *Sandbank*, has been considered in the model simulations, to avoid superposition of neighboring wind farms. Simulations start on June 1, 2013, 00:00.

4 Study III – Regional Modeling of Structure Drag

This chapter contains the third manuscript, which has not yet been published:

Christiansen, N., Carpenter, J.R., Daewel, U., Suzuki, N. and Schrum, C. (2022). **Regional modeling of structure-induced mixing at offshore wind farm sites.**

Author Contributions:

NC initiated the study, set up the numerical model, generated the data sets, performed the data analysis and wrote the manuscript. NS contributed to the implementation of the drag parameterization. JRC, UD and NS contributed to the data analysis and discussion of the results. CS contributed to the discussion and the design of the study. All authors participated in the conception of this study, and revised and approved the manuscript.

Regional modeling of structure-induced mixing at offshore wind farm sites

Nils Christiansen^{1,*}, Jeffrey R. Carpenter¹, Ute Daewel¹, Nobuhiro Suzuki¹, Corinna Schrum^{1,2}

¹Institute of Coastal Systems, Helmholtz-Zentrum Hereon, Max-Planck-Straße 1, 21502 Geesthacht, Germany

²Institute of Oceanography, Center for Earth System Research and Sustainability, Universität Hamburg, Bundesstraße 53, 20146 Hamburg, Germany

*Corresponding author. Email address: nils.christiansen@hereon.de

Abstract

Structure drag by offshore wind turbines is among the physical stressors of offshore wind energy on marine environments. The flow past vertical cylinders, such as wind turbine foundations, has long been studied through laboratory experiments and model simulations, which showed the development of turbulent mixing downstream of the cylinders. However, questions remain about far field and regional implications of offshore wind infrastructure, as potential effects of structure-induced mixing on physical and biogeochemical processes have been discussed. Here we present two existing modeling approaches for implementing wind turbine foundation effects into ocean models and discuss the problematic use of high resolution in hydrostatic regional modeling. By implementing a low resolution structure drag parameterization into an unstructured-grid model, we demonstrate the impact of monopile drag at regional scale for the German Bight, validated against recent in-situ measurements. Our simulations show that additional turbulence is the driving mechanism behind the monopile impact, affecting not only the mixing but also horizontal currents at wind farm sites. While structure-induced changes are mainly within natural variability, the effects extend over wide areas of the model domain with the most significant changes in stratification development and mean horizontal circulation. This study gives new insights into the hydrodynamic impact of offshore wind farms and emphasizes the need for further research in view of potential restructuring of the future coastal environment.

Keywords: offshore wind farms, structure-induced mixing, turbulence, stratification, modeling

1 Introduction

5,402 offshore wind turbines had been installed in European waters by the end of 2020, and the development is still growing (WindEurope, 2021, 2022). Set out by the EU's Offshore

Renewable Energy Strategy, the EU's offshore wind capacity is expected to increase from the current 12 GW in 2020 (excluding UK) to at least 60 GW in 2030 and 300 GW by 2050 (European Commission, 2020). This implies a massive expansion of offshore wind infrastructure in the European shelf seas and particularly the North Sea, which currently accounts for about 79 % of the total European capacity (WindEurope, 2021). With that in mind, recent studies addressed the potential consequences of offshore wind energy production for the marine environment, emphasizing the need for further investigations with regard to the future coastal ocean (van Berkel et al., 2020; Daewel et al., 2022; Dorrell et al., 2022). The effects of offshore wind farms include, on the one hand, large-scale reductions in wind speed and associated changes in wind-driven hydrodynamic processes (Ludewig, 2015; Christiansen et al., 2022a), and, on the other hand, turbulent mixing processes at local wind farm sites due to flow obstructions from offshore wind turbine foundations (Rennau et al., 2012; Carpenter et al., 2016). Here we focus on the latter effects, in particular the potential influence of additional mixing induced by offshore wind turbine foundations on regional hydrodynamics.

Flow past offshore wind turbine foundations is comparable to cylindrical structures in a horizontal flow. The flow characteristics around a vertical cylinder in a steady homogenous current have long been studied by numerous studies using laboratory experiments or high-resolution numerical simulations (Williamson, 1996; Sumer and Fredsøe, 2006). The cylindrical obstacles hinder the horizontal flow and create complex downstream wake patterns consisting of different shear layer at the boundary of the structures and in the downstream wake area (Williamson, 1996). In unstratified waters, arising flow patterns are determined by the ratio of inertial forces to viscous forces, described by the Reynolds number

$$Re = \frac{u_{\infty} d}{\nu}, \quad (1)$$

where u_{∞} is the undisturbed flow velocity, d the diameter of cylinder and ν the kinematic viscosity of the fluid. The dominant feature of the downstream wake pattern is the development of a Karman vortex street due to vortex shedding, which occurs already for laminar flows with $Re > 40$ (Williamson, 1996; Sumer and Fredsøe, 2006). With increasing Reynolds number, the vortex street changes from laminar to turbulent ($200 < Re < 300$) and from two-dimensionality to three-dimensionality ($Re > 300$), eventually becoming unsteady and highly turbulent (Sumer and Fredsøe, 2006). In contrast, flow past a cylinder in stratified waters is yet less well understood (Dorrell et al., 2022).

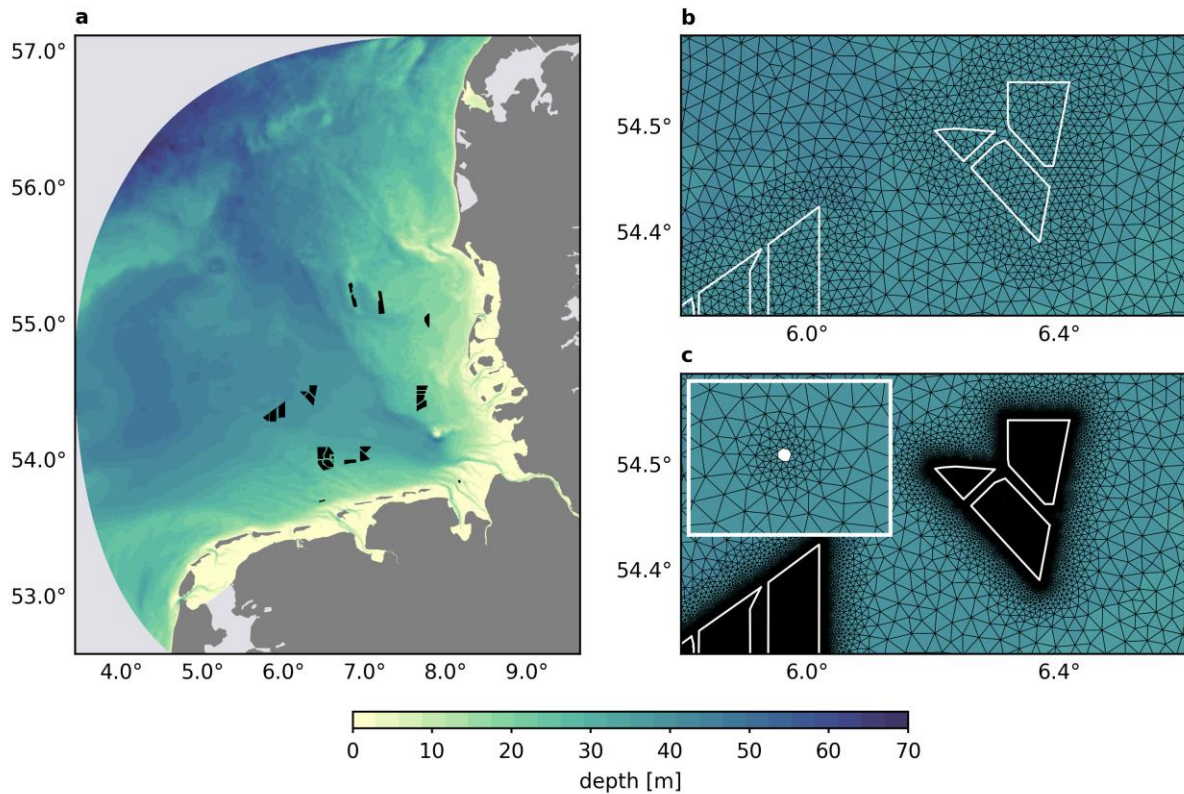


Figure 1: Bathymetry of the German Bight setup (a). Black polygons represent commissioned and under construction offshore wind farms in the German Exclusive Economic Zone (status as of November 2021; data obtained from <https://www.4coffshore.com/windfarms/>). (b) Horizontal grid resolution for the body force approach, using a grid size of about 1000 m inside wind farms. (c) Horizontal grid resolution for the dry cell method around the wind farms (white polygons) and a single wind turbine (small panel). The wind turbine locations have been obtained from <https://www.marktstammdatenregister.de/MaStR>.

Generally speaking, cylindrical obstacles in horizontal flows reduce the downstream flow velocity and create turbulence depending on the Reynolds number. In shelf seas, such as the North Sea, turbulence results in high Reynolds number flows (Simpson and Sharples, 2012) and thus typical Reynolds numbers at offshore wind turbine foundations are expected to be at least $Re > 10^5$ (Dorrell et al., 2022). Consequently, the wakes behind offshore wind farms can be expected highly turbulent and three-dimensional. There are few studies that measured occurring turbulent wakes under natural conditions. In an early study, Lass et al. (2008) showed that turbulent wakes behind bridge piles, analogous to turbine foundations, enhanced the vertical mixing within a distance of about 50 pile diameters at high Reynolds numbers in a stratified flow in the Baltic Sea and ultimately affected the stratification strength behind the piles. Vanhellemont and Ruddick (2014) and Forster (2018) showed observations of turbulent sediment plumes downstream of offshore wind turbines in the southern North Sea with wake lengths exceeding 1000 m. Recent observations in the German Bight confirmed the assumptions about induced mixing at wind farm sites and emphasized

the effects on density stratification (Floeter et al., 2017; Schultze et al., 2020). On the one hand, Floeter et al. (2017) measured high-resolution vertical profiles through different offshore wind farms, demonstrating the weakening of stratification within the wind farms associated to increased vertical mixing. Although not completely separable from natural variability, potential energy anomaly within wind farms decreased by about 5-10 J/m³. On the other hand, the survey by Schultze et al. (2020) showed that the induced mixing by a wind turbine foundation in a stratified environment reduced the potential energy anomaly along the wake by about 65 % at maximum (Dorrell et al., 2022). At this, mixing by a single monopile accounted for about 10 % of the mixing triggered by bottom boundary layer turbulence (Schultze et al., 2020).

In order to estimate the magnitude of structure-induced mixing at offshore wind farm side, modeling approaches started to consider additional turbulence production by offshore wind farms (Rennau et al., 2012; Carpenter et al., 2016). By adding additional production terms in the turbulence closure scheme of a regional-scale model, Rennau et al. (2012) showed that vertical mixing by hypothetical offshore wind turbines in the western Baltic Sea reduced local bottom salinities by about 0.2 g/kg. At this, occurring salinity anomalies extended several tens of kilometers into the Baltic Sea. With a similar approach deriving a TKE production model, Carpenter et al. (2016) estimated that structure-induced turbulence is associated to a loss of tidal energy of about 4-20 % of that by bottom boundary layer turbulence in seasonally stratified waters. However, both studies concluded that the impact on regional stratification at recent states of offshore wind energy development (2010 and 2016, respectively) is small and comparable to natural variability, whereas with regard to future offshore wind expansion significant effects on stratification could emerge in the German Bight and the Baltic Sea, respectively.

Effects on stratification raise concerns about the environmental impact of offshore wind infrastructure, particularly with respect to future development. However, apart from the initial estimates by Carpenter et al. (2016), implications by structure-induced turbulence have yet rarely been addressed at regional scales. In shelf and marginal seas such as the North Sea, stratification plays an important role in hydrodynamics and particularly biogeochemical processes, like nutrient availability and primary production, which are determined by the physical processes (Simpson and Sharples, 2012; Daewel and Schrum, 2013). Therefore, enhanced mixing rates due to offshore wind turbine foundations could not only strongly affect the thermocline evolution but also ecosystem dynamics at temporal and spatial scales (Dorrell et al., 2022). Investigations of the processes at offshore wind turbine foundations and their environmental impact, however, become complex due to the

scale of the effects of $\mathcal{O}(10^{-2}-10^4)$ m (Dorrell et al., 2022). While laboratory experiments and high-resolution non-hydrostatic models enable to resolve fine scale processes at the foundations, low-resolution hydrostatic models are necessary to capture the large-scale aspects of the wake effects. Further research into the impact by structure-induced mixing is nevertheless essential to assess potential changes to the marine environment and identify possible mitigation measures for negative impact by renewable energy production.

In this study, we approach the complexity of structure-induced mixing at offshore wind turbine foundations by using low-resolution numerical modeling. In this context, we aim to evaluate the environmental impact by offshore wind turbines and to determine the necessity of regional consideration of the pile effects. We address different approaches how to incorporate the pile effects into the regional model framework, following previous studies, e.g., by Rennau et al. (2012) and Cazenave et al. (2016), and discuss their strengths and weaknesses and limitations of the hydrostatic assumptions. The groundwork for the analysis is a three-dimensional hydrodynamic model setup for the German Bight, which allows resolving structure-induced processes at high resolution by unstructured horizontal grids.

2 Methods

2.1 Model Description

Focus of this study is on the German Bight region and the physical implications by German offshore wind farms in the shallow coastal waters. As part of the southern North Sea, the German Bight is characterized by oceanic influences from the central North Sea, but is mainly influenced by coastal features such as fresh water inflow and shallow bathymetry (Sündermann and Pohlmann, 2011). Tidal energy and wind forcing determine the dynamics of the shallow waters and result in different hydrodynamic regimes of well-mixed waters and seasonally stratified waters, depending on local bathymetry (Otto et al., 1990; Sündermann and Pohlmann, 2011; van Leeuwen et al., 2015).

To enable representation of the wake effects inside offshore wind farms at higher resolution, we developed a model setup grounded on unstructured horizontal grids. For this, we utilized the three-dimensional Semi-implicit Cross-scale Hydroscience Integrated System Model (SCHISM), which is a hydrostatic numerical model using Reynolds-averaged Navier-Stokes equations based on the Boussinesq approximation (Zhang et al., 2016). The model domain covers the German Bight region, from the northeastern Dutch coast in the south to the northeastern Danish coast in the north (Figure 1a). At this, our model setup acts as a nested domain within a larger Southern North Sea model introduced by Christiansen et al. (2022a),

as the simulations were driven at the lateral open boundary by the output data from the enveloping model simulations. Note that wind wake effects from offshore wind farms, which have been studied by Christiansen et al. (2022a), were not included in the boundary data.

The model simulations were conducted for the time period of May to September 2013, to emphasize the effect of structure-induced mixing on the stratification development and to allow comparison to the demonstrated wind wake effects (Christiansen et al., 2022a; 2022b). For the initial state of the new model setup and the open boundary conditions, we obtained sea surface elevation, temperature, salinity, and horizontal velocity from the enveloping Southern North Sea model. Additionally, tidal forcing by eight constituents (M_2 , S_2 , K_2 , N_2 , K_1 , O_1 , Q_1 , P_1), daily river discharge, and hourly atmospheric forcing were applied similarly to the governing simulations. A detailed description of the Southern North Sea model setup can be found in Christiansen et al. (2022a; 2022b).

Horizontal and vertical grid cell resolution have been adjusted compared to the former setup. Here, we used an overall finer horizontal grid resolution varying between 750 m at the coast and 2000 m in the open ocean. The final number of horizontal grid cells depended on the wind turbine implementation used. Vertically, the depth-depending layer thickness of the localized sigma coordinates (Zhang et al., 2015) varied between one meter near the sea surface to four meters in deep bottom layers, resulting in a maximum of 36 vertical layers. The time step of the simulations was between 90 s to 120 s, depending on the wind turbine implementation. Output data is written with an hourly time step.

For the analysis, we illustrate the changes between simulations with wind farm effects (*OWF*) and reference simulations without wind farm effects (*REF*) by depicting the differences (*OWF-REF*). In this context, the data are averaged over time before the differences are calculated. For vector quantities, like velocities, we distinguish between the differences in absolute values of velocity Δu_{abs} (*current speed*) and the differences in the velocity vector Δu (*current velocity*):

$$\Delta u_{abs} = \langle |\vec{u}_{OWF}| \rangle - \langle |\vec{u}_{REF}| \rangle, \quad \Delta u = |\langle \vec{u}_{OWF} \rangle| - |\langle \vec{u}_{REF} \rangle|, \quad (2)$$

where $\langle \rangle$ indicates the temporal mean and $||$ the absolute value of the velocity vector.

2.2 Implementation of Offshore Wind Turbine Effects

Incorporating the small-scale processes at vertical cylinders into the regional model frame presents a number of numerical challenges. The extreme scale differences of the processes associated with flow past vertical cylinders ($\mathcal{O}(10^{-2}-10^4)$ m) make it nearly impossible to capture all flow characteristics with the same modeling approach, and therefore models

require certain limitations and assumptions. Here, we focus on the two most prominent approaches used in the recent literature, namely drag parameterization at low resolution (Rennau et al., 2012) and explicit representation of wind turbine foundations at very high resolution (Christie et al., 2012; Cazenave et al., 2016). While these approaches have been able to resemble wake processes, the regional modeling approaches should be adopted with care, as the actual processes are still not fully understood (Dorrell et al., 2022) and results are difficult to validate due to a lack of comparable observations and measurements.

Perhaps the greatest limitation in modeling of the small-scale pile effects arises from the hydrostatic assumptions in regional applications. For geophysical flows, like ocean currents, the horizontal scales are usually much larger than vertical scales and therefore the latter are typically neglected in the equations of regional models (Haidvogel and Beckmann, 1998; Cushman-Roisin and Beckers, 2011). This concerns the equations of motion but also the turbulence closure. Consequently, hydrostatic regional modeling becomes appropriate for mesoscale features or larger dynamics, but is limited in the treatment of small-scale non-hydrostatic processes (Haidvogel and Beckmann, 1998). Therefore, high grid resolution, which contradicts the hydrostatic assumption, can cause problems, regardless of the implementation approach. On the other hand, the hydrostatic model by definition underrepresents the non-hydrostatic wake turbulence that is expected for highly turbulent wakes at $Re > 10^5$ in the shelf sea waters.

2.2.1 Parameterization of Monopile Drag and Wake Turbulence

Structure-induced mixing by offshore wind turbine foundations can be accounted for by parameterizing the drag force that a vertical cylinder exerts on the horizontal flow. In an unstratified flow perpendicular to a vertical cylinder, the drag by the cylinder can be expressed as

$$\vec{F}_d = -\frac{1}{2}\rho_0 C_d A |\vec{u}| \vec{u}, \quad (3)$$

where ρ_0 is the density of the fluid, C_d is the drag coefficient, A is the frontal area of the cylinder that is exposed to the free stream, and \vec{u} is the velocity of the free stream (Carpenter et al., 2016). This parameterization is similar to vegetation canopy models (Wilson and Shaw, 1977; Svensson and Häggkvist, 1990) and has been used by different studies to estimate additional anthropogenic mixing from offshore wind turbine foundations (Rennau et al., 2012; Carpenter et al., 2016; Rivier et al., 2016). Although the parameterization was developed for unstratified flow, Rennau et al. (2012) suggested that the basic principles of the approach also apply for stratified flow.

Here, we consider the pile drag via the model equations, following Rennau et al. (2012) and Rivier et al. (2016). For the implementation into the model equations, the horizontal drag per grid box divided by mass is given by

$$\vec{G}_d = -\frac{1}{2}C_d N \frac{d}{A_c} |\vec{u}| \vec{u}, \quad (4)$$

where d is the diameter of the cylinder, A_c is the horizontal area of the grid cell containing the cylinders, and N is the number of cylinders per grid cell (Rennau et al., 2012). To account for deceleration at grid cells containing offshore wind turbines, the drag parameterization is added to the hydrostatic momentum equation of the SCHISM model, defined as

$$\frac{D\vec{u}}{Dt} = \frac{\partial}{\partial z} \left(\nu \frac{\partial \vec{u}}{\partial z} \right) - g \nabla \eta + \vec{F} + \vec{G}_d, \quad (5)$$

with the vertical coordinate z and the time t , g as the gravitational acceleration, \vec{u} as the horizontal velocity, ν as the vertical eddy viscosity, η as the free-surface elevation, and \vec{F} as additional forcing terms, such as baroclinic gradient, horizontal viscosity or Coriolis force (Zhang et al., 2016). Note that in SCHISM horizontal velocities are calculated at the sides of grid elements.

In order to account for the production of subgrid-scale wake turbulence, the drag force is also added to the turbulence closure scheme for turbulent kinetic energy and its dissipation (Svensson and Häggkvist, 1990; Rennau et al., 2012; Rivier et al., 2016). Using the generic length-scale model (Umlauf and Burchard, 2003) in SCHISM, the modified turbulent kinetic energy k and dissipation ε are calculated as

$$\frac{\partial k}{\partial t} = \frac{\partial}{\partial z} \left(\nu_k \frac{\partial k}{\partial z} \right) + P + B - \varepsilon + P_d, \quad (6)$$

$$\frac{\partial \varepsilon}{\partial t} = \frac{\partial}{\partial z} \left(\nu_\varepsilon \frac{\partial \varepsilon}{\partial z} \right) + \frac{\varepsilon}{k} (c_1 P + c_3 B - c_2 \varepsilon F_{wall} + c_4 P_d), \quad (7)$$

where ν_k and ν_ε are vertical turbulent diffusivities, F_{wall} is a wall proximity function, P is the shear production, B is the buoyancy production, and $P_d = -\vec{G}_d \cdot \vec{u}$ is the additional production term due to wake turbulence. $c_1 - c_4$ are model-specific weighting parameters for the dissipation source and sink terms (Umlauf and Burchard, 2003), defined in SCHISM as $c_1 = 1.44$, $c_2 = 1.92$ and $c_3 = -0.52$ for the $k - \varepsilon$ model. While Rivier et al. (2016) defined $c_4 = c_2$, Rennau et al. (2012) demonstrated the importance of the definition of c_4 and its physical implications by showing that mixing efficiency is reduced for $c_4 > c_1$ and enhanced for $c_4 < c_1$. In this context, Rennau et al. (2012) determined a critical upper limit value of $c_4 = 1.75$ and suggested $c_4 = 0.6$ for strong mixing scenarios and $c_4 = 1.4$ for weak mixing scenarios.

In general the results of the drag parameterization are strongly dependent on the choice of scaling parameters in the drag formulation, more precisely the diameter d and the drag

coefficient C_d , of which the latter has the largest uncertainty. From experimental studies, drag coefficients by a cylinder in an unstratified fluid are expected between $C_d = 0.2$ and $C_d = 1.3$ (Shih et al., 1993; Sumer and Fredsøe, 2006), depending on, for example, the turbulence intensity and the surface roughness. As these conditions can vary by location and flow properties, choosing a fixed drag coefficient may continuously over- or underestimate the frictional processes. Furthermore, in stratified fluids, the drag coefficient becomes additionally dependent on local stratification and thus eventually a function of location, depth and time, in addition to the structure geometry (Dorrell et al., 2022). Carpenter et al. (2016) showed how different drag conditions influence the results of the drag parameterization. For a low-turbulence scenario ($C_d = 0.35$) with *tripile* foundations and a high-turbulence scenario ($C_d = 1.0$) with *tripod* foundations, structure-induced power removal can differ by a factor of 4.6, demonstrating the uncertainty in structure-induced mixing as a function of structure properties. This uncertainty has to be taken into account when interpreting the results of the canopy-like approach.

In the following, the drag parameterization approach is referred to as the *body force* approach or *body force* method.

2.2.2 Explicit Implementation of Monopile Cylinders

Another, more obvious, approach is to incorporate offshore wind turbine foundations as full-depth vertical cylinders into the horizontal model grid, i.e., as fine-scale islands. This *dry cell* method requires very high grid resolution around wind turbine locations in order to resolve the small-scale structures. As this implies a large number of small grid cells around the cylinders, the computational effort of this approach can be huge. Using the dry cell method in regional unstructured-grid models, recent studies (Christie et al., 2012; Cazenave et al., 2016) have been able to resemble downstream wake patterns at offshore wind turbines, looking similar to sediment plume patterns observed by Forster (2018). However, while this approach has been used in literature before, the dry cell method is associated to a number of numerical challenges, which will be presented and discussed in this study.

The limitations of the explicit representation of monopile foundations in the regional model do not arise from the dry cells themselves but from the use of very high resolution, which is incompatible with the hydrostatic assumptions and the numerical constraints of the region model. On the one hand, small grid cells near the wind turbine foundations permit the development of non-hydrostatic vertical circulation that are not accounted for by the hydrostatic model equations and thus lead to spurious modes and invalid results. On the other hand, the small grid cells violate the stability criteria of the semi-implicit SCHISM

model at an invariant time step, leading to instabilities and physically unreasonable simulations.

As a semi-implicit model, the SCHISM model uses a combination of implicit and explicit schemes, which results in two constraints for the temporal and spatial discretization: an inverse Courant–Friedrichs–Lewy criterion of $CFL \approx \frac{dt}{dx} > 0.4$, and an operating range for the time step between 100–200 s for baroclinic applications (*SCHISM v5.7 User Manual*). Given that, small grid sizes of $\mathcal{O}(10^0\text{--}10^1)$ m cannot satisfy both constraints simultaneously and thus results in numerical diffusion in form of noise or dissipation.

Eventually, the dry cell approach is creating spurious modes and numerical noise in small-scale grid cells, due to numerical or model-specific limitations. These instabilities can be mitigated by using additional viscosity implementations in the small grid cells, which remove spurious modes below the sampling limit of the horizontal resolution by averaging velocities of neighboring grid nodes (Zhang et al., 2016). While recent studies used the Smagorinsky model to control sub-grid scale instabilities (Christie et al., 2012; Cazenave et al., 2016), here we use the 5-point Shapiro filter implemented in the SCHISM model (Zhang et al., 2016). Note that despite filtering, contradiction between high grid resolution and the hydrostatic model assumptions remain.

2.3 Model Simulations

Using the two implementations, we conducted several studies to analyze the methods and the impact of structure-induced mixing, while taking into account offshore wind farms in the German Exclusive Economic Zone (Figure 1a). The simulation period was chosen between May and September 2013. This period was chosen to analyze the impact of wake turbulence on summer stratification on the one hand and to allow comparison to demonstrated effects by atmospheric wind wakes from offshore wind farms (Christiansen et al., 2022a; Christiansen et al., 2022b) on the other hand. For both implementations, we assumed monopile foundations for simplicity with a diameter of $d = 8$ m, based on available industry information (Merkur Offshore). Regarding the many factors influencing the foundation drag, the monopile assumption is reasonable for a generalized impact study.

For the body force approach, we selected different combinations of drag coefficients and mixing parameters (see Table 1) in order to discuss their impact on the resulting wake effects. The values are based on earlier studies (Rennau et al., 2012; Carpenter et al., 2016). Whereas Rennau et al. (2012) used a horizontal grid resolution of 900 m, here, we will discuss the impact of different horizontal discretizations between 250 m and 1000 m at offshore wind farm sites. For the latter (Figure 1b), the horizontal grid of the body force approach results in

approximately 78 K nodes and 152 K triangles. Simulations were conducted with the a time step of 120 s, similar to governing Southern North Sea simulation (Christiansen et al., 2022a).

Due to its limitations, the dry cell approach requires a tradeoff between process accuracy, numerical stability, and computational efficiency. Although numerical instabilities are inevitable for this approach, we aimed to moderate the numerical noise by using coarser resolution than previous studies, who used 2.5 m resolution or lower at the monopile foundations (Christie et al., 2012; Cazenave et al., 2016). Here, we chose a grid resolution of about 4 m around the cylinders, almost linearly increasing to about 1000 m over a five-kilometer radius of the wind turbines (Figure 1c). In addition, we applied the Shapiro filter with a maximum damping factor of 0.5 and in five-fold iteration. While stronger iteration of the filter would increase the effect on spurious modes, we tried not to manipulate the hydrodynamics significantly, since stronger filtering implies stronger artificial viscosity around the wind turbines. In order to reduce the computational cost and allow seasonal simulations, we reduced the number of wind farms to six, which are all located in stratified deep waters of the German Bight (see Figure 1c). Still, the setup results in approximately 1.4 million nodes and 2.8 million triangles. Simulations were conducted with a time step of 90 s to relax the stability criterion violations in small grid cells. Although this time step already falls below the suggested operating range, numerical diffusion takes place in any case due to the very high resolution.

Table 1: List of conducted model simulations involving wind turbine implementations.

Simulation Parameters			Foundation Parameters			
method	dt [s]	dx [m]	d [m]	C_d	c_4	
dry cell	90	4	-	-	-	-
body force	120	250	8	0.63	1.0	
body force	120	1000	8	0.35	1.4	
body force	120	1000	6	0.63	1.0	
body force	120	1000	8	0.63	1.0	
body force ^a	120	1000	8	0.63	1.0	
body force ^b	120	1000	8	0.63	1.0	
body force	120	1000	8	1.0	1.0	
body force	120	1000	8	1.0	0.6	

^a drag only in momentum equations, ^b drag only in turbulence closure

3 German Bight Scenarios

3.1 Validation of Wind Turbine Implementations

Both the flow resistance of the dry cells and the drag of the body force affect the hydrodynamics in adjacent grid cells of offshore wind turbines. The main difference lies in the physical representation of the downstream wake structures related to the choice of horizontal grid resolution, which is discussed in the following. In fact, the comparison elucidates the usage of high and low resolution in hydrostatic regional modeling, while showing the consequences in relation to structure-induced mixing by offshore wind turbine foundations. Note that due to the different time steps of the simulations, the two approaches may exhibit minor differences in general.

The small-scale vertical structures in the dry cell approach deflect the local horizontal flow and generate distinct wake patterns downstream of the wind turbines (Figure 2a). The wakes extend well downstream of the monopiles with an average length of about 600 m (Supplementary Figure 1) are consistent with recent sediment plume observations by Vanhellemont and Ruddick (2014) and Forster (2018). At this, wake lengths exceed the spacing distance between neighboring wind turbines and affect upstream flow conditions. The magnitudes of the reductions in depth-averaged velocity are on average about 0.11 m/s in 10 m distance behind the monopiles and about 0.01-0.02 m/s in 50-100 m downstream distance (Supplementary Figure 1b). While this is in agreement with the surface velocity anomalies of about 0.05 m/s simulated by Cazenave et al. (2016), momentum extraction is strongly underrepresented by the hydrostatic dry cell method. Using the drag equation (Equation (3)) and assuming an average velocity of about 0.3 m/s, theoretical estimates result in reductions of about 0.34 m/s and 0.03-0.06 m/s, respectively, and thus flow alterations about three times larger as simulated here. The underestimation of momentum extraction by the dry cell approach might be related to insufficient drag of the vertical cylinders at a horizontal resolution of $\mathcal{O}(10^0)$ m, but more importantly is the result of the numerical constraints in the small grid cells.

To obtain appropriate wake structures as shown here, the application of the viscosity-like filter, e.g., the Shapiro filter, is necessary to avoid severe numerical noise. Otherwise, numerical instabilities and non-hydrostatic spurious modes originating from the small grid cells around the turbines superimpose the actual wake patterns (see Supplementary Figure 2a). Here, five-fold iteration of the Shapiro filter and a resolution of 4 m at monopiles seems to be sufficient to mitigate noise. However, not only instabilities but also the wakes are sensitive to the filtering, as this adds artificial viscosity to the small grid cells. The filter

attenuates spurious modes but also affects the dynamic properties of the horizontal flow. Consequently, in the present case, for example, a twenty-fold iteration of the Shapiro filter would result in shorter and broader downstream wake structures (see Supplementary Figure 2c), and affects the drag processes.

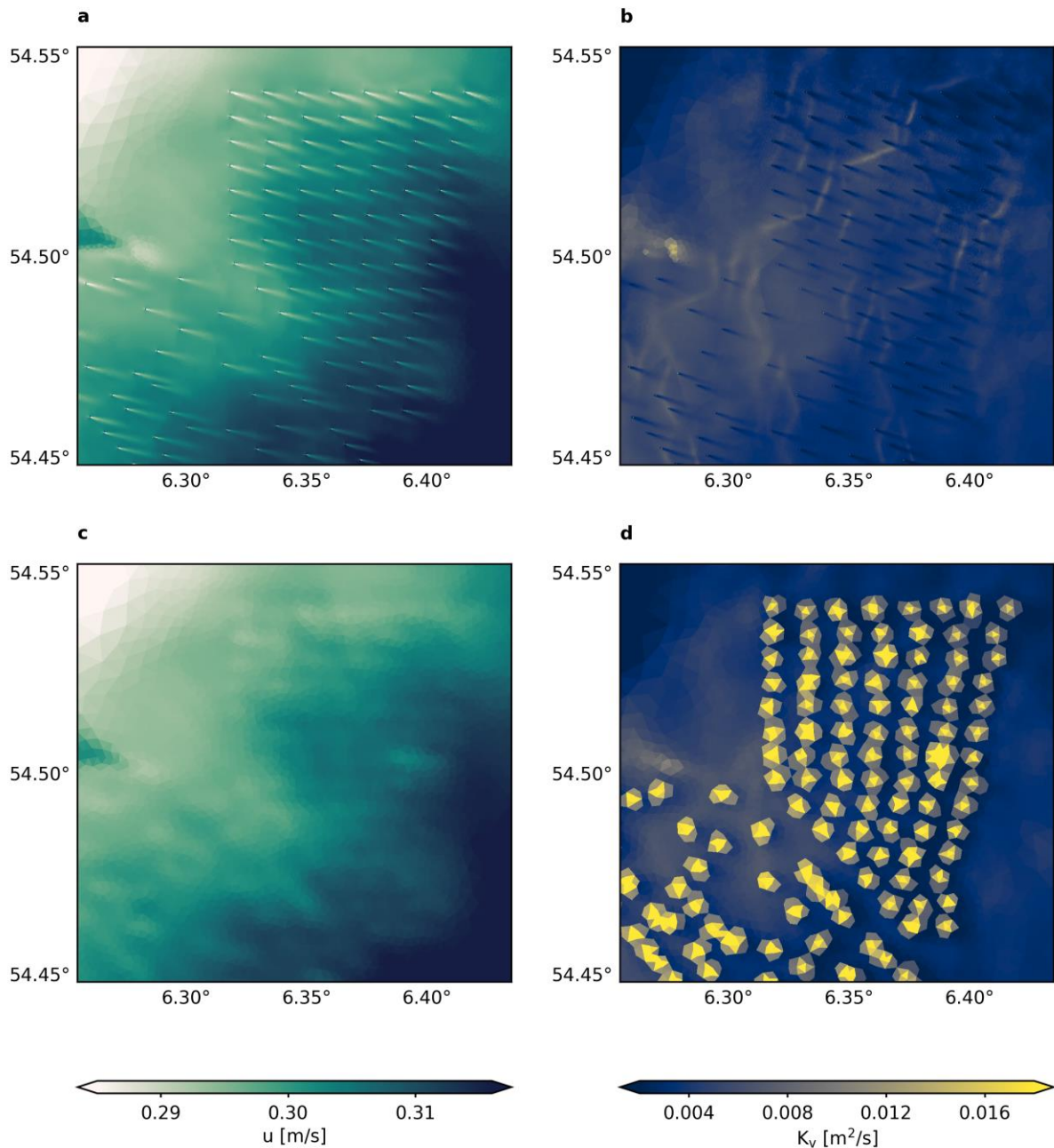


Figure 2: Simulated wake effects at Global Tech I after one hour of simulation for depth-averaged horizontal velocity u (a,c) and depth-averaged vertical eddy diffusivity K_v (b,d). Top panel show wake patterns for the dry cell approach (a,b), bottom panels show wake effects for the body force approach ($C_d = 0.63$ and $c_4 = 1.0$) at 1000 m resolution (c,d). Note that minor deviations between the two approaches may generally occur due to the different time steps used for the simulations.

Apparently, very high horizontal grid resolution in hydrostatic regional models produces insufficient wake patterns, which are strongly sensitive to the numerical measures, making the dry cell approach seem inappropriate for studying the effects of monopile drag. This assumption is emphasized by the associated patterns in the vertical diffusivity, which is a measure for the vertical mixing rate. Unlike laboratory experiments (Williamson, 1996), the hydrostatic dry cell approach does not produce additional turbulent mixing along the wakes. Instead, the vertical mixing rates downstream of the wind turbine foundations even decrease (Figure 2b). The absence of additional turbulence is related to the reduction of vertical shear inside the wakes and the lack of horizontal shear production in the turbulence closure equations (Equation (6),(7)) due to the hydrostatic assumption. Consequently, structure-induced mixing is significantly underrepresented in the hydrostatic dry cell approach, which will bias the effects on density stratification and turbulent mixing. Thus, as also noted by van Berkel et al. (2020), regional implementation of the dry cell approach without additional mixing parameterization should be interpreted with caution.

The body force approach allows to use low resolution at wind farm sites and thus to avoid numerical instabilities or contradictions with the hydrostatic assumptions. Here, we start by using a horizontal resolution of about 250 m inside wind farms for illustration of the momentum extraction and additional wake turbulence at monopile grid cells. However, note that this horizontal discretization is slightly below the lower limit of the CFL criterion and thus might bias the magnitudes. At scales on the order of 10^2 m, the processes at wind farm can be considered hydrostatic, while the amount of turbulence from non-hydrostatic sub-grid scale processes can be prescribed by the drag equation. Consequently, the body force approach becomes much more reliable, despite not resolving the actual wakes.

The drag parameterization generates generally weaker, indistinct velocity anomalies at wind turbines sites due to consideration of the larger grid cell size (Figure 2c). Nevertheless, the anomalies in depth-averaged horizontal velocity extend similarly in downstream directions as the highly resolved wake patterns. The disadvantage of the body force method is the use of uncertain model parameters, like the drag coefficient, which can lead to uncertainties with regard to the simulated magnitudes. Here, the initial values for the drag coefficient C_d and the mixing parameter c_4 are based on Rennau et al. (2012), assuming moderate mixing with $C_d = 0.63$ and $c_4 = 1.0$. Using these values, depth-averaged horizontal velocity decreases by about 0.01 m/s compared to adjacent grid cells.

In terms of turbulent mixing, the SCHISM model limits the advantages of the body force approach, as the $k - \varepsilon$ equations do not account for advection of turbulence and therefore structure-induced mixing cannot be transported downstream. Consequently, additional

vertical diffusivity develops locally at the predefined wind turbine elements (Figure 2d). Since wakes have been shown to extend much further than 250 m (Vanhellemont and Ruddick, 2014; Forster, 2018; Schultze et al., 2020), the small grid cells might underrepresent the turbulent mixing inside offshore wind farms. Thus, to account for advection of turbulence, horizontal grid resolution should be of similar magnitude to the expected wake structures. Here, we propose a horizontal resolution of about 1000 m, covering the observations of both Forster (2018) and Schultze et al. (2020). The importance of resolution inside wind farms will be discussed later.

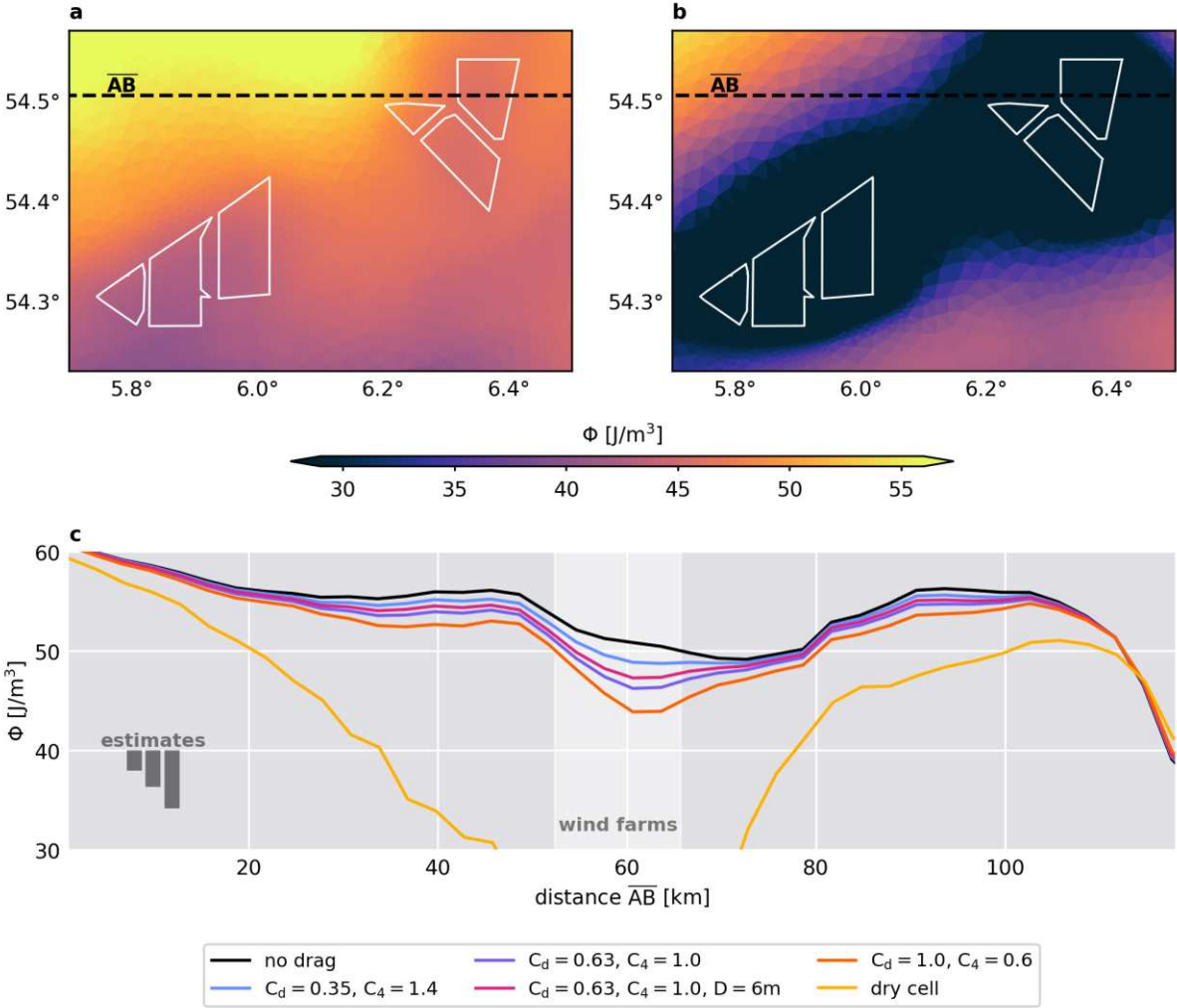


Figure 3: Mean potential energy anomaly Φ in July 2013 for the body force approach (a) and the dry cell approach (b). White polygons represent offshore wind farms, black dashed line indicates the course of profile \overline{AB} . (c) Potential energy anomaly Φ along profile \overline{AB} for different scenarios. White area indicates location of the intersected wind farms. Gray vertical bars show estimated changes in potential energy anomaly, using $C_d = 0.35, C_d = 0.63, C_d = 1.0$ (left to right).

Since additional mixing is added via the wind turbine implementation, it is important to validate its influences on physical ocean processes. To date, however, there are few in-situ measurements of turbine wake structures within offshore wind farms, especially in stratified waters (Floeter et al., 2017; Schultze et al., 2020). Following the observation period given in Floeter et al. (2017), we analyze here the changes in summer stratification and compare them with the observations. Figure 3 shows the mean stratification strength, described by the potential energy anomaly, in July 2013 in the region of the Global Tech I wind farm. As the wind farms are located near frontal regions and water depth decreases, stratification generally decreases from northwest to southeast in the example region and the spatial variability of stratification is about 10–15 J/m³ without offshore wind farms. For the moderate mixing case, using $C_d = 0.63$ and $c_4 = 1.0$, the body force approach produces small anomalies in mean potential energy anomaly around offshore wind farms, with reductions of about 5–10 J/m³ compared to surrounding areas (Figure 3a). At this, stratification changes can vary by location or wind turbine density. While these magnitudes are within the spatial variability and also natural annual and interannual variability, the changes are comparable to the observations of Floeter et al. (2017), although fewer wind farms were installed at the time of the measurements.

To verify the simulated stratification changes, the theoretical model derived by Carpenter et al. (2016) is used here as additional reference. The model estimates structure-induced changes in stratification by offshore wind farms based on the time a water parcel spends inside a wind farm, the power removed by the structure from the flow, and the pycnocline thickness at the wind farm site. Here, we use Equation (4) to calculate the power consumption per unit area, estimate the thermocline thickness using a threshold of vertical temperature difference of 0.2 °C (Boyer Montégut et al., 2004), and calculate residence times through the mean current velocity and the size of the Global Tech I wind farm. For $C_d = 0.63$ and an estimated thermocline thickness of 9 m, the theoretical reduction in mean potential energy anomaly at Global Tech I here can be calculated as about 3.6 J/m³, which agrees well with the simulated changes (Figure 3c). However, there is an uncertainty about these estimates as the simulated thermocline might be too diffusive (Luneva et al., 2019) and the mixing at Global Tech I is influenced by neighboring wind farms. Furthermore, calculated stratification changes between 1–5 J/m³ are within the uncertainty of the drag coefficient (Figure 3c). Nonetheless, profiles of potential energy anomaly across the Global Tech I wind farm comparable to the observed changes by Floeter et al. (2017), suggesting that the body force approach produces reasonable results for structure-induced mixing.

In contrast, the results of the dry cell approach are also shown here to illustrate the problems of the high resolution and the spurious modes due hydrostatic assumptions and numerical instabilities. Despite five-fold iteration, the high-resolution approach exhibits extensive reductions in potential energy anomaly of more than 20 J/m^3 at wind farm locations, which extend far from the associated wind farms (Figure 3b,c). In fact, mean potential energy anomaly decreases to below 10 J/m^3 within wind farms, implying a nearly well-mixed water column in the stratified region. Adjustments of the Shapiro filter can reduce these effects (see Supplementary Figure 2d-f), however, even with twenty-fold iteration of the Shapiro filter, which apparently influences the wake characteristics, the stratification anomalies deviate significantly from the observation values and theoretical estimates. These results underline the problematic use of small grid cells with hydrostatic assumptions and make the dry cell approach unsuitable for hydrostatic regional modelling. Hence, in the following we use the body force approach at low resolution for the model simulations and impact assessment of structure-induced mixing.

3.2 Local Impact of Structured-Induced Mixing

To understand the regional impact of flow disturbance and mixing from offshore wind farms, we start by examining the local processes at wind farm sites, focusing on density stratification and horizontal currents. For this, we analyze impact of horizontal grid resolution and separate the processes of momentum extraction and turbulence production, in order to determine their impact on the hydrodynamics. For the process separation, we performed individual simulations in which the drag term (Equation (4)) was considered in either the momentum equation (Equation (5)) or the turbulence closure scheme (Equations (6),(7)). At this, horizontal resolution was kept at 1000 m. The associated hydrodynamic changes averaged over the first month of the simulation (May 2013) are depicted in Figure 4 and Supplementary Figure 3. Furthermore, we used the simulations with higher resolution of about 250 m to determine the impact of the horizontal spatial discretization at wind farms.

In general, Figure 4 shows that smaller grid cells increase variability inside wind farms and enable processes in between monopiles, but have no influence on the large-scale effects of structure drag. Consequently, higher resolution at wind farm sites does not seem to add significant value to the regional impact, but is primarily relevant in the local analysis of wake effects inside of offshore wind farms, suggesting that including small-scale dry cells into regional models is not worth the numerical effort. However, more research on the small-scale processes within wind farms is needed to understand their relevance and to improve parameterizations at coarser resolution. In the present case, higher resolution increases the

amplitudes of the monopile effects (Figure 4), but this might be related to the critical resolution, which is already below the lower bound of 300 m of the stability criterion.

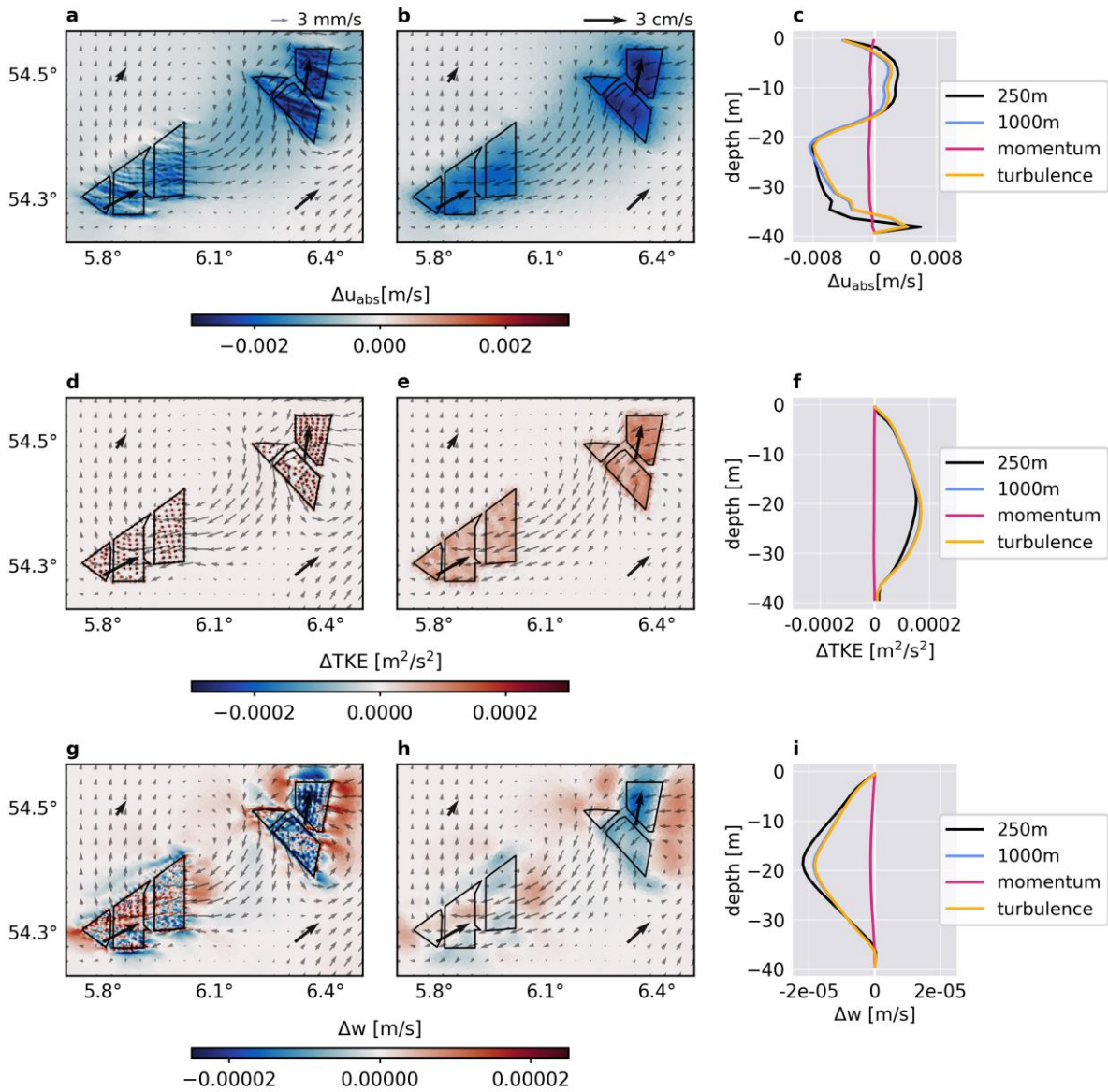


Figure 4: Time-averaged structure-induced changes after the first month of simulation (May 2013) in horizontal current speed u_{abs} (a-c), turbulent kinetic energy TKE (d-f) and vertical velocity w (g-i). Horizontal patterns are depicted for 250 m resolution (left) and 1000 m resolution (right). Gray and black arrows show the changes and reference values of the mean horizontal velocity. Black polygons indicate wind farms. Vertical profiles show changes at Global Tech I for the full drag parameterization (Equation (4)) at different resolutions and for the differentiated momentum extraction (Equation (5)) and turbulence production (Equations (6),(7)) at 1000 m resolution.

The structure-induced drag influences the horizontal velocities and attenuates the monthly mean horizontal flow, whereas the additional turbulence disturbs the incoming velocity field. In consequence, the horizontal current speed averaged over depth and time decreases at wind farms, causing horizontal gradients in the surrounding velocity field and affecting the

downstream currents (Figure 4a,b). The magnitudes of the changes in mean current speed are about 1–3 mm/s, which is about 1 % of the simulated mean depth-averaged currents in May (0.3 m/s). However, looking at a vertical profile of mean horizontal current speed at the Global Tech I wind farm shows that the changes behave differently over depth and can become much stronger than integrated over depth (Figure 4c). In fact, the structure-induced drag causes negative and positive changes in mean current speed of up to –8 mm/s and +4 mm/s, respectively. The vertical profiles show notable differences between the processes related to momentum extraction and to turbulence production, which is also visible in the depth average (Supplementary Figure 3a,d). On the one hand, momentum extraction causes minor reduction in mean current speed of the order of about 0.5 mm/s, which is nearly constant over depth. On the other hand, turbulence appears to be the driving mechanism, resulting in mean current speed changes similar to the combined effect of momentum and turbulence, and thus positive and negative speed changes. Consequently, the variations in amplitude over depth are clearly related to the additional turbulence in the water column, which will be discussed later in the regional analysis.

While also affecting the current speed, the additional structure-induced turbulence primarily changes the amount of turbulent mixing at offshore wind farm sites. As a result, mean turbulent kinetic energy averaged over depth increases at wind farms (Figure 4d,e). Here, we clearly see the limitation of missing turbulence advection in the mixing schemes of the model, since additional turbulent kinetic energy occurs only in grid cells connected to the wind turbine locations. However, averaged over the wind farm area, the vertical profiles show that both grid resolution result in similar increases in turbulent kinetic energy over depth (Figure 4f). Again, turbulence production is the dominating factor of the monopile effects, while, if not additionally parameterized, the turbulent kinetic energy remains almost unchanged for momentum extraction.

The changes in horizontal flow and turbulence affect other hydrodynamic processes near wind farms, such as vertical velocities. As the structure-induced drag deflects the incoming currents, the mixing leads to upwelling and downwelling, which remains consistent regardless of horizontal grid resolution, but patterns are inconsistent across different wind farms (Figure 4g,h). The changes in mean depth-averaged vertical velocity are on the order of 0.01–0.02 mm/s and thus around 1 m/day. These changes are much more significant than the demonstrated effects due to wind wakes, which are of similar order but on daily rather than monthly average (Ludewig, 2015; Christiansen et al., 2022b).

At Global Tech I, the mean vertical velocity decreases inside the wind farm and increases at the sides of the wind farm relative to the mean flow direction (Figure 4g-i). While this

indicates a blockage the incoming currents, the upwelling and downwelling anomalies resemble the observations of Floeter et al. (2017) at the same location. The former study suggested the blocking effects as a result of increased vertical mixing inside the wind farms, similar to the island stirring effect by Simpson et al. (1982), with the increased mixing inside the wind farms leading to destratification and local upwelling. Indeed, the simulated effects here agree well with the assumptions by Floeter et al. (2017), however, local upwelling relative to the mean flow direction does not occur at other simulated wind farms but seems to be determined by other factor as well (Supplementary Figure 4c).

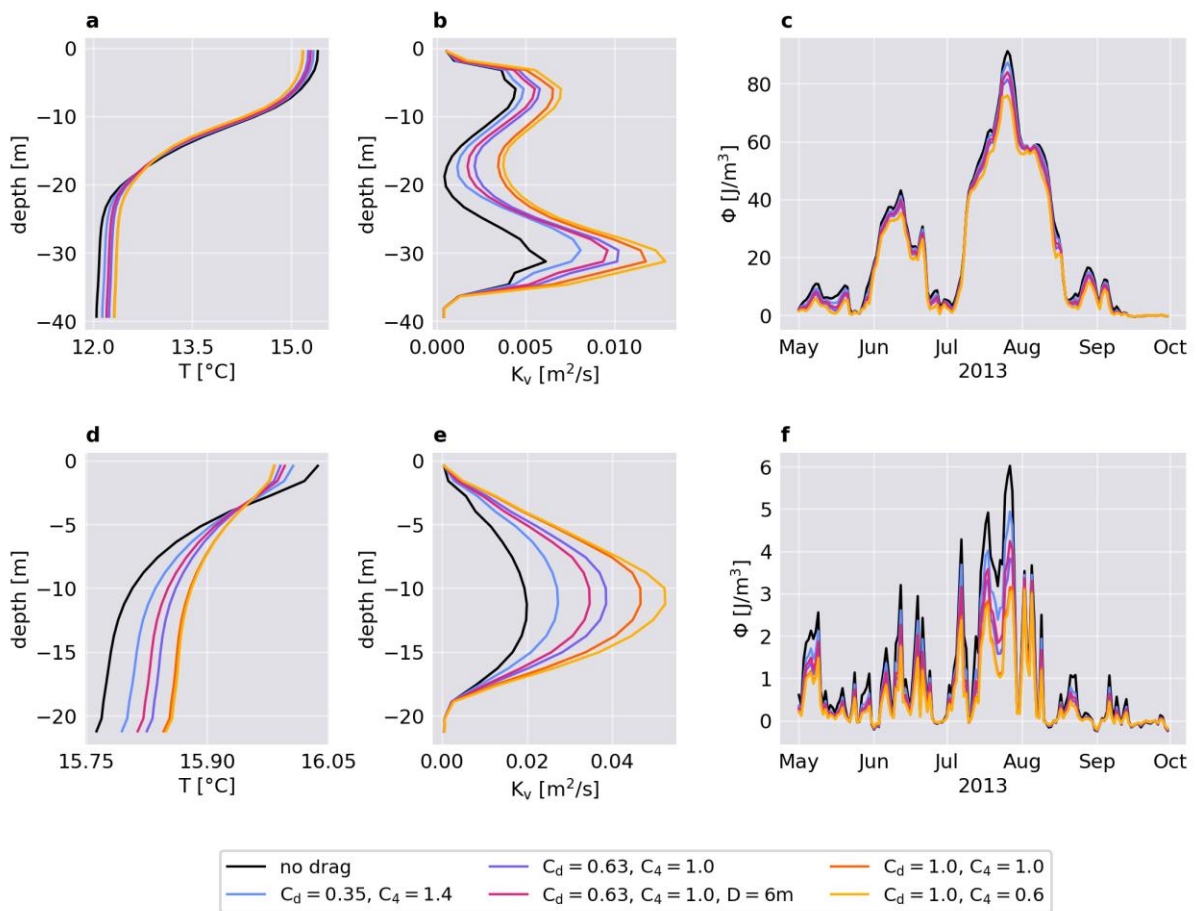


Figure 5: Vertical changes in temperature T (a,d) and vertical eddy diffusivity K_v (b,e) averaged between June and August, and temporal changes in potential energy anomaly ϕ (c,f) from May to October, each for different scenarios of the body force approach. The upper panels show changes in stratified waters at the Global Tech I wind farm and the lower panels show changes in well-mixed waters at the Riffgat wind farm.

Turbulent mixing appears to be the most dominant consequence of structure-induced drag at offshore wind turbine foundations, implying implications for local stratification. Vertical profiles of water temperature and vertical eddy diffusivity, averaged over the summer months of June through August, and the respective evolution of seasonal stratification are shown in Figure 5 for two different wind farm locations. The two examples correspond to the

Global Tech I wind farm, located in seasonally stratified deeper waters, and the smaller Riffgat wind farm, located in unstratified waters northwest of the East Frisian island of Borkum. At Global Tech I, summer stratification is strong with a mean temperature gradient of more than 3°C and a pycnocline thickness of about 9 m (Figure 5a). Here, mixing predominantly occurs in the surface and bottom mixed layers, and decreases in the pycnocline (Figure 5b). Stratification strength reaches its maximum at the end of July with more than 80 J/m^3 in magnitude (Figure 5c). In contrast, the temperature gradient at Riffgat is small. Here, the mean temperature gradient is about 0.3°C during summer (Figure 5d) and the potential energy anomaly does not exceed 6 J/m^3 (Figure 5f). As a result, the vertical mixing rate is significantly stronger than at Global Tech I, with the most pronounced mixing occurring in the middle of the water column (Figure 5e).

Despite different stratification conditions, the processes behave similarly at the two wind farms with regard to temperature and diffusivity changes. In consequence of the additional structure-induced turbulence, the mean temperature gradients at wind farm sites decrease and mean vertical diffusivities increase (Figure 5). Here, the magnitudes of the perturbations depend strongly on the scaling parameters used in the simulations and on local conditions. For instance, mean vertical diffusivity increases by about 25 % for a low turbulence scenario ($C_d = 0.35$, $c_4 = 1.4$), but by about 100 % for the scenario of very strong turbulence ($C_d = 1.0$, $c_4 = 0.6$), indicating a strong uncertainty about the amount of additional mixing at individual wind farms. In this context, parameters of the drag parameterization (C_d and d) significantly affect both the changes in stratification and the turbulent mixing rates, whereas the parameter c_4 appears to determine primarily the latter. The uncertainty caused by the drag parameters has been mentioned in earlier studies (Carpenter et al., 2016; Dorrell et al., 2022) and must be taken into account for the application of the body force approach and the interpretation of the simulation results. Nevertheless, using moderate values for the scaling parameters, e.g. $C_d = 0.35$ and $c_4 = 1.4$, will in general provide sufficient results for the regional impact, though effects might be under- or overestimated in some regions.

Regardless of stratification conditions, the additional mixing by monopiles alters and, in particular, reduces the potential energy anomaly inside offshore wind farms (Figure 5c,f). If the water column is stable ($\phi > 0$), the magnitudes of these changes vary between $0\text{--}15 \text{ J/m}^3$ and account for more than $10\text{--}50 \%$ of the actual potential energy anomaly. In this context, the changes are stronger in stratified waters, as here the turbulence has a bigger potential to disturb the vertical density distribution and affect the stability of the water column. However, percentage changes are more pronounced for weaker stratification. The

stratification changes are in general more than twice as strong for high turbulence cases than for low turbulence cases, indicating again the uncertainty due to drag conditions.

The impact on stratification and changes of more than 10 J/m^3 support the concerns of Dorrell et al. (2022) about the implications of future offshore wind development. With expansion into stratified deeper waters (WindEurope, 2022), offshore wind infrastructure could fundamentally change temporal and spatial stratification development, which is essential for associated biogeochemical processes in the central and southern North Sea (van Leeuwen et al., 2015). This includes, for example, nutrient and light availability in surface layers or oxygen concentration in deeper layers, ultimately affecting the productivity and cascading up the trophic levels (Dorrell et al., 2022). However, with regard to ecological impact, atmospheric wake effects and their influence on stratification and biogeochemistry (Daewel et al., 2022) have to be considered as well, which makes the overall impact of offshore wind farms very complex.

3.3 Regional Impact of Structured-Induced Mixing

As horizontal momentum and turbulent mixing are disturbed locally, the regional dynamics respond to the local alterations at offshore wind farm sites. This may include advection of disturbances into the far field or larger scale structural changes due to perturbations of mesoscale circulation and baroclinic flows, affecting the hydrodynamics well beyond associated wind farms. Regional-scale alterations due to structure-induced mixing have been shown by Rennau et al. (2012) for a case study in the Baltic Sea and develop in various hydrodynamic parameters such as horizontal and vertical currents, sea surface elevation or density stratification. Here, we focus on key processes related to the structure-induced mixing, namely the extraction of horizontal momentum, the generation of turbulent mixing, and the implications for the stratification. Figure 6 shows the differences in the hydrodynamic parameters averaged over the simulation period from May to September. For further insights into other parameters, see Supplementary Figure 4.

Structure drag reduces the depth-averaged current speeds inside offshore wind farms and influences downstream currents (Figure 4a-c). Although the reductions thereby originate at wind farm sites, the simulations show that the average depth-integrated current speed decreases extensively over the entire German Bight area (Figure 6a). This includes changes advecting along the predominant downstream directions, as well as a general reduction in current speed of about 0.5 mm/s along the German coast. The most pronounced changes occur at wind farm sites with average magnitudes of $1\text{-}2 \text{ mm/s}$, and especially at wind farm clusters with high turbine density, where magnitudes can exceed 3 mm/s . These changes

are minor compared to the actual average current speeds in the German Bight (0.20–0.45 m/s), but extend significantly on a spatial scale. Moreover, the structure-induced changes exhibit magnitudes in the same order as the alterations due to wind stress reduction from wind wakes (Christiansen et al., 2022a; Christiansen et al., 2022b), suggesting that the ultimate impact by offshore wind farms on the marine environment will be a complex interaction of atmospheric and hydrodynamic effects.

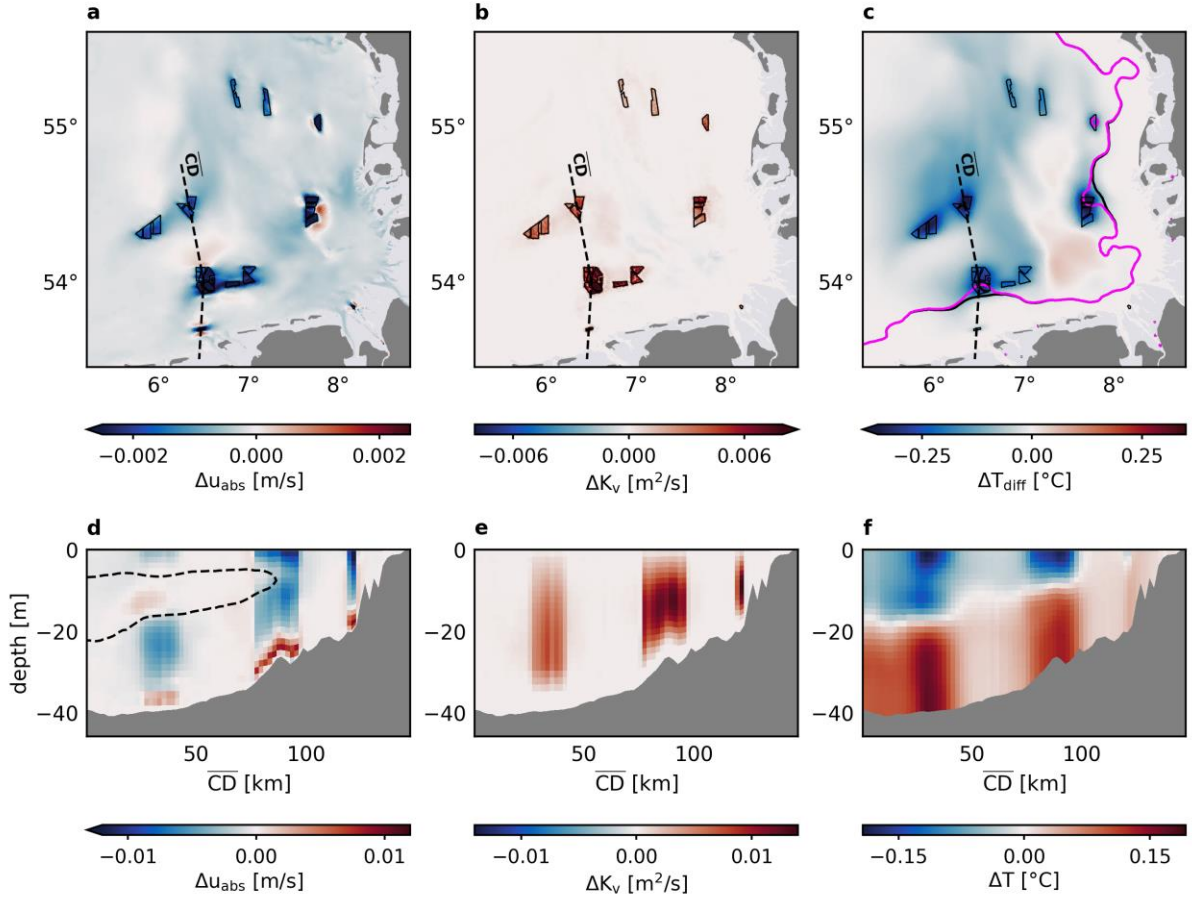


Figure 6: Changes in depth-averaged current speed u_{abs} , depth-averaged vertical eddy diffusivity K_v averaged and temperature gradient T_{diff} averaged between May and September for the canopy approach. Black dashed lines indicate profile \overline{CD} , black polygons indicate wind farms. Gray arrows in (a) show direction of mean depth-averaged horizontal velocity u . Respective changes in absolute velocity, eddy diffusivity and temperature averaged between May and September along profile \overline{CD} are depicted in (d)–(f). Black dashed line in (d) indicates pycnocline, based on buoyancy frequency $N^2 \geq 5 \times 10^{-4} \text{ s}^{-1}$ (Dorrell et al., 2022).

The processes behind changes in the average current speed become clearer looking at a vertical cross section through different wind farm clusters from deep stratified waters to shallow mixed waters (Figure 6d). In fact, the changes are about one order of magnitude larger over depth than in the depth average, with more than 1 cm/s and thus up to 5% of the actual average current speed. As seen in Figure 4c, turbulence becomes a decisive factor

for structure-induced speed changes at wind farm sites, causing both positive and negative anomalies. The turbulence increases viscosity and penetrates areas of lower mixing rates such as the pycnocline or bottom boundary layer, making the current speed and density vertically more diffused and results in more uniform vertical shear. In consequence, current speed increases in the low mixing areas compared to the reference simulation, whereas it decreases in areas where current speed is faster than the depth average (Figure 6d). In this context, the positive anomalies disappear as stratification declines towards the well-mixed shallower waters and occur solely inside the bottom boundary layer, which remains the only area with lower current speed than the depth average speed.

While affecting other parameters like currents and density far from the monopiles, structure-induced mixing increases turbulence and vertical mixing rates mainly at wind farm sites (Figure 6b, Supplementary Figure 4d). Since wake turbulence has been shown to be confined to the near field of the narrow monopile wakes (Schultze et al., 2020), these localized changes in turbulence and mixing rates are expected and consistent with the observations. Here, the changes in mean vertical diffusivity are around $0.005\text{--}0.01\text{ m}^2/\text{s}$ and are thus up to twice as strong as the actual mean vertical diffusivity, particularly in stratified waters. In this context, magnitudes increase towards the shallower waters (Figure 6e), where tidal velocities are generally stronger and thus enhance the velocity-dependent turbulence production. The increase in additional mixing towards the coast is also reflected in changes in horizontal current speed (Figure 6d). Compared to wind wake effects (Christiansen et al., 2022a; Christiansen et al., 2022b), the local mixing by monopiles is significantly stronger by at least one order of magnitude, indicating that structure-induced mixing will dominate the wind-driven effects at wind farm sites.

Ultimately, structure-induced mixing influences the vertical density distribution and the seasonal stratification development. Although the mixing effects, in this context, occur at wind farm sites, mixed water conditions can be detected across the entire German Bight area. Here, the vertical temperature differential from surface to bottom layer is used as a measure for stratification, meaning the stronger the surface-bottom differential the stronger the stratification. The additional mixing reduces the temperature differentials average over the period from May to September by about $0.1\text{--}0.2^\circ\text{C}$ with the strongest stratification reductions of more than 0.3°C occurring at wind farm sites (Figure 6c). These changes are quite substantial accounting for up to 50 % of the actual mean vertical temperature differentials. At this, strong mixing at densely built wind farms near tidal mixing fronts can even shift the mean frontal position to deeper waters as the vertical temperature stratification collapses.

In stratified months, the structure-induced mixing transports colder water from the bottom layers to the surface and warm surface water into deeper layers (Figure 6f), reducing the vertical temperature gradient at wind farm sites, as also seen for the temperature profiles at the Global Tech I wind farm (Figure 5a). In this process, the vertical boundary between temperature reductions and increases follows the course of the thermocline here. The changes in mean temperature at wind farms reach up to $\pm 0.2^\circ\text{C}$ in stratified waters, and thus up to 20% of the interannual variability of sea surface and bottom temperatures in the southern North Sea (Daewel and Schrum, 2017). Here, the mean sea surface cooling between May and September is up to five times stronger than the mean sea surface warming that occurs in the context of atmospheric wind wake effects (Christiansen et al., 2022a), and thus likely superimpose the latter when looking at the total wind farm effect. However, again, effects of structure-induced mixing are most pronounced at wind farm sites, while wind wakes effects are less confined to the wind farms and occur as regional patterns.

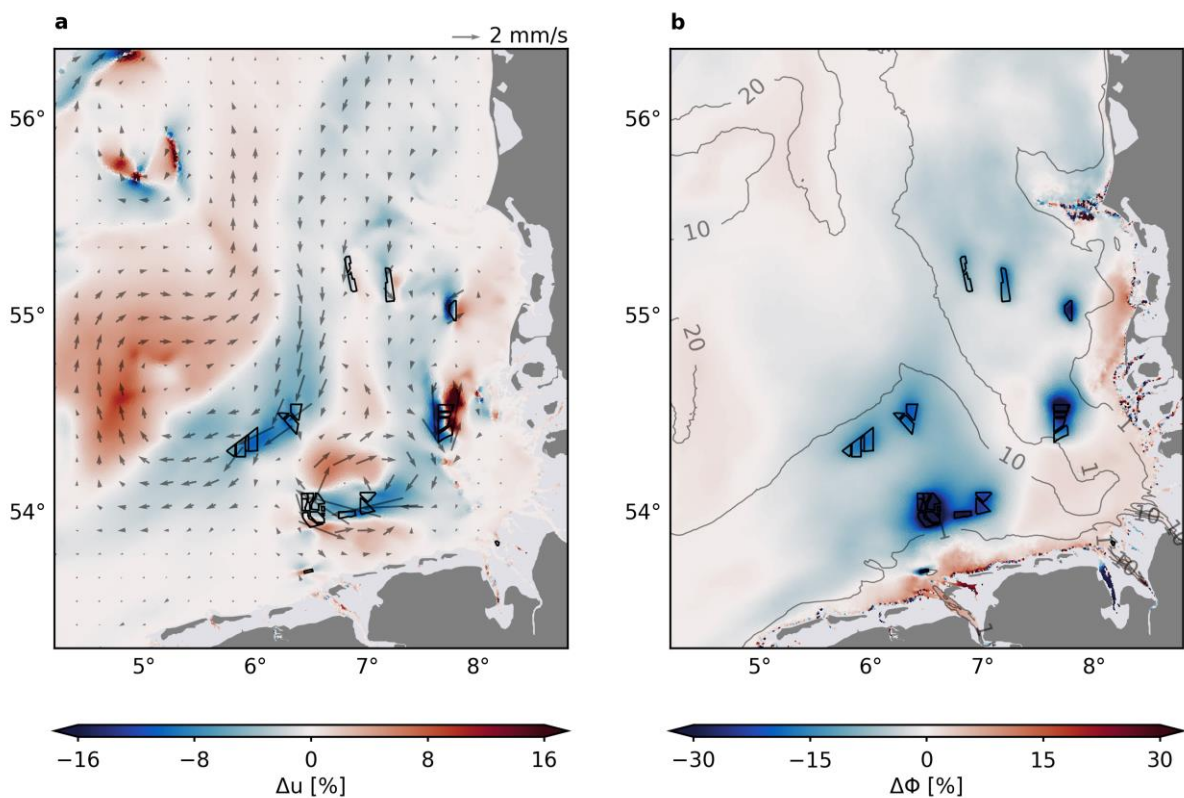


Figure 7: Long-term percentage changes in depth-averaged horizontal velocity u (a) and potential energy anomaly Φ (b) averaged over the years 2011-2015. Gray arrows indicate direction of mean velocity changes in (a), contour lines indicate mean potential energy anomaly in (b). Black polygons indicate wind farms. Water depths below 3 m are masked.

Similar to wind wake effects, the regional effects of structure drag are sensitive to hydrodynamic conditions, such as horizontal advection, baroclinic conditions or the stratification, which may vary over time, e.g., seasonally or annually. Thus, it becomes important with regard to the impact assessment to distinguish temporal signals from persistent changes in the local dynamics. For this reason, we conducted additional long-term simulations of the monopile effects, covering the years 2011 to 2015. Here, the focus is on mean changes in horizontal flow velocity and stratification strength over the five-year period (Figure 7), as these become critical for biogeochemical processes and the environmental impact. Note that here we look at changes in the mean current velocity, not the average current speeds (see Equations (2)).

The five-year average of changes in depth-averaged horizontal velocity shows distinct velocity reductions near offshore wind farms, which extend far downstream along the predominant northward circulation (Figure 7a). The local changes in momentum and turbulence influence the surrounding dynamics and lead to an attenuation of the mean current in the center of the German Bight, where the wind farms are located. In addition, mean horizontal flows increase laterally of the large-scale reductions, including increasing mean current velocity along the coast and towards the northeastern part of the Dogger Bank. Nevertheless, mean flow directions are still not affected visibly by the velocity changes. The changes in mean horizontal velocity are around ± 1 mm/s on average and reach up to ± 4 mm/s at wind farm sites, accounting for about ± 5 -15 % of the mean horizontal flow locally (Figure 7a, Supplementary Figure 5a). The structure drag alters the horizontal velocity on a similar order of magnitude to the annual and interannual variability in the southern North Sea (Daewel and Schrum, 2017), which can be substantial to associated velocity-dependent biogeochemical processes like sedimentation or migration processes (van Berkel et al., 2020). Increasing and area-wide offshore wind development in the German Bight could result in large-scale blocking effects and deflection of coastal circulation towards central North Sea areas, where horizontal current velocities increase. Furthermore, the reduction in mean currents may create positive feedback on mixing processes by increasing the time as water parcel spends inside the wind farm area. At Global Tech I, for example, mean velocity decreases by 6.4 % of the mean current, which result in a 6.8 % longer residence time τ_{adv} at Global Tech I, using $\tau_{adv} = L/\bar{u}$ and $L = 8$ km from Carpenter et al. (2016).

The structure-induced mixing changes the stratification conditions in the German Bight. On the five-year average the potential energy anomaly decreases by 10-15 % at wind farm sites, at which maximum values of more than 30 % reduction emerge at wind farms in shallower waters near the tidal mixing fronts (Figure 7b). The advection of mixed water masses

distributes the anomalies along the northward circulation, reducing the area-wide stratification by about 5 %. These effects are accompanied by an increase in potential energy anomaly of about 5 % along the shallow German coast and about 1 % near the Dogger Bank area. Although the strongest changes in potential energy anomaly occur in stratified waters during the summer periods (Figure 5c,f), we see that also in mixed and unstable waters the mixing changes the potential energy anomaly, where the percentage changes become most substantial. However, note that averaging over winter conditions may bias the annual mean changes at seasonally stratified wind farms, where stratification can decrease by up to 15 J/m^3 during the summer.

In general, the long-term changes in stratification have the potential to influence the ecosystem dynamics in the German Bight. Stratification provides a natural barrier for vertical exchange of nutrients, oxygen or phytoplankton in the water column and significantly determines the seasonal shelf sea productivity (Simpson and Sharples, 2012). The strong local mixing at wind farms will translate to local biogeochemical processes such as nutrient dynamics and light availability (Floeter et al., 2017; Dorrell et al., 2022). In addition, large-scale perturbations of the pycnocline and increased mixing can affect regional ecosystem productivity, which becomes particularly critical for structure-induced mixing in stratified waters. Dorrell et al. (2022) discussed that these changes could ultimately affect higher trophic levels, such as fish or seabird populations that adapt to phytoplankton growth, demonstrating the need for further investigations of the biogeochemical consequences of structure-induced mixing and extensive future offshore wind scenarios.

4 Conclusion

With increasing offshore wind energy development in coastal seas, investigations of the consequences for the marine environment are becoming more important. Here, we presented two methods of implementing structure-induced mixing by offshore wind turbine foundations at the scale of regional numerical models and discussed the improper use of high resolution with the hydrostatic approximation. We show that the dry cell method encounters numerical problems and inappropriate results, since at very high resolution the hydrostatic model does not fulfill its purposes and further physics must be added to simulate small-scale processes. In contrast, the body force approach appears as a suitable method to account for subgrid-scale wake turbulence, while complying with the hydrostatic assumptions. Thus, we conclude that for assessing the large-scale impacts of structure-induced mixing it is more reasonable to use low-resolution parameterizations supported by high-resolution non-hydrostatic modeling, e.g., Large Eddy Simulations as in Schultze et al.

(2020), which can be used to analyze small-scale wake processes and upscale the effects for regional models.

Using the drag parameterization, our results show that monopile drag not only influences local processes at wind farms, but that local mixing and flow disturbances are advected by the prevailing currents and extensively affect the far field of offshore wind farms. In this context, additional wake turbulence dominates the extraction of momentum and becomes the driving mechanism of structure-induced processes. Mean horizontal currents and density stratification can change locally by about 10 % on average and are on the order of interannual variability. However, the magnitudes of these changes should still be interpreted with caution, since turbulent mixing processes in stratified waters are still uncertain (Dorrell et al., 2022) and mixing schemes can bias the effects on stratification (Luneva et al., 2019). In general, more observations are needed to validate modeling approaches and support the simulation results. Nonetheless, this study gives first insights into the expected dimension of the structure-induced effects of offshore wind infrastructure and emphasizes that these processes must be considered at a regional scale for impact assessment, similar to the much larger wind wake effects.

In view of future European offshore wind development (WindEurope, 2022), the demonstrated effects of structure-induced mixing will increase, raising the question about the consequences for the marine environment of not only the German Bight, but the entire North Sea. These include perturbations of the regional circulation as well as changes in timing and intensity of seasonal stratification development. Given the amount of wind farms planned, structure-induced mixing could thus alter the prevailing dynamics on a large scale, shaping a "new normal" (Dorrell et al., 2022) in the physical and associated biogeochemical system of the North Sea. In this context, however, wind wake effects, which influence stratification in similar order of magnitude (Christiansen et al., 2022a; Christiansen et al., 2022b) and have been shown to impact biogeochemistry (Daewel et al., 2022), have to be considered as well. Interaction between the atmospheric and hydrodynamic wake effects could increase or attenuate the local effects of structure-induced mixing. Hence, to come up with assumptions about the regional impact of offshore wind energy of the North Sea dynamics, the combined effect has to be investigated further.

Funding

This project is a contribution to the EXC 2037 'Climate, Climatic Change, and Society (CLICCS)' (Project Number: 390683824) funded by the German Research Foundation (DFG), to the CLICCS-HGF networking project funded by the Helmholtz Association of German Research Centers (HGF), and to the Helmholtz Research Program "Changing Earth – Sustaining our Future", Topic 4. Furthermore, this work contributes to the DAM Research Mission sustainMare and the project CoastalFutures.

References

- Boyer Montégut, C. de, Madec, G., Fischer, A. S., Lazar, A., and Iudicone, D. (2004). Mixed layer depth over the global ocean: An examination of profile data and a profile-based climatology. *J. Geophys. Res.* 109. doi: 10.1029/2004JC002378
- Carpenter, J. R., Merckelbach, L., Callies, U., Clark, S., Gaslikova, L., and Baschek, B. (2016). Potential Impacts of Offshore Wind Farms on North Sea Stratification. *PLOS ONE* 11, e0160830. doi: 10.1371/journal.pone.0160830
- Cazenave, P. W., Torres, R., and Allen, J. I. (2016). Unstructured grid modelling of offshore wind farm impacts on seasonally stratified shelf seas. *Progress in Oceanography* 145, 25–41. doi: 10.1016/j.pocean.2016.04.004
- Christiansen, N., Daewel, U., Djath, B., and Schrum, C. (2022a). Emergence of Large-Scale Hydrodynamic Structures Due to Atmospheric Offshore Wind Farm Wakes. *Frontiers in Marine Science* 9. doi: 10.3389/fmars.2022.818501
- Christiansen, N., Daewel, U., and Schrum, C. (2022b). Tidal mitigation of offshore wind wake effects in coastal seas. *Frontiers in Marine Science* 9. doi: 10.3389/fmars.2022.1006647
- Christie, E., Li, M., and Moulinec, C. (2012). Comparison of 2D and 3D large scale morphological modeling of offshore wind farms using HPC. *Int. Conf. Coastal. Eng.* 1, sediment.42. doi: 10.9753/icce.v33.sediment.42
- Cushman-Roisin, B., and Beckers, J.-M. (2011). *Introduction to geophysical fluid dynamics: physical and numerical aspects*. Academic Press.
- Daewel, U., Akhtar, N., Christiansen, N., and Schrum, C. (2022). Offshore wind farms are projected to impact primary production and bottom water deoxygenation in the North Sea. *Communications Earth & Environment* 3, 292. doi: 10.1038/s43247-022-00625-0
- Daewel, U., and Schrum, C. (2013). Simulating long-term dynamics of the coupled North Sea and Baltic Sea ecosystem with ECOSMO II: Model description and validation. *Journal of Marine Systems* 119–120, 30–49. doi: 10.1016/j.jmarsys.2013.03.008
- Daewel, U., and Schrum, C. (2017). Low-frequency variability in North Sea and Baltic Sea identified through simulations with the 3-D coupled physical-biogeochemical model ECOSMO. *Earth System Dynamics* 8, 801–815. doi: 10.5194/esd-8-801-2017

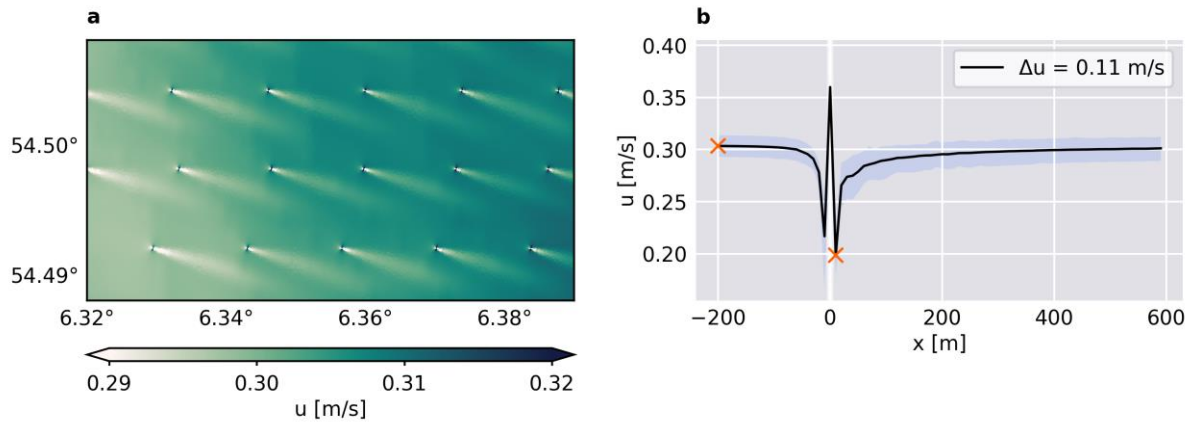
- Dorrell, R. M., Lloyd, C. J., Lincoln, B. J., Rippeth, T. P., Taylor, J. R., Caulfield, C.-c. P., et al. (2022). Anthropogenic Mixing in Seasonally Stratified Shelf Seas by Offshore Wind Farm Infrastructure. *Frontiers in Marine Science* 9. doi: 10.3389/fmars.2022.830927
- European Commission (2020). *Offshore renewable energy strategy*. Directorate-General for Energy, <https://data.europa.eu/doi/10.2833/219143>
- Floeter, J., van Beusekom, J. E., Auch, D., Callies, U., Carpenter, J., Dudeck, T., et al. (2017). Pelagic effects of offshore wind farm foundations in the stratified North Sea. *Progress in Oceanography* 156, 154–173. doi: 10.1016/j.pocean.2017.07.003
- Forster, R. M. (2018). *The effect of monopile-induced turbulence on local suspended sediment patterns around uk wind farms: field survey report*. An IECS report to The Crown Estate. ISBN 978-1-906410-77-3.
- Haidvogel, D. B., and Beckmann, A. (1998). Numerical models of the coastal ocean. *The Global Coastal Ocean, Processes and Methods*, 457–482.
- Lass, H. U., Mohrholz, V., Knoll, M., and Prandke, H. (2008). Enhanced mixing downstream of a pile in an estuarine flow. *Journal of Marine Systems* 74, 505–527. doi: 10.1016/j.jmarsys.2008.04.003
- Ludewig, E. (2015). *On the Effect of Offshore Wind Farms on the Atmosphere and Ocean Dynamics*. Cham, s.l. Springer International Publishing.
- Luneva, M. V., Wakelin, S., Holt, J. T., Inall, M. E., Kozlov, I. E., Palmer, M. R., et al. (2019). Challenging Vertical Turbulence Mixing Schemes in a Tidally Energetic Environment: 1. 3-D Shelf-Sea Model Assessment. *J. Geophys. Res. Oceans* 124, 6360–6387. doi: 10.1029/2018JC014307
- Merkur Offshore. *Merkur Offshore – Technology: Balance of Plant, Foundations*. Accessed December 07, 2022, <https://www.merkur-offshore.com/technology/>
- Otto, L., Zimmerman, J., Furnes, G. K., Mork, M., Saetre, R., and Becker, G. (1990). Review of the physical oceanography of the North Sea. *Netherlands Journal of Sea Research* 26, 161–238. doi: 10.1016/0077-7579(90)90091-T
- Rennau, H., Schimmels, S., and Burchard, H. (2012). On the effect of structure-induced resistance and mixing on inflows into the Baltic Sea: A numerical model study. *Coastal Engineering* 60, 53–68. doi: 10.1016/j.coastaleng.2011.08.002
- Rivier, A., Bennis, A.-C., Pinon, G., Magar, V., and Gross, M. (2016). Parameterization of wind turbine impacts on hydrodynamics and sediment transport. *Ocean Dynamics* 66, 1285–1299. doi: 10.1007/s10236-016-0983-6
- SCHISM v5.7 User Manual*. Accessed December 07, 2022, http://ccrm.vims.edu/schismweb/SCHISM_v5.7-Manual.pdf
- Schultze, L. K. P., Merckelbach, L. M., Horstmann, J., Raasch, S., and Carpenter, J. R. (2020). Increased Mixing and Turbulence in the Wake of Offshore Wind Farm Foundations. *J. Geophys. Res. Oceans* 125, e2019JC015858. doi: 10.1029/2019JC015858

- Shih, W., Wang, C., Coles, D., and Roshko, A. (1993). Experiments on flow past rough circular cylinders at large Reynolds numbers. *Journal of Wind Engineering and Industrial Aerodynamics* 49, 351–368. doi: 10.1016/0167-6105(93)90030-R
- Simpson, J. H., and Sharples, J. (2012). *Introduction to the physical and biological oceanography of shelf seas*. Cambridge University Press.
- Simpson, J. H., Tett, P. B., Argote-Espinoza, M. L., Edwards, A., Jones, K. J., and Savidge, G. (1982). Mixing and phytoplankton growth around an island in a stratified sea. *Continental Shelf Research* 1, 15–31. doi: 10.1016/0278-4343(82)90030-9
- Sumer, B. M., and Fredsøe, J. (2006). *Hydrodynamics Around Cylindrical Structures*. WORLD SCIENTIFIC.
- Sündermann, J., and Pohlmann, T. (2011). A brief analysis of North Sea physics. *Oceanologia* 53, 663–689. doi: 10.5697/oc.53-3.663
- Svensson, U., and Häggkvist, K. (1990). A two-equation turbulence model for canopy flows. *Journal of Wind Engineering and Industrial Aerodynamics* 35, 201–211. doi: 10.1016/0167-6105(90)90216-Y
- Umlauf, L., and Burchard, H. (2003). A generic length-scale equation for geophysical turbulence models. *Journal of Marine Research* 61, 235–265. doi: 10.1357/002224003322005087
- van Berkel, J., Burchard, H., Christensen, A., Mortensen, L. O., Svenstrup Petersen, O., and Thomsen, F. (2020). The Effects of Offshore Wind Farms on Hydrodynamics and Implications for Fishes. *Oceanography* 33, 108–117. doi: 10.5670/oceanog.2020.410
- van Leeuwen, S., Tett, P., Mills, D., and van der Molen, J. (2015). Stratified and nonstratified areas in the North Sea: Long-term variability and biological and policy implications. *J. Geophys. Res. Oceans* 120, 4670–4686. doi: 10.1002/2014JC010485
- Vanhellemont, Q., and Ruddick, K. (2014). Turbid wakes associated with offshore wind turbines observed with Landsat 8. *Remote Sensing of Environment* 145, 105–115. doi: 10.1016/j.rse.2014.01.009
- Williamson, C. H. K. (1996). Vortex Dynamics in the Cylinder Wake. *Annu. Rev. Fluid Mech.* 28, 477–539. doi: 10.1146/annurev.fl.28.010196.002401
- Wilson, N. R., and Shaw, R. H. (1977). A Higher Order Closure Model for Canopy Flow. *Journal of Applied Meteorology (1962-1982)* 16, 1197–1205.
- WindEurope (2021). *Offshore Wind in Europe: Key trends and statistics in 2020*, <https://windeurope.org/intelligence-platform/product/offshore-wind-in-europe-key-trends-and-statistics-2020/>
- WindEurope (2022). *Wind Energy in Europe: 2021 Statistics and the outlook for 2022–2026*, <https://windeurope.org/intelligence-platform/product/wind-energy-in-europe-2021-statistics-and-the-outlook-for-2022-2026/>

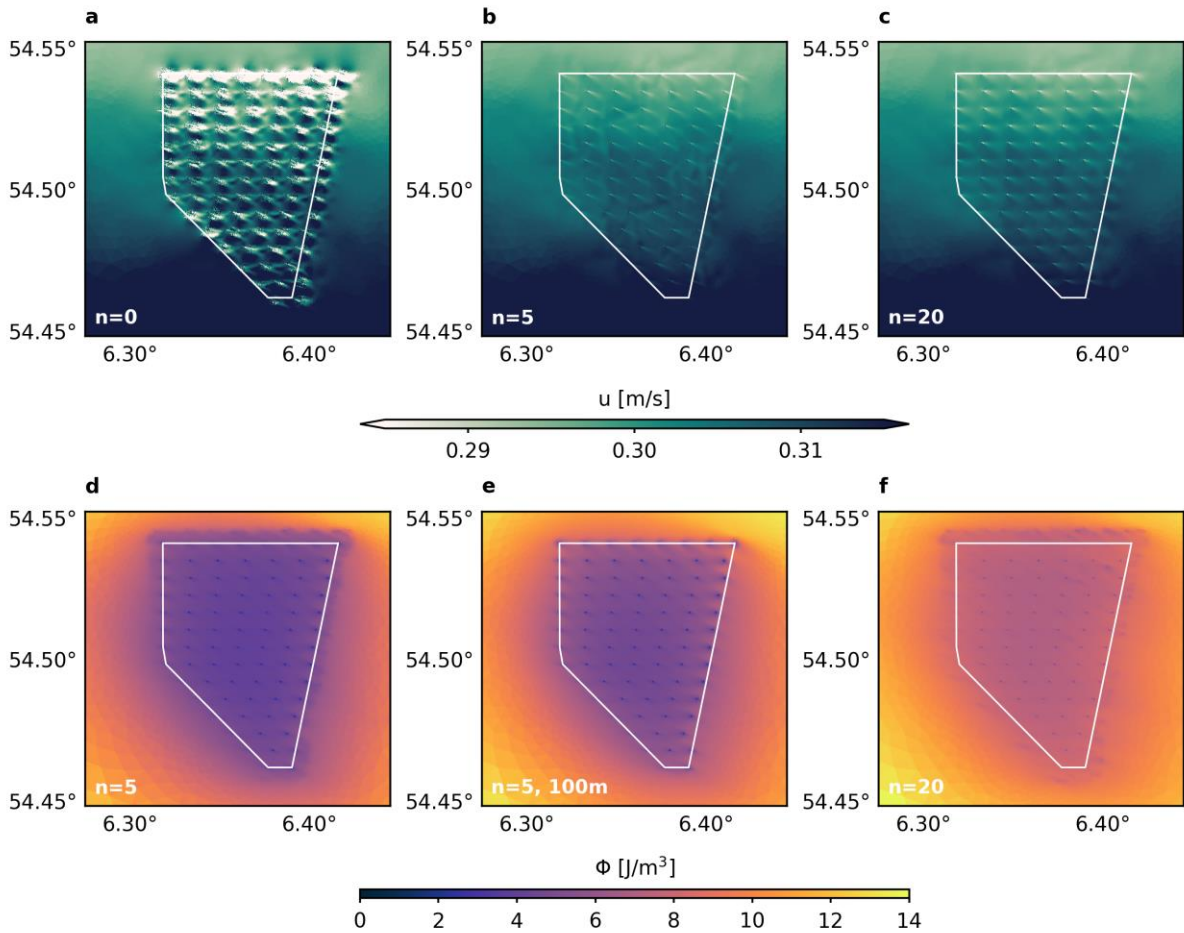
Zhang, Y. J., Ateljevich, E., Yu, H.-C., Wu, C. H., and Yu, J. C. (2015). A new vertical coordinate system for a 3D unstructured-grid model. *Ocean Modelling* 85, 16–31. doi: 10.1016/j.ocemod.2014.10.003

Zhang, Y. J., Ye, F., Stanev, E. V., and Grashorn, S. (2016). Seamless cross-scale modeling with SCHISM. *Ocean Modelling* 102, 64–81. doi: 10.1016/j.ocemod.2016.05.002

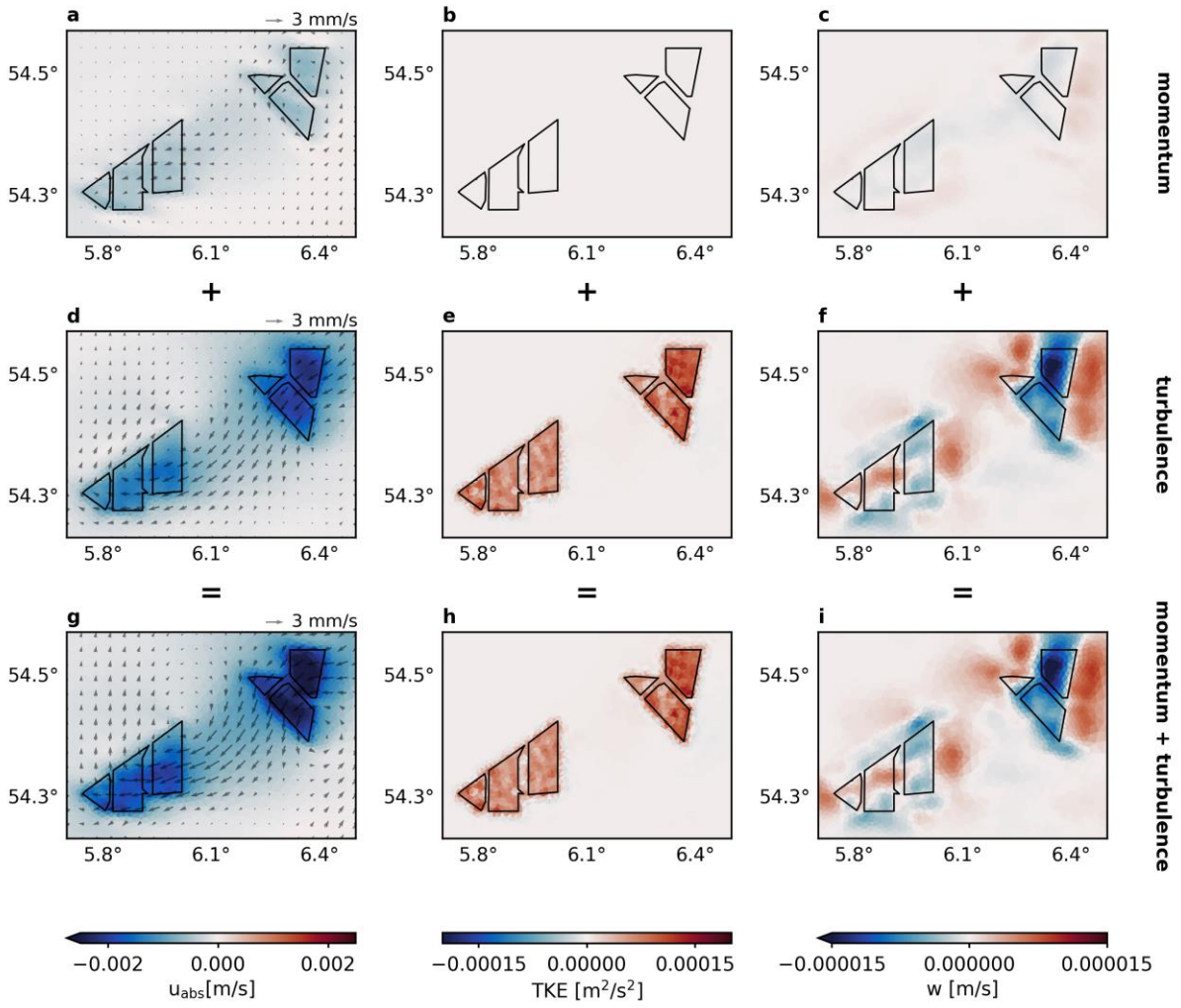
Supplementary Figures

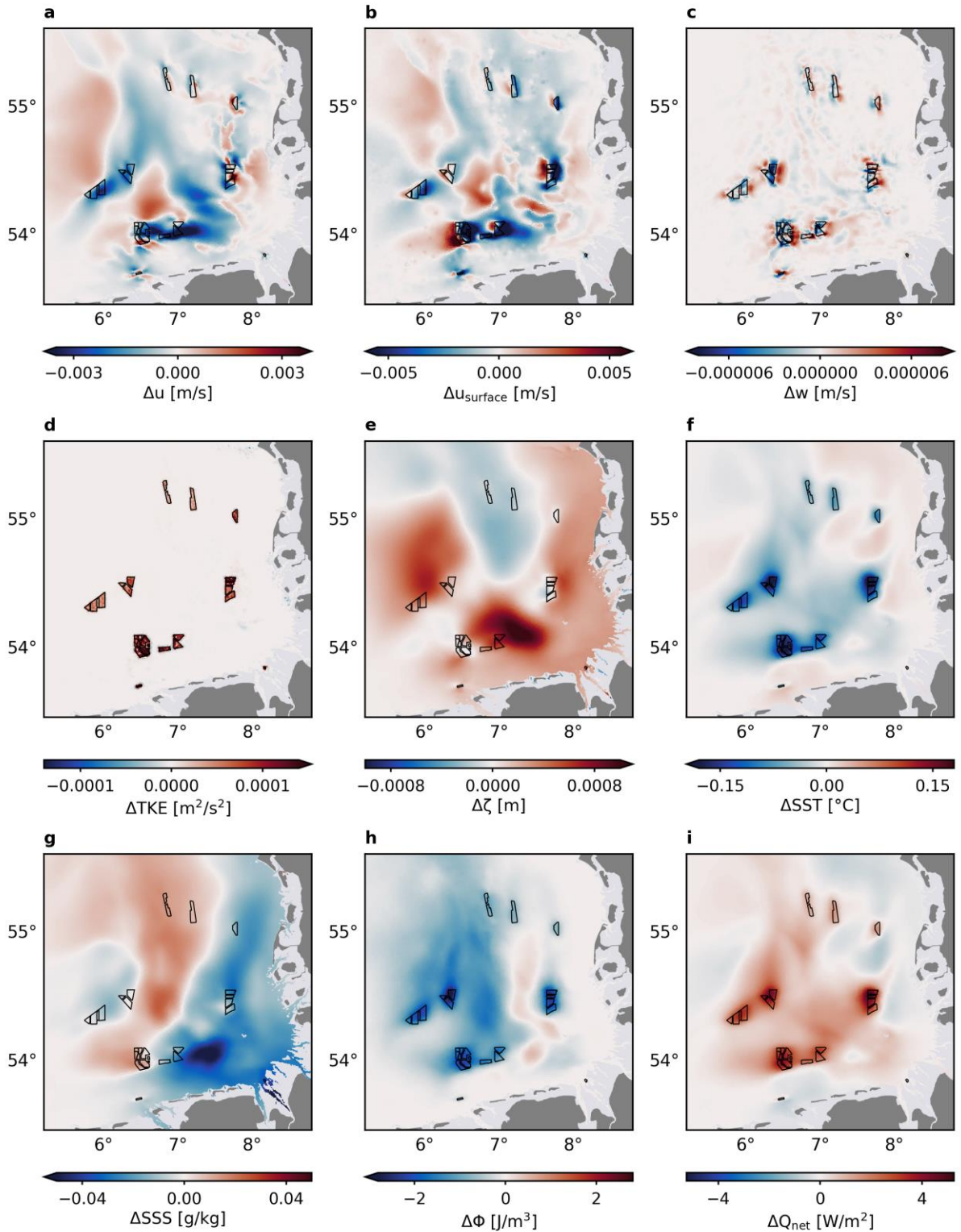


Supplementary Figure 1: Changes in depth-averaged horizontal velocity u after the first time step at the Global Tech I wind farm. (a) Wake patterns inside the wind farm. (b) Mean velocity profile of the wake patterns (black line) and the respective minimum-maximum range (blue envelope). Orange crosses indicate locations of upstream and downstream measurement points.

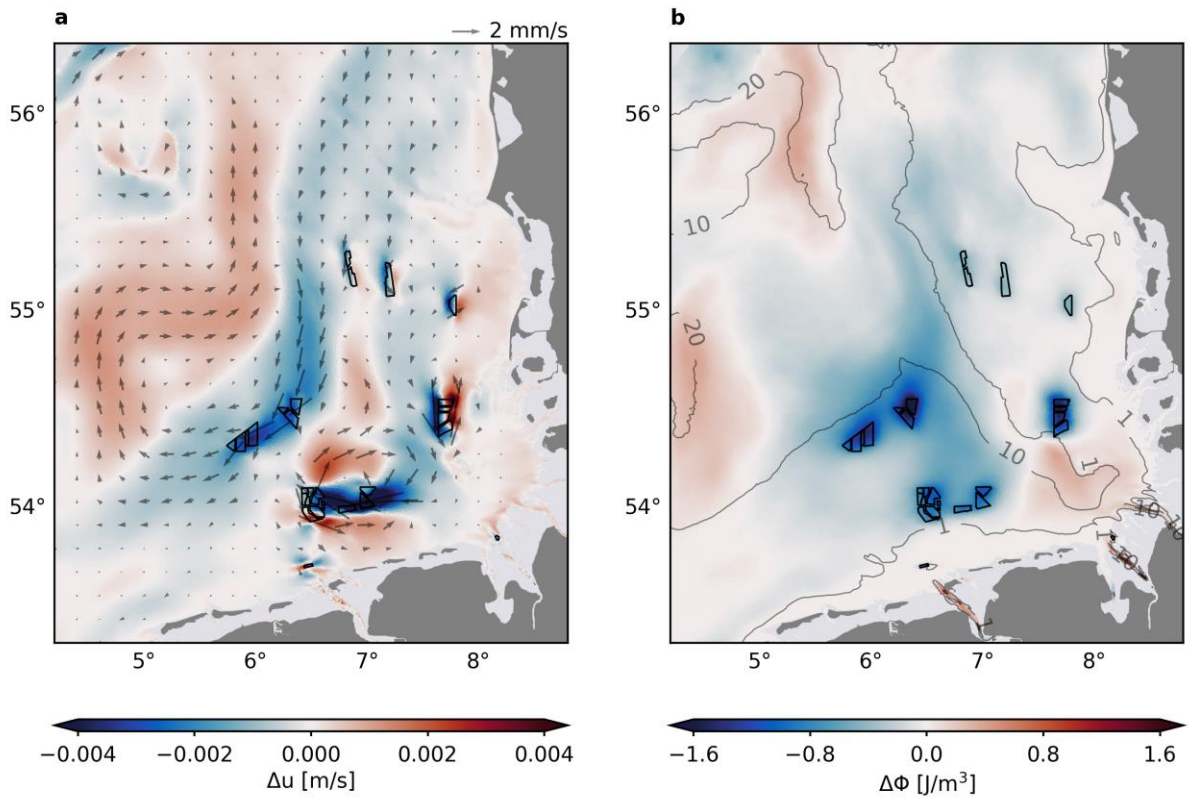


Supplementary Figure 2: Wake patterns in depth-averaged horizontal velocity u after the first time step (a-c), and the mean potential energy anomaly ϕ in the first 14 days of July (d-f) for different iterations n of the Shapiro filter using the dry cell approach. White polygons indicate borders of Global Tech I wind farm.





Supplementary Figure 4: Structure-induced changes in depth-averaged horizontal velocity u (a), horizontal surface velocity u_{surface} (b), depth-averaged vertical velocity w (c), depth-averaged turbulent kinetic energy TKE (d), sea surface elevation ζ (e), sea surface temperature SST (f), sea surface salinity SSS (g), potential energy anomaly Φ (h) and net surface heat flux Q_{net} (i) averaged over the period May to September 2013. Black polygons indicate wind farms. Water depths below 2 m are masked.



Supplementary Figure 5: Long-term changes in depth-averaged horizontal velocity u (a) and potential energy anomaly ϕ (b) averaged over the years 2011–2015. Gray arrows indicate direction of mean velocity changes in (a), contour lines indicate mean potential energy anomaly in (b). Black polygons indicate wind farms. Water depths below 3 m are masked.

5 Discussion and Outlook

Offshore wind farm effects occur at a variety of horizontal scales, from local mixing at turbine foundations to large-scale wind speed reductions downstream of wind farms. Combining these different effects into a single model framework requires appropriate modeling approaches and simplification of processes (Q1), in order to determine their impacts on the ocean physics (Q2) and the consequences for the regional hydrodynamics (Q3). Each of the studies presented here adds to these research objectives and helps to advance the knowledge of the physical offshore wind farm impacts. While previous literature addressed the impacts mainly at local scales, this thesis puts the wind farm effects into perspective with regional dynamics and environmental consequences.

Accounting for wind farm effects in regional models

The studies of this thesis provide new understanding about the physical implications of offshore wind farms, specifically into the magnitudes and spatial scales of atmospheric and hydrodynamic wake effects. For this, a combination of flexible unstructured grids and simplified first-order parameterizations were used, describing the wind speed reduction and the structure-induced mixing caused by an offshore wind farm. The demonstrated methods are easily applicable to regional-scale models and flexible in terms of defining wind farm scenario, since no coupling between models or specific boundary conditions are needed for the model setup. The unstructured grids allow capturing submesoscale processes near offshore wind farms while simulating the larger scale dynamics in the model domain equally well. At this, enhanced grid resolution at wind farm sites of about 500 m, as applied in **Study I,II**, enables a detailed simulation of wake-related processes, while coarser grid resolution of about 2000 m is still sufficient to reproduce the regional anomalies (Figure IV). Hence, the horizontal grid resolution can be chosen according to the individual research objectives. However, with regard to small-scale ocean wake turbulence, **Study III** discourages the use of very high resolution while using hydrostatic models, to avoid problems with the hydrostatic assumptions and numerical instability. To represent both the wind wake and hydrodynamic wake effects in the regional model properly, a wind farm resolution of about 1000 m seems most appropriate.

While the introduced methods allow for flexible application in numerical models and can sufficiently reproduce wind farm effects, these simplified approximations have their limitations and offer room for improvements. On the one hand, both parameterizations

generalize the impact by wind speed reduction and structure drag independent of local conditions or wind farm characteristics. On the other hand, the parameterizations lack important physical processes. For instance, the wind wake parameterization in **Study I,II** excludes atmospheric boundary layer stability (Platis et al., 2020), which is critical for the actual wake lengths, and additional effects on near-surface temperature and humidity (Akhtar et al., 2022), which could enhance the impacts on stratification. These processes could be accounted for by replacing the simplified wake parameterization with data from regional climate modeling including wind farm parameterizations (Akhtar et al., 2021), as done by Daewel et al. (2022). This would result in more realistic atmospheric wake effects and individual wind speed reductions. On the other hand, the drag parameterization in **Study III** does not consider the drag coefficient dependency on the flow and stratification conditions (Dorrell et al., 2022) or the small-scale processes inside offshore wind farms. While numerical constraints limit the capabilities of this method, high-resolution Large Eddy Simulations or non-hydrostatic approaches could be used to determine local processes inside offshore wind farms and to improve and validate the results of the drag parameterization at coarse resolutions.

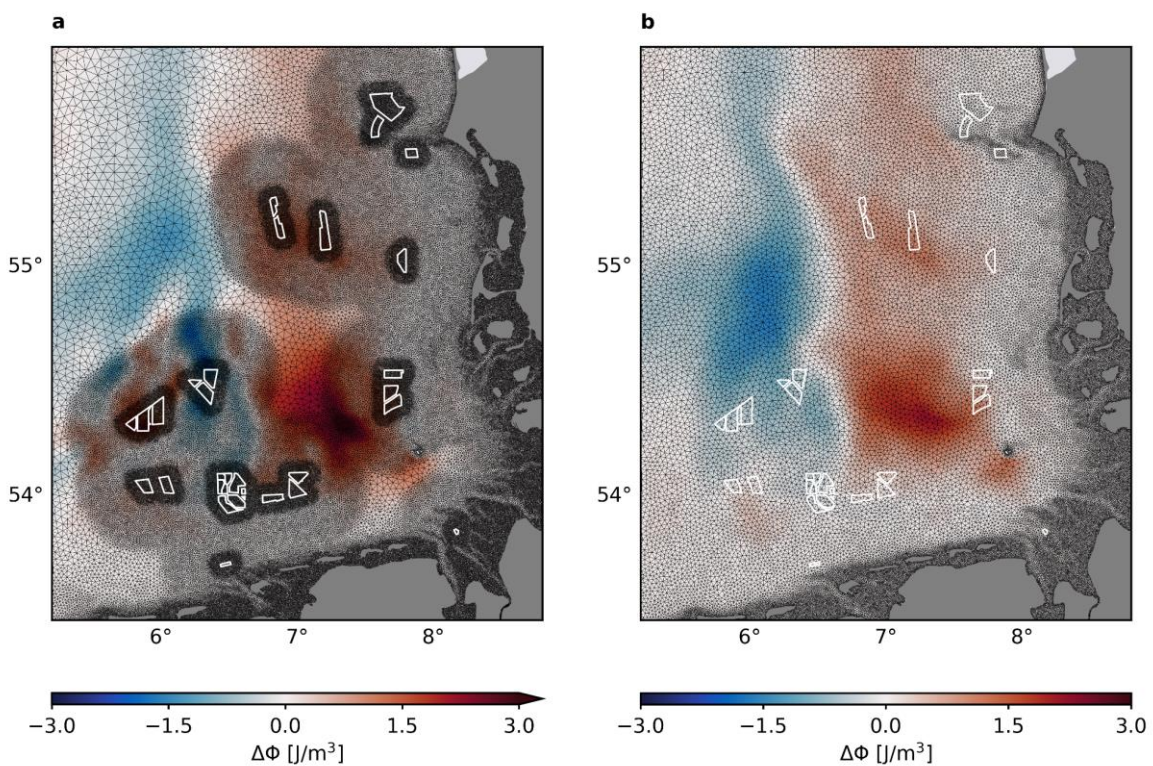


Figure IV | Comparison of different grid resolutions at wind farm sites with respect to summer stratification anomalies: (a) resolution refinement around wind farms as used in **Study I,II**, (b) alternative resolution of uniformly 2000 m around wind farms.

Implications for regional hydrodynamics

Using the simplified parameterizations, **Study I-III** demonstrate the hydrodynamic processes related to the physical offshore wind farm effects and how these alterations propagate through the system. The studies suggest the emergence of large spatial anomalies in ocean dynamics, which show temporal and spatial variability depending on atmospheric and hydrodynamic conditions. In this context, both processes, i.e., wind speed reduction and structure-induced mixing, extend regionally and cause large-scale structural changes whose magnitudes are similar to natural variability when averaged over time.

The downstream wind speed reductions at offshore wind farms add up to extensive anomalies in the wind field over time, with surface wind speed reductions around 0.2 m/s. Here, the simplified approximations presented in **Study I** agree well with recent regional climate modeling by Akhtar et al. (2021; 2022), considering that future scenarios have been used for the latter. The surface wind speed reductions translate to wind-driven processes in the ocean, particularly surface layer mixing and Ekman dynamics, and affect the hydrodynamics well beyond the wind farm sites, as also shown by Ludewig (2015). In this context, **Study I** emphasizes the implications for seasonal stratification development between spring and autumn, with perturbations around 10% in stratification strength. The simulated magnitudes of the changes in mean current speed and mean stratification of the simplified method are in agreement with the more sophisticated approach by Daewel et al. (2022). Nevertheless, it should be noted that the generalized parameterization used here might over- or underrepresent individual wind wake effects. Additional sensitivity studies for different wind wake intensities and lengths could help to classify the significance of individual wake representation on the mean hydrodynamic impact.

While the processes related to wind wakes are driven by changes in horizontal shear and induced vertical transport, **Study II** emphasizes that the actual impact on the ocean is determined by local hydrodynamic conditions. Changing surface currents in relation to the wind field and strong vertical mixing rates, e.g., from tides, can disturb and mitigate the mean effects by wind speed reduction over time. Here, **Study II** shows that tides in the North Sea can decrease the magnitudes of wind wake-induced changes locally by about 50% or more, as tidal currents disturb the wind wake effects and tidal stirring superimposes Ekman processes and impedes stratification. These mitigation processes are likely not only associated with wind wake effects, but also with structure-induced mixing, which is dependent on local tidal currents and turbulence levels.

Discussion and Outlook

Mixing at offshore wind turbine structures occurs on much smaller scales (10^2 m), in contrast to wind speed reduction (10^4 m). Nonetheless, **Study III** also suggests regional impact of similar magnitude by structure-induced mixing driven by additional wake turbulence at wind farm sites. While here the strongest changes occur within the wind farms, the mixing disturbs horizontal velocities and density-driven currents so that changes in hydrodynamics occur well beyond wind farms or propagate by advection. On a five-year average, structure drag changes the mean residual circulation in the German Bight by about $\pm 5\%$, whereas stratification decreases by about 10% on a large scale due to the additional mixing. Although the simplified approach in **Study III** agrees well with observational data, structure-induced mixing in stratified waters is yet poorly understood, and the magnitudes of the modified turbulent mixing scheme should be interpreted with caution (Dorrell et al., 2022). This, applies to both the turbulent mixing schemes themselves, which have been shown to underrepresent pycnocline depths and lack important physical processes (Luneva et al., 2019), and the drag parameterization, which is strongly sensitive to local turbulence conditions (Carpenter et al., 2016). High-resolution modeling and further in-situ measurements at offshore wind farm sites are needed to better evaluate the results of structure-induced mixing.

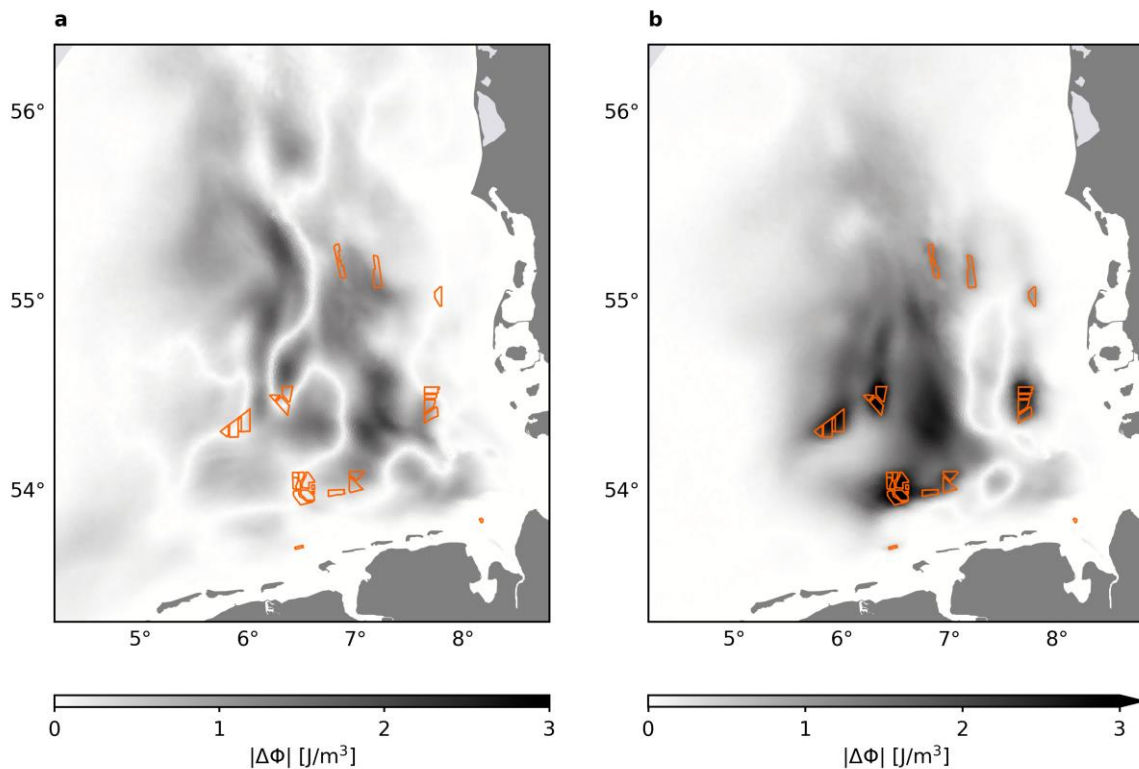


Figure V | Comparison of absolute stratification anomalies in summer (June-August) due to wind speed reduction (a) and structure-induced mixing (b) for the German Bight model setup (**Study III**).

The studies indicate that despite their different spatial scales, wind speed reduction and structure-induced mixing lead to similar magnitudes in the hydrodynamic changes, e.g., in mean current velocity on the order of mm/s, or in mean vertical density stratification (Figure V). As in this context, both effects extend largely into the far field of offshore wind farms, the effects are assumed to influence each other by amplification or attenuation of local amplitudes. However, as the different wake effects are determined by different influencing factors, interaction between atmospheric and hydrodynamic wake effects becomes complex. For instance, perturbations related to surface wind speed reduction depend on the wind field and the atmospheric boundary layer stability, and therefore vary seasonally with the climatic conditions. On the other hand, structure-induced mixing primarily depends on local turbine foundation properties and tidal flow characteristics, which differ in particular spatially with the wind farm locations. In addition, the effects may act into opposite directions, as wind and ocean currents are not always aligned. Consequently, the interaction between the wind farm effects becomes sensitive to the driving mechanisms. Nevertheless, the outcomes of the studies suggest that wake turbulence dominates inside and in the near-field of offshore wind farms, whereas wind wake effects spread over larger areas in the far field (Figure V). This is accompanied by areas of similar and opposite amplitudes. Further research is required to understand the interaction between the different wake effects and to address the complexity of the combined offshore wind farm impact.

A new normal for the marine environment

The monthly-mean changes induced by offshore wind farms are small compared to prevailing oceanic conditions and mostly do not exceed natural variability in the dynamic southern North Sea. Nonetheless, the stressors cause spatial redistributions and large-scale anomalies, which have the potential to influence the marine environment, especially given future offshore wind development and expected impact amplification. Physical processes are pivotal for ecosystem dynamics and determine, for example, the nutrient availability in surface and bottom waters (Sverdrup, 1953; Simpson and Sharples, 2012). At this, small variations in regional stratification of similar magnitude to interannual variability are sufficient to influence chlorophyll production and shift the spring bloom of phytoplankton by up to one month (Luneva et al., 2019). Hence, disturbances from offshore wind farms are strong enough to cause interannual fluctuations in hydro and ecosystem dynamics.

Atmospheric wakes reduce the momentum transfer from the atmosphere to the ocean and thereby decrease shear production of turbulent kinetic energy in the surface layers.

Discussion and Outlook

In consequence, wind-induced mixing diminishes near wind farms, as shown in **Study I,II**. The reduced mixing associates with reduction in turbidity and resuspension, eventually leading to locally increasing primary production as light availability increases (van der Molen et al., 2014; Daewel et al., 2022). In a recent study, Daewel et al. (2022) showed that extensive wind speed reduction and associated fluctuations in mixed layer depth cause large-scale positive and negative changes in annual averaged net primary production of up to $\pm 10\%$ locally and influence the bottom oxygen concentrations. Current velocity changes from wind speed reductions of similar magnitude to those in **Study I,II** were shown to reduce the bottom shear stress locally and increase annual mean sediment organic carbon by up to 10% at the wind farm locations (Daewel et al., 2022).

The extensive changes in current velocity from structure drag, shown in **Study III**, suggest similar implications for bottom shear stress and sediment resuspension. In addition, the structure-induced mixing is assumed to weaken the pycnocline as a barrier for vertical transport, thus increasing the exchange of nutrients and oxygen between the surface and bottom water (Floeter et al., 2017; Dorrell et al., 2022). Nutrient supply to upper layers might increase productivity in surface water, however the net effect phytoplankton growth will depend on the balance between nutrient and light availability, as additional mixing might also affect photosynthesis (Dorrell et al., 2022). The potential stirring effects at offshore wind farms (Floeter et al., 2017), involve consequences for local mixing and nutrient concentrations throughout the wind farms, which are likely to propagate downstream with the residual currents (Dorrell et al., 2022). In view of future offshore wind development, large-scale stirring effects of neighboring wind farm clusters could have systematic implications for marine ecosystem dynamics, changing the nutrient supply and oxygen concentrations over extensive areas.

Eventually, both wake effects alter ecosystem dynamics through the changes in current velocity and stratification, at which the combined impact will depend on the interaction between the physical processes such as the balance between reduced and enhanced mixing. Redistribution of primary production and sedimentation are likely to cascade up to higher trophic levels of the marine ecosystem and benthic species (van Berkel et al., 2020; Daewel et al., 2022). At this, wind farm effects can influence ecological processes on small time scales, such as transport changes during the tidal cycle, or on larger time scales, such as changes in seasonal primary production. As mentioned by Daewel et al. (2022), the systematic response to the offshore wind farm effects will likely consolidate in the marine environment of the North Sea, but with interannual variations depending to the environmental conditions. Persistent changes in surface water properties due to the perturbations of the pycnocline are likely to alter processes at the air-sea interface, such

as heat exchange and other surface fluxes or the oxygen and CO₂ uptake by the ocean (Dorrell et al., 2022). These effects might feed back on the atmosphere, for example, on the boundary layer stability, which in turn becomes critical for the magnitudes of atmospheric wakes.

Regional-scale changes in surface water density can become important with regard to climate change effects. The studies show ambient sea surface temperature changes near offshore wind farms of ± 0.05 °C, with maximum changes up to ± 0.1 - 0.2 °C. These changes correspond to 1-20% of the expected sea surface heating based on climate change projections for the North Sea (Schrum et al., 2016; Dieterich et al., 2019), in which mean sea surface temperature is projected to increase by about 1-3 °C by the end of the century. More importantly, changes in mean stratification strength (Figure V) are of similar magnitude as projected climate change alterations of about 1-5 J/m³ in the southern North Sea (Dieterich et al., 2019). Consequently, perturbations induced by wind speed reduction and mixing from offshore wind farms are sufficient to imitate or mitigate the impact of global warming. In this context, structure-induced mixing primarily counteracts the climate change effects by lowering sea surface temperatures, while wind speed reduction could both mitigate and imitate the effects, depending on the anomaly patterns.

In addition to the potential environmental changes on the one hand, the physical effects of extensive offshore wind development might also be beneficial to environmental and societal needs on the other. Besides potentially lowering the surface warming from climate change, for example, additional mixing within extensive future wind farm clusters could dominate wind wake effects over large areas and increase nutrient availability and production in surface layers, with beneficial effects on various higher trophic levels. From another perspective, such wind farm clusters in coastal regions, which reduce the momentum from surface winds and currents, could lead to a reduction of nearshore current speeds and wave heights, and thus contribute to coastal protection by lowering storm surges and erosion along the coastlines. van der Molen et al. (2014) showed that a 10 % reduction in surface winds can reduce the wave height within a large wind turbine array by about 17 %, which is assumed to be enhanced by the underwater structure drag. However, these assumptions are rather hypothetical and need to be tested by additional studies, especially since the magnitudes of average wind farm effects are suggested within natural variability.

Concluding remarks

Ultimately, interference between offshore renewable energy and the marine ecosystem becomes inevitable, given that marine energy resources are essential for sustainable energy production and reduction of greenhouse gas emissions. Therefore, it is important to understand the physical effects of offshore wind farms and their consequences, and to identify potential mitigation measures. This thesis provides innovative results on the long-term consequences of physical offshore wind farm effects in the southern North Sea. The studies of this thesis show how wind speed reduction and additional mixing by offshore wind farms influence the ocean physics and, in particular, stratification during the summer season. The studies identify large-scale restructuring and spatially and temporally varying redistributions in ocean physics, which are on the order of interannual variability in the monthly means, but much stronger on smaller time scales.

Questions remain about the interaction between effects from wind speed reduction and structure drag, and thus the ultimate impact of offshore wind farms on hydrodynamics. The simplified approaches need to be developed further, accounting for missing physical processes and individual wind farm characteristics, and should be complemented by more reliable but less flexible methods, such as using regional climate modeling as done by Daewel et al. (2022). In general, there is great need for more in situ measurements to support all the modeling studies and to assure that simulations and assumptions are reasonable.

As offshore wind farms will become an integral part of coastal seas, their implications should be given greater consideration in coastal ocean modeling and marine spatial planning. Although the magnitudes of hydrodynamic perturbations from wind speed reduction and structure-induced mixing are below or similar to natural variability, offshore wind farms cause systematic structural changes and redistributions of hydrodynamic properties on a regional scale. These spatial scales should be taken into account with regard to the environmental impact, as offshore wind infrastructure is often built in close proximity to marine protected areas or ecologically important areas (Daewel et al., 2022). Especially in dynamic systems like the North Sea, physical effects will propagate beyond the boundaries of wind farm clusters and affect far field ecosystem dynamics.

Future work will require impact assessment for more specific scenarios with respect to future marine spatial planning to mitigate consequences for the marine environment or make targeted use of inevitable changes. Long-term analyses of future scenarios are needed to determine persistent changes in the North Sea hydrodynamics and

ecosystem, and to understand variability and intensity of the systematic restructuring. As these effects are highly dependent on environmental conditions, climate change scenarios for atmosphere and ocean should be taken into account in future studies, as well as interaction with other anthropogenic stressors to the marine environment. In the end, this thesis might serve as groundwork for mitigation strategies and creates awareness for potential changes in the future North Sea.

References

- Akhtar, N., Geyer, B., Rockel, B., Sommer, P. S., and Schrum, C. (2021). Accelerating deployment of offshore wind energy alter wind climate and reduce future power generation potentials. *Scientific reports* 11, 11826. doi: 10.1038/s41598-021-91283-3
- Akhtar, N., Geyer, B., and Schrum, C. (2022). Impacts of accelerating deployment of offshore windfarms on near-surface climate. *Scientific reports* 12, 18307. doi: 10.1038/s41598-022-22868-9
- Baeye, M., and Fettweis, M. (2015). In situ observations of suspended particulate matter plumes at an offshore wind farm, southern North Sea. *Geo-Marine Letters* 35, 247–255. doi: 10.1007/s00367-015-0404-8
- Bergström, L., Kautsky, L., Malm, T., Rosenberg, R., Wahlberg, M., Åstrand Capetillo, N., et al. (2014). Effects of offshore wind farms on marine wildlife—a generalized impact assessment. *Environmental Research Letters* 9, 34012. doi: 10.1088/1748-9326/9/3/034012
- Boehlert, G. W., and Gill, A. B. (2010). Environmental and Ecological Effects of Ocean Renewable Energy Development: A Current Synthesis. *Oceanography*. doi: 10.5670/oceanog.2010.46
- Broström, G. (2008). On the influence of large wind farms on the upper ocean circulation. *Journal of Marine Systems* 74, 585–591. doi: 10.1016/j.jmarsys.2008.05.001
- Cañadillas, B., Foreman, R., Barth, V., Siedersleben, S., Lampert, A., Platis, A., et al. (2020). Offshore wind farm wake recovery: Airborne measurements and its representation in engineering models. *Wind Energy* 23, 1249–1265. doi: 10.1002/we.2484
- Carpenter, J. R., Merckelbach, L., Callies, U., Clark, S., Gaslikova, L., and Baschek, B. (2016). Potential Impacts of Offshore Wind Farms on North Sea Stratification. *PLOS ONE* 11, e0160830. doi: 10.1371/journal.pone.0160830
- Cazenave, P. W., Torres, R., and Allen, J. I. (2016). Unstructured grid modelling of offshore wind farm impacts on seasonally stratified shelf seas. *Progress in Oceanography* 145, 25–41. doi: 10.1016/j.pocean.2016.04.004
- Christiansen, M. B., and Hasager, C. B. (2005). Wake effects of large offshore wind farms identified from satellite SAR. *Remote Sensing of Environment* 98, 251–268. doi: 10.1016/j.rse.2005.07.009
- Clark, S., Schroeder, F., and Baschek, B. (2014). *The influence of large offshore wind farms on the North Sea and Baltic Sea – a comprehensive literature review*. HZG Report 2014-6.

- Daewel, U., Akhtar, N., Christiansen, N., and Schrum, C. (2022). Offshore wind farms are projected to impact primary production and bottom water deoxygenation in the North Sea. *Communications Earth & Environment* 3, 292. doi: 10.1038/s43247-022-00625-0
- Dieterich, C., Wang, S., Schimanke, S., Gröger, M., Klein, B., Hordoir, R., et al. (2019). Surface Heat Budget over the North Sea in Climate Change Simulations. *Atmosphere* 10. doi: 10.3390/atmos10050272
- Djath, B., and Schulz–Stellenfleth, J. (2019). Wind speed deficits downstream offshore wind parks? A new automatised estimation technique based on satellite synthetic aperture radar data. *Meteorologische Zeitschrift* 28, 499–515. doi: 10.1127/metz/2019/0992
- Djath, B., Schulz–Stellenfleth, J., and Cañadillas, B. (2018). Impact of atmospheric stability on X-band and C-band synthetic aperture radar imagery of offshore windpark wakes. *Journal of Renewable and Sustainable Energy* 10, 43301. doi: 10.1063/1.5020437
- Dorrell, R. M., Lloyd, C. J., Lincoln, B. J., Rippeth, T. P., Taylor, J. R., Caulfield, C.-c. P., et al. (2022). Anthropogenic Mixing in Seasonally Stratified Shelf Seas by Offshore Wind Farm Infrastructure. *Frontiers in Marine Science* 9. doi: 10.3389/fmars.2022.830927
- Emeis, S. (2010). A simple analytical wind park model considering atmospheric stability. *Wind Energ.* 13, 459–469. doi: 10.1002/we.367
- European Commission (2020). *Offshore renewable energy strategy*. Directorate-General for Energy, <https://data.europa.eu/doi/10.2833/219143>
- Floeter, J., Pohlmann, T., Harmer, A., and Möllmann, C. (2022). Chasing the offshore wind farm wind-wake-induced upwelling/downwelling dipole. *Frontiers in Marine Science* 9. doi: 10.3389/fmars.2022.884943
- Floeter, J., van Beusekom, J. E., Auch, D., Callies, U., Carpenter, J., Dudeck, T., et al. (2017). Pelagic effects of offshore wind farm foundations in the stratified North Sea. *Progress in Oceanography* 156, 154–173. doi: 10.1016/j.pocean.2017.07.003
- Forster, R. M. (2018). *The effect of monopile-induced turbulence on local suspended sediment patterns around uk wind farms: field survey report*. An IECS report to The Crown Estate. ISBN 978-1-906410-77-3.
- Frandsen, S., Barthelmie, R., Pryor, S., Rathmann, O., Larsen, S., Højstrup, J., et al. (2006). Analytical modelling of wind speed deficit in large offshore wind farms. *Wind Energ.* 9, 39–53. doi: 10.1002/we.189
- Grashorn, S., and Stanev, E. V. (2016). Kármán vortex and turbulent wake generation by wind park piles. *Ocean Dynamics* 66, 1543–1557. doi: 10.1007/s10236-016-0995-2
- Inger, R., Attrill, M. J., Bearhop, S., Broderick, A. C., James Grecian, W., Hodgson, D. J., et al. (2009). Marine renewable energy: potential benefits to biodiversity? An urgent call for research. *Journal of Applied Ecology* 46, 1145–1153. doi: 10.1111/j.1365-2664.2009.01697.x

- Ludewig, E. (2015). *On the Effect of Offshore Wind Farms on the Atmosphere and Ocean Dynamics*. Cham, s.l. Springer International Publishing.
- Luneva, M. V., Wakelin, S., Holt, J. T., Inall, M. E., Kozlov, I. E., Palmer, M. R., et al. (2019). Challenging Vertical Turbulence Mixing Schemes in a Tidally Energetic Environment: 1. 3-D Shelf-Sea Model Assessment. *J. Geophys. Res. Oceans* 124, 6360–6387. doi: 10.1029/2018JC014307
- Mineur, F., Cook, E. J., Minchin, D., Bohn, K., MacLeod, A., and Maggs, C. A. (2012). Changing Coasts: Marine Aliens and Artificial Structures. *Oceanography and Marine Biology: An Annual Review*, 189–234. doi: 10.1201/b12157-6
- Otto, L., Zimmerman, J., Furnes, G. K., Mork, M., Saetre, R., and Becker, G. (1990). Review of the physical oceanography of the North Sea. *Netherlands Journal of Sea Research* 26, 161–238. doi: 10.1016/0077-7579(90)90091-T
- Paskyabi, M. B., and Fer, I. (2012). Upper Ocean Response to Large Wind Farm Effect in the Presence of Surface Gravity Waves. *Selected papers from Deep Sea Offshore Wind R&D Conference, Trondheim, Norway, 19-20 January 2012* 24, 245–254. doi: 10.1016/j.egypro.2012.06.106
- Platis, A., Bange, J., Bärfuss, K., Cañadillas, B., Hundhausen, M., Djath, B., et al. (2020). Long-range modifications of the wind field by offshore wind parks? Results of the project WIPAFF. *Meteorologische Zeitschrift* 29, 355–376. doi: 10.1127/metz/2020/1023
- Rennau, H., Schimmels, S., and Burchard, H. (2012). On the effect of structure-induced resistance and mixing on inflows into the Baltic Sea: A numerical model study. *Coastal Engineering* 60, 53–68. doi: 10.1016/j.coastaleng.2011.08.002
- Schrum, C., Lowe, J., Meier, H. E. M., Grabemann, I., Holt, J., Mathis, M., et al. (2016). "Projected Change - North Sea," in *North Sea Region Climate Change Assessment*, eds. M. Quante, and F. Colijn (Cham: Springer International Publishing), 175–217.
- Schultze, L. K. P., Merckelbach, L. M., Horstmann, J., Raasch, S., and Carpenter, J. R. (2020). Increased Mixing and Turbulence in the Wake of Offshore Wind Farm Foundations. *J. Geophys. Res. Oceans* 125, e2019JC015858. doi: 10.1029/2019JC015858
- Shih, W., Wang, C., Coles, D., and Roshko, A. (1993). Experiments on flow past rough circular cylinders at large Reynolds numbers. *Journal of Wind Engineering and Industrial Aerodynamics* 49, 351–368. doi: 10.1016/0167-6105(93)90030-R
- Simpson, J. H., and Sharples, J. (2012). *Introduction to the physical and biological oceanography of shelf seas*. Cambridge University Press.
- Sumer, B. M., and Fredsøe, J. (2006). *Hydrodynamics Around Cylindrical Structures*. WORLD SCIENTIFIC.
- Sündermann, J., and Pohlmann, T. (2011). A brief analysis of North Sea physics. *Oceanologia* 53, 663–689. doi: 10.5697/oc.53-3.663

- Sverdrup, H. U. (1953). On Conditions for the Vernal Blooming of Phytoplankton. *ICES J Mar Sci* 18, 287–295. doi: 10.1093/icesjms/18.3.287
- van Berkel, J., Burchard, H., Christensen, A., Mortensen, L. O., Svenstrup Petersen, O., and Thomsen, F. (2020). The Effects of Offshore Wind Farms on Hydrodynamics and Implications for Fishes. *Oceanography* 33, 108–117. doi: 10.5670/oceanog.2020.410
- van der Molen, J., Smith, H. C., Lepper, P., Limpenny, S., and Rees, J. (2014). Predicting the large-scale consequences of offshore wind turbine array development on a North Sea ecosystem. *Continental Shelf Research* 85, 60–72. doi: 10.1016/j.csr.2014.05.018
- van Leeuwen, S., Tett, P., Mills, D., and van der Molen, J. (2015). Stratified and nonstratified areas in the North Sea: Long-term variability and biological and policy implications. *J. Geophys. Res. Oceans* 120, 4670–4686. doi: 10.1002/2014JC010485
- Vanhellemont, Q., and Ruddick, K. (2014). Turbid wakes associated with offshore wind turbines observed with Landsat 8. *Remote Sensing of Environment* 145, 105–115. doi: 10.1016/j.rse.2014.01.009
- Williamson, C. H. K. (1996). Vortex Dynamics in the Cylinder Wake. *Annu. Rev. Fluid Mech.* 28, 477–539. doi: 10.1146/annurev.fl.28.010196.002401
- WindEurope (2021). *Offshore Wind in Europe: Key trends and statistics in 2020*, <https://windeurope.org/intelligence-platform/product/offshore-wind-in-europe-key-trends-and-statistics-2020/>
- WindEurope (2022). *Wind Energy in Europe: 2021 Statistics and the outlook for 2022–2026*, <https://windeurope.org/intelligence-platform/product/wind-energy-in-europe-2021-statistics-and-the-outlook-for-2022-2026/>
- Zhang, Y. J., Ye, F., Stanev, E. V., and Grashorn, S. (2016). Seamless cross-scale modeling with SCHISM. *Ocean Modelling* 102, 64–81. doi: 10.1016/j.ocemod.2016.05.002

Acknowledgements

I would like to take this opportunity to thank all the people who accompanied me on this journey.

First and foremost, I would like to thank Corinna Schrum, who came up with the idea for this intriguing topic and gave me the opportunity to grow with the challenge despite my non-oceanographic scientific background. Thank you for all the support, advice and guidance throughout my PhD, for sharing your experience and knowledge, and for all the fruitful discussion that got me back on track. I am very grateful for the opportunity to work with you.

I would like to thank Ute Daewel for her mentorship, her commitment and her support. Thank you for always being there for me when I needed advice, scientific or personal, even on stressful working days or late Friday afternoons. Thank you for being my 'OWF workmate', spending hours trying to understand the processes or find solutions to my problems. I am grateful for all your creative ideas, your inspiration and the knowledge you shared with me. Your enthusiasm has motivated me.

I would also like to thank the many colleagues I met during my PhD who inspired me to come up with new ideas, helped me with technical problems, or gave me advice and constructive criticism, especially Johannes Schulz–Stellenfleth and Bughsin Djath for their collaborations on the wind wakes, Jeff Carpenter and Nobuhiro Suzuki for their help and discussions on the pile effects, Johannes Pein for his help with modeling, and Andreas Kannen for giving me a platform in a world outside numerical modeling. Thank you to all my KST colleagues who made my working life more enjoyable and introduced me to the HZG/Hereon world. Special thanks to Jan Kossack, Peter Arlinghaus and Lucas Porz, who helped me with all my struggles, scientific or work-related, and for the many discussions and troubleshooting during the modeling.

Finally, I would not have made it to this point without my family. Thank you for all the love, support and motivation throughout the last nine years of my studies. Thank you for giving me the opportunities in life, always believing in me and making me the person I am today. Most of all, thank you Jana for all your encouragement and love. Thank you for always supporting me and being there for me. Thank you for your ideas, for being my personal reviewer and for tolerating all my spontaneous flashes of inspiration, whether at home, while going out for dinner or even on vacations. I could not have done this without you.

Eidesstattliche Versicherung | Declaration on Oath

Hiermit erkläre ich an Eides statt, dass ich die vorliegende Dissertationsschrift selbst verfasst und keine anderen als die angegebenen Quellen und Hilfsmittel benutzt habe.

I hereby declare upon oath that I have written the present dissertation independently and have not used further resources and aids than those stated.

Hamburg, 17.12.2022

A handwritten signature in black ink that reads "Christiansen". The script is cursive and somewhat stylized.

Nils Christiansen

